

**SURFACE AND BIOLOGICAL EFFECTS
OF PEPTIDE ORIENTATION**

**Surface and Biological Effects of
Peptide Orientation Evaluated
Using Gold-Coated Polyurethanes**

By

BRANDI MEEKS, B.A.Sc.

A Thesis

**Submitted to the School of Graduate Studies
in Partial Fulfillment of the Requirements
for the Degree
Master of Engineering**

McMaster University

©Copyright by Brandi Meeks, January 2001

**MASTER OF ENGINEERING (2001)
(Chemical Engineering)**

**McMaster University
Hamilton, Ontario**

**TITLE: Surface and Biological Effects of Peptide Orientation
 Evaluated Using Gold-Coated Polyurethanes**

AUTHOR: Brandi Meeks, B.A.Sc. (University of Ottawa)

SUPERVISOR: Professor Heather Sheardown

NUMBER OF PAGES: xii; 115

ABSTRACT

Cell adhesion and growth are central issues in the otherwise promising method of endothelialization of materials for improving blood compatibility. To improve cell adhesion to biomaterial surfaces, surface modification with cell adhesion peptides is often used. In particular, arginine-glycine-aspartic acid (RGD), long recognized as a peptide sequence that plays an important role in cell adhesion, has been covalently attached to surfaces to enhance cell adhesion. In this work, the effect of the orientation of the cell adhesion peptide immobilized on the surface was studied through using gold surfaces, which can be readily modified with thiols and sulfur-containing groups. Peptide orientation was controlled by the placement of the cysteine (C) at either the C- or N-terminus. Two cell adhesion peptides, the non-specific RGD and more endothelial cell specific REDV (arginine-glutamic acid-aspartic acid-valine), were studied for their effect on the surface chemical and biological properties, including effects on the interactions with the endothelial cell line ECV304. Vitronectin adsorption to the modified surfaces was specifically examined as a possible reason for differences noted. The results suggest that peptide orientation plays an important role in the interactions of cells and proteins to the modified surfaces. Peptides with the cysteine at the N-terminus showed increased adhesion of endothelial cells from the ECV304 line, with the greatest adhesion noted consistently on the CREDEV-modified surfaces. Differences in surface chemistry as evaluated by x-ray

photoelectron spectroscopy were also found higher levels of bonded peptide when the thiol-containing cysteine was in the N-terminal position. These results suggest that the secondary structure of the peptide can be used to enhance or to limit its reaction with the surface. Furthermore, while cell adhesion was noted during culture in the absence of serum, significant increases in the numbers of adherent cells were noted on all surfaces when the cells were grown in the presence of serum. Immunoblotting and culture with antibodies demonstrated that this increase in the adhesion of the cells is likely mediated primarily by the cell adhesion peptide vitronectin.

ACKNOWLEDGEMENTS

The author would like to thank a number of people who have contributed to the completion of this thesis. My sincere thanks go out to my thesis supervisor, Dr. Heather Sheardown who provided unlimited guidance, expertise and assistance. I would like to thank Dr. Brash and his entire research group for their guidance, particularly Rena Cornelius, Glenn McClung and Jacques Archambault for dealing with my endless questions in the lab. I would also like to thank Dr. Tom Podor who provided expertise as well as the required resources for the cell adhesion assays. Thanks also to Farid Bensebaa, Yves Deslandes and Gerry Pleizier of NSERC who provided XPS analysis. Special thanks also go out to my loving family, especially my understanding and supportive husband, Trevor Kooistra.

Thank you.

TABLE OF CONTENTS

Title Page	i
Descriptive Note	ii
Abstract	iii
Acknowledgements	iv
Table of Contents	v
List of Figures	ix
List of Tables	xi
Abbreviations	xii
1. Introduction	1
2. Literature Review	4
2.1 Blood-Biomaterial Interactions	4
2.1.1 Protein Adsorption	4
2.1.2 Hemostasis	5
2.1.3 Platelet Reactions	5
2.1.4 Coagulation	6
2.1.5 Fibrinolysis	7
2.2 Vascular Physiology	8
2.2.1 Blood Vessel Physiology	8
2.2.2 Extracellular Matrix	9
2.2.3 Endothelial Cells	10
2.3 Cell Adhesion	11
2.3.1 Integrins	11
2.3.2 Cell Adhesion Peptides	13
2.3.3 Vitronectin	15
2.4 Blood Compatible Materials	19
2.4.1 Biomaterials	19
2.4.2 Surface Modification for Modulating Protein Surface Interactions	19
2.4.3 Endothelialization to Promote Blood Compatibility	21
2.4.4 Peptide Modification of Surfaces to Improve Blood Compatibility	22
2.5 Gold-Thiol Chemistry	24
2.5.1 Gold-Thiol Chemistry as a Surface Modification Technique	24

2.5.2	Self-Assembled Monolayers on Gold Substrates	25
2.5.3	Gold-Thiol Surfaces In Biomedical Applications	26
2.6	Characterization Techniques	31
2.6.1	Water Contact Angles	31
2.6.2	X-ray Photoelectron Spectroscopy	33
2.6.3	Scanning Electron Microscopy	34
2.6.4	SDS-Polyacrylamide Gel Electrophoresis	34
2.7	Project Rationale	35
3.	Experimental Procedures	37
3.1	Surface Preparation and Modification	37
3.1.1	Polyurethane Synthesis	37
3.1.2	Polyurethane Film Casting	38
3.1.3	Gold Evaporation on Polyurethane Films	38
3.1.4	Peptide Chemisorption	38
3.2	Surface Characterization	40
3.2.1	Water Contact Angles	40
3.2.2	X-ray Photoelectron Microscopy	41
3.2.3	Scanning Electron Microscopy	42
3.3	Protein Adsorption Studies	42
3.3.1	Protein Adsorption from Plasma	42
3.3.2	Total Protein Assay	43
3.3.3	SDS-Polyacrylamide Gel Electrophoresis	43
3.3.4	Immunoblotting	44
3.3.5	Vitronectin Adsorption and Immunoblotting	46
3.3.5.1	¹²⁵ I Labeled Vitronectin	46
3.3.5.2	Vitronectin Adsorption from Plasma	47
3.3.5.3	Vitronectin Immunoblot	48
3.4	<i>In Vitro</i> Cell Attachment Studies	48
3.4.1	Cell Reagents, Maintenance and Subculture	48
3.4.2	Cell Attachment Assay	49
4.	Results	51
4.1	Surface Preparation and Modification	51
4.1.1	Polyurethane Synthesis	51
4.1.2	Gold Evaporation on Polyurethane Films	51
4.1.3	Cleaning Gold Coated Polyurethanes	52
4.2	Surface Characterization	53
4.2.1	Water Contact Angles	53
4.2.2	Scanning Electron Microscopy	55

4.2.3 X-ray Photoelectron Microscopy	58
4.3 Protein Adsorption Studies	61
4.3.1 Total Protein Adsorption	61
4.3.2 Total Protein Immunoblot	63
4.3.4 Vitronectin Immunoblot	68
4.3.5 Vitronectin Adsorption	69
4.4 <i>In Vitro</i> Cell Attachment Studies	72
4.4.1 Peptide and Serum Protein Effects	72
4.4.2 Peptide and Vitronectin Effects	75
5. Discussion	77
5.1 Peptide Modification of Gold Surfaces	77
5.2 Surface Characterization	78
5.3 Biological Characterization	82
6. Conclusions	90
7. Recommendations for Future Studies	94
References	95
Appendix A: Reagents, Solvents, and Materials	103
Appendix B: Peptide Chromatograms	105
Appendix C: Preparation of Buffers	109
Appendix D: Determination of Free Iodide Concentration	110
Appendix E: SDS-PAGE and Western Blotting Technique	111

LIST OF FIGURES

Figure 2.1	General blood responses to biomaterials	4
Figure 2.2	The coagulation cascade	7
Figure 2.3	Schematic representation of the fibrinolytic system	8
Figure 2.4	Illustration of the extracellular matrix	10
Figure 2.5	Schematic structure of a typical integrin	13
Figure 2.6	Structure of the peptides Arginine-Glycine-Aspartic Acid and Arginine-Glutamic Acid-Aspartic Acid-Valine	15
Figure 2.7	Schematic illustration of alkyl thiolate monolayer on Au(111)	25
Figure 2.8	Schematic model of L-Cysteine on a gold surface	28
Figure 2.9	Schematic illustration of contact angles on hydrophilic and hydrophobic surfaces	32
Figure 2.10	Advancing and receding contact angles as measured by the sessile drop method	32
Figure 4.1	Advancing and receding sessile drop water contact angles for the unmodified and peptide-modified surfaces	54
Figure 4.2	Scanning electron microscope images (2000x) of unmodified and peptide-modified surfaces	56
Figure 4.3	Scanning electron microscope images (5000x) of unmodified and peptide-modified surfaces	57
Figure 4.4	Total amount of protein adsorption to the unmodified and peptide-modified surfaces following a two-hour incubation in 100% plasma	62
Figure 4.5	Immunoblot from SDS-PAGE 12% reduced gel probing for numerous plasma proteins in the eluate obtained from the unmodified gold surface and the cysteine-modified surface following a two-hour incubation in plasma	65

Figure 4.6	Immunoblot from SDS-PAGE 12% reduced gel probing for numerous plasma proteins in the eluate obtained from the CRGD-modified and the RGDC-modified surface following a two-hour incubation in plasma66
Figure 4.7	Immunoblot from SDS-PAGE 12% reduced gel probing for numerous plasma proteins in the eluate obtained from the CREDV-modified and the REDVC-modified surface following a two-hour incubation in plasma67
Figure 4.8	Immunoblot from SDS-PAGE 9% gel (reduced) probing for vitronectin in the proteins eluted from the unmodified and modified surfaces following a two-hour incubation in plasma 68
Figure 4.9	The adsorption of ¹²⁵ I labeled vitronectin from plasma solutions to the unmodified and peptide-modified surfaces71
Figure 4.10	Percentage of cells attached on the various surfaces after a four-hour incubation at 37°C. The media was either serum-free or serum-free containing 10% fetal calf serum74
Figure 4.11	Normalized cells attachment on the various surfaces following a four-hour incubation at 37°C. The media was serum-free containing 10% fetal calf serum containing either anti-vitronectin or non-immune IgG 76

LIST OF TABLES

Table 3.1	Polyclonal antibodies to human proteins in the form of fractionated antisera (IgG fractions) developed in goat, sheep, or rabbit	45
Table 3.2	Affinity purified alkaline phosphatase conjugated secondary antibodies	46
Table 4.1	Summary of representative XPS results for the unmodified and peptide-modified surfaces	60
Table 5.1	Summary of results for the immunoblot probing for vitronectin in the proteins eluted from the unmodified and modified surfaces	87

LIST OF ABBREVIATIONS

BAEC	bovine aortic endothelial cell
BCIP	5-bromo-4-chloro-3-indolyl phosphate
CREDV	Cysteine-Arginine-Glutamic Acid-Aspartic Acid-Valine
CRGD	Cysteine-Arginine-Glycine-Aspartic Acid
DMF	dimethylformamide
DMSO	dimethyl sulfoxide
EC	endothelial cells
ED	ethylene diamine
FCS	fetal calf serum
GP	glycoprotein
HUVEC	human umbilical vein endothelial cells
kDa	kiloDalton
MDI	4,4'-methylene-di-p-phenyl diisocyanate
NBT	nitroblue tetrazolium
PAGE	polyacrylamide gel electrophoresis
PAI	plasminogen activator inhibitor
PBS	phosphate buffered saline
PEG	polyethylene glycol
PEO	polyethylene oxide
PTFE	polytetrafluoroethylene
PTMO	Polytetramethylene oxide
PU	polyurethane
REDV	Arginine-Glutamic Acid-Aspartic Acid-Valine
REDVC	Arginine-Glutamic Acid-Aspartic Acid-Valine-Cysteine
RGD	Arginine-Glycine-Aspartic Acid
RGDC	Arginine-Glycine-Aspartic Acid-Cysteine
SAM	self-assembled monolayer
SDS	sodium dodecyl sulfate
SEM	scanning electron microscopy
tPA	tissue plasminogen activator
uPA	urokinase plasminogen activator
XPS	x-ray photoelectron spectroscopy

1. INTRODUCTION

Protein adsorption to a biomaterial is the first and most critical event following blood-biomaterial contact [1]. Subsequent phenomena, including platelet reactions, coagulation, fibrinolysis and inflammation, are largely a result of interactions between blood and the adsorbed protein layer. Though some biomaterials have seen limited clinical success, there remains considerable room for improvement, particularly in terms of specificity.

Polymers, while ideal for biomaterials due to their strength, durability and flexibility, generally induce unfavourable biological responses upon contact with blood. The biocompatibility of polymer-based biomaterials can be improved by surface modification, while still maintaining the other essential properties of the material [2]. Increasing hydrophobicity, chemical modification, attachment of anti-thrombotic agents, treatment of surfaces with protein, and biomembrane-mimetic surfaces are examples of modification techniques commonly used [3].

The development and maintenance of a material adherent endothelial cellular layer similar to that present *in vivo* has been widely proposed as a method of decreasing deleterious blood-biomaterial interactions by providing a bioactive and biological blood-graft interface. Such a surface would have the potential for reducing the instances of neointimal hyperplasia, and would possess

the coagulant and fibrinolytic properties present in the native vessel. One method of effecting the adhesion and growth of an endothelial cell lining involves surface modification with cell adhesion proteins and peptides similar to those present *in vivo*. It has been shown that short peptides, including arginine-glycine-aspartic acid (RGD), found in the adhesion proteins vitronectin, collagen, fibrinogen, thrombospondin and von Willebrand factor [4], possess cell adhesive properties similar to the intact protein [5]. Surface modification with cell adhesion peptides is preferred to modification by either passive adsorption or covalent attachment of the entire protein for a number of reasons, including the lower immunogenicity, and higher specificity of surface attachment as well as the stability of the resulting surfaces [6]. Surface immobilization of RGD-containing synthetic peptides has been shown to promote cell attachment in a similar fashion as fibronectin itself [7]. REDV, a sequence found in fibronectin, has been suggested to interact with the $\alpha_4\beta_1$ receptor on endothelial cells, and has also been used to enhance endothelial cell adhesion [8] with some endothelial cell specificity.

Gold surfaces are attractive for studies of surface modification and show promise in biomaterials applications. Gold, while inert to most chemical functionalities, interacts strongly with thiol-containing moieties. The regular spacing of the gold atoms on a 111 gold surface and the ease of modification with thiol-containing compounds therefore results in the potential for generating surfaces of high density and specificity [9]. In particular, gold surfaces can be readily modified with cysteine-containing peptides to generate surfaces with a

high concentration of surface bound ligand. Cell adhesion peptide modified gold-coated metal [10], glass [11] and polymeric surfaces [12] have been studied for interactions with cells of a variety of origins. The orientation of the peptides on the gold-coated surfaces in these studies, controlled through the placement of the cysteine in the peptides was apparently randomly selected. However, by modification of the location of the cysteine in the peptide, fundamental studies of the effect of peptide surface orientation are possible. In this work, gold-coated polyurethanes were surface modified with cell adhesion peptides to improve interactions with vascular endothelial cells. Peptide orientation on the surfaces was controlled by the placement of the cysteine and thus the thiol group in the peptide. The effect of peptide orientation on the surface properties of the modified surfaces was studied using x-ray photoelectron spectroscopy, scanning electron microscopy, and sessile drop water contact angles. The biological properties of the surfaces were examined using protein adsorption and vascular endothelial cell attachment studies. In particular, the protein studies focused on the interactions of the surfaces with vitronectin, a 75 kDa multifunctional adhesive plasma glycoprotein protein known to play a role in the coagulation, complement and fibrinolytic pathways. Vitronectin has also been found to be a plasma protein adsorbed to biomaterials in contact with blood. The results of these studies are useful in establishing parameters necessary for the development of an endothelialized surface and potentially for the development of an implantable material for blood contacting applications.

2. LITERATURE REVIEW

2.1 BLOOD-BIOMATERIAL INTERACTIONS

2.1.1 Protein Adsorption

The first and most critical event following contact of a biomaterial with blood is the adsorption of proteins from plasma to the material surface [1]. Subsequent phenomena are largely a result of interactions between blood and the adsorbed protein layer (as depicted in Figure 2.1). Once adsorbed, many proteins have the ability to promote both the adherence and activation of a number of blood cell types (platelets, leukocytes) resulting in thrombosis and inflammation [13]. Furthermore, adsorption of proteins can inhibit cell adhesion to a surface by competing with cell adhesion proteins present in blood or by blocking surface access to the cell surface receptors.

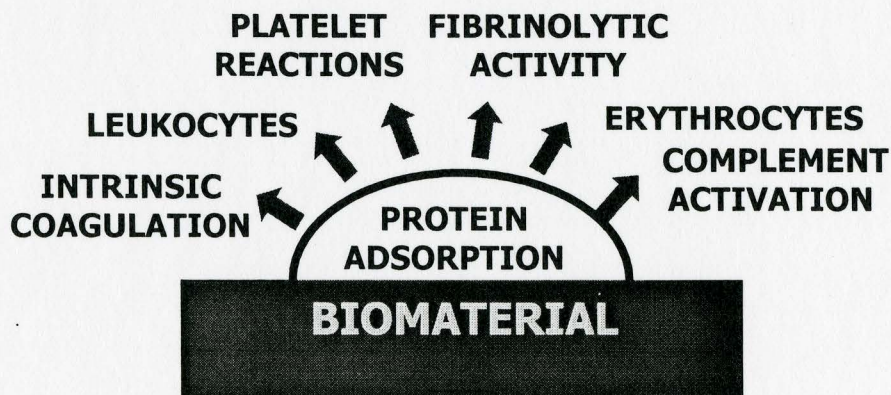


Figure 2.1 General blood responses to biomaterials. (Adapted from Courtney *et al.*, 1994. [3])

2.1.2 Hemostasis

Hemostasis involves coordination between the coagulation and fibrinolytic systems. Coagulation controls bleeding via formation of fibrin clots while fibrinolysis maintains vascular patency by clot dissolution and removal. The hemostatic response is fast, localized and extremely well controlled involving a number of blood coagulation factors normally present in plasma as well as some substances that are released by platelets and injured tissue cells.

2.1.3 Platelet Reactions

In a number of pathophysiologic events, including inflammation, blood coagulation and the immune response, the recruitment of circulating blood cells to specific sites is crucial. At sites of vascular injury, platelets adhere to the sub-endothelial matrix of the damaged vessel, spread over the surface, secrete granule products and recruit additional platelets [14]. Platelet adhesion is mediated by glycoproteins embedded in the platelet's membrane that serve as receptors for activation and interaction with other cells. The glycoprotein GPIb/IX mediates platelet adhesion to subendothelial collagen via von Willebrand factor, GPIa mediates platelet adhesion via binding to collagen, and GPIIb/IIIa serves as the binding site for adhesive molecules that possess the Arginine-Glycine-Aspartic Acid (RGD) peptide sequence [15].

Following platelet adhesion, the resulting aggregate is stabilized in a continuing process by fibrin formation. This process, referred to as primary

hemostasis, is followed by platelet retraction. During platelet retraction, myosin and actin filaments within platelets that are linked via the integrin $\alpha_{1b}\beta_3$ to extracellular fibrin, draws the edges of a wound together, reducing bleeding and supporting the healing process [16]. On artificial surfaces, platelet adhesion follows the adsorption of plasma proteins to the surface. Thrombus formation on an artificial surface can occur via intrinsic coagulation initiated by either the release of thromboplastins by platelets or by factor XII activation caused by platelets stimulated by adenosine diphosphate [3].

2.1.4 Coagulation

The coagulation cascade involves the conversion of a series of inactive proenzymes to activated enzymes, ultimately resulting in the formation of thrombin. Thrombin then converts the soluble plasma protein fibrinogen into the insoluble fibrous protein fibrin, which polymerizes incorporating platelets to form the thrombus or blood clot. The coagulation cascade has been divided into two pathways: the extrinsic and intrinsic pathways. The intrinsic pathway, of concern in biomaterials development, is initiated by activation of Hageman factor (factor XII), while the extrinsic pathway is activated by tissue factor, a cellular lipoprotein present at sites of tissue injury [14]. The two pathways converge at the point where factor X is activated as shown in Figure 2.2.

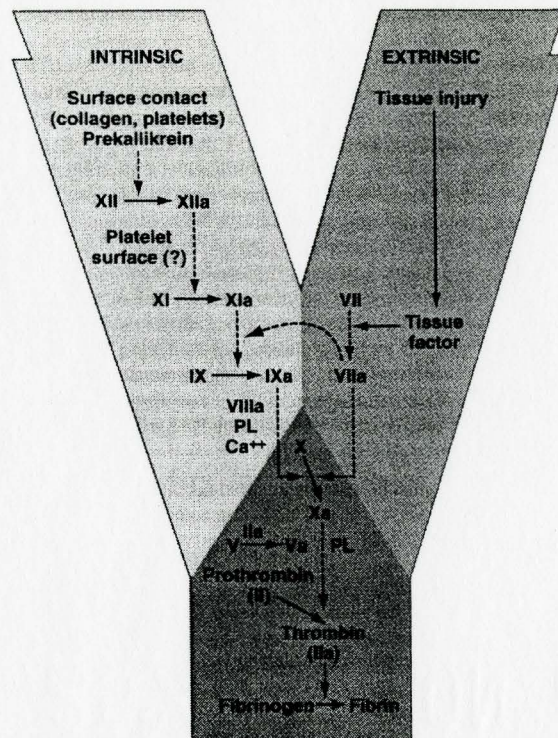


Figure 2.2 The coagulation cascade. (Taken from Kumar *et al.*, 1997. [14])

2.1.5 Fibrinolysis

Fibrinolysis results in the dissolution of thrombi. The inactive proenzyme, plasminogen is converted to the active enzyme plasmin, which degrades fibrin into soluble fibrin degradation products as shown in Figure 2.3. Tissue-type plasminogen activator (tPA) and urokinase-type plasminogen activator (uPA) have been identified as two immunologically distinct types of plasminogen activators responsible for converting plasminogen to plasmin. Inhibition of the fibrinolytic system may occur with plasminogen activator inhibitors such as PAI-1 and PAI-2, or with the plasmin inhibitor, α_2 -antiplasmin [17].

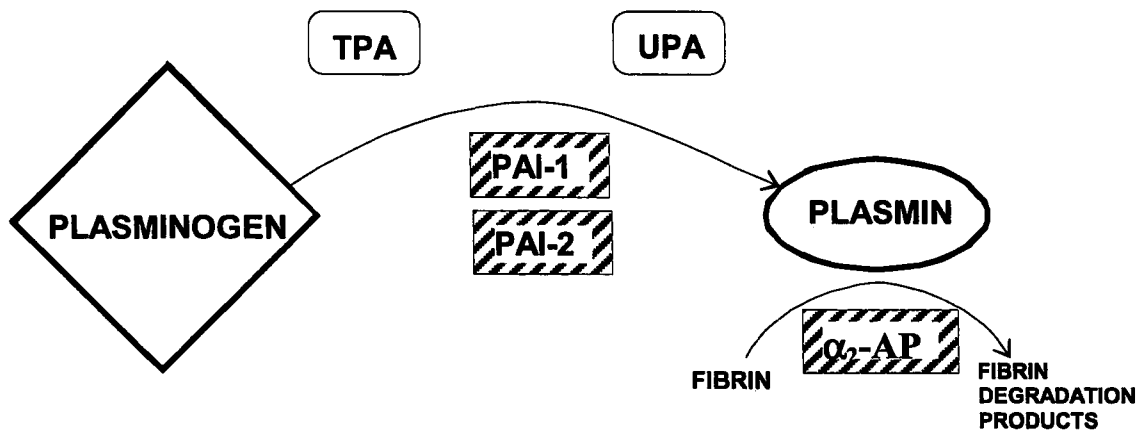


Figure 2.3 Schematic representation of the fibrinolytic system. (Adapted from Collen, 1999. [17])

2.2 VASCULAR PHYSIOLOGY

2.2.1 Blood Vessel Physiology

There are two major cell types in the blood vessel, namely, endothelial cells and smooth muscle cells [18]. The walls of all but the smallest blood vessels are composed of three distinct layers (tunics) which surround a central blood-containing space, the vessel lumen. The innermost tunic consists of a single layer of vascular endothelial cells, supported by a basement membrane in vessels larger than 1 mm in diameter [19]. This layer provides a smooth, low-friction surface for the movement of blood through the vessel lumen. The middle tunic is mostly smooth muscle cells and sheets of elastin and is innervated by nerve fibers. This layer controls blood flow and pressure via vasoconstriction or vasodilation. The outermost layer is composed mainly of collagen fibers that protect the blood vessel and anchor it to surrounding structures.

2.2.2 Extracellular Matrix

Cell adhesion is key in tissue organization during development, platelet plug formation in hemostasis, recruitment of neutrophils, monocytes, and lymphocytes from the circulation during wound healing, inflammation, and infection, and in tumor cell metastasis [20]. Furthermore, cell adhesion to artificial surfaces may be crucial to the development of tissue engineered implants. *In vivo*, the extracellular matrix (ECM) plays an important role in tissue development; supplying a substratum for cell adhesion, as well as influencing cell development, migration, proliferation, shape, and metabolic functions [14]. The ECM (Figure 2.4) consists of two major classes of extracellular macromolecules: adhesive glycoproteins and fibrous proteins, both often secreted by fibroblasts. The adhesive glycoproteins consist of polysaccharide glycosaminoglycans (GAGs) usually linked to proteoglycans. GAGs form a highly hydrated gel in which the fibrous proteins are embedded. This gel resists any compressive forces on the matrix [21]. Fibrous proteins are of two types; structural proteins include collagen and elastin and adhesive proteins include fibronectin and laminin. Collagen provides tensile strength while elastin gives the blood vessel its resilience. Fibronectin promotes cells such as fibroblasts to adhere to the matrix, whereas laminin promotes attachment of endothelial cells to the basal lamina.

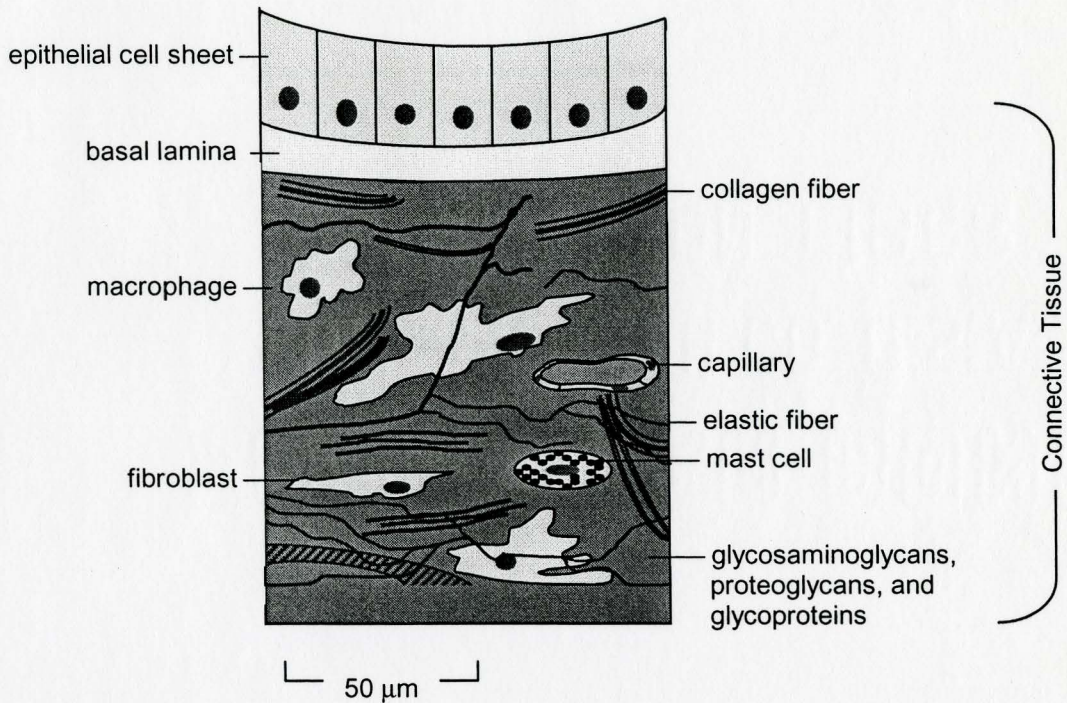


Figure 2.4 Illustration of the extracellular matrix. (Adapted from Alberts *et al.*, 1994. [21])

2.2.3 Endothelial Cells

The vasculature is lined with a monolayer of endothelial cells attached both to each other and to the underlying basement membrane or basal lamina. This cell layer is crucial to the modulation of blood supply to the tissues as well as to the maintenance of hemostasis. Endothelial cells are also responsible for tissue growth and repair. Following denudation, neighbouring cells migrate and proliferate to repair the wound. In canine models, endothelial cells have been shown to form a complete monolayer on the surface of an artificial blood vessel [22]. In culture, human endothelial cells require specific growth factors in order to

proliferate and subcultivation can lead to morphological changes. Thus, immortalized cell lines, such as ECV304, which are typically used for endothelial cell research [23], give results that are therefore not necessarily reflective of true human endothelial cells.

Endothelial cells modulate several, and frequently opposing, aspects of normal hemostasis. They normally possess anti-platelet, anticoagulant, and fibrinolytic properties, but are also capable after injury or activation of exerting pro-coagulant functions [14]. The anti-coagulant properties of endothelium include inhibition of platelet adhesion and activation, production of thrombomodulin, and synthesis of Protein S. Pro-coagulant properties include the production of von Willebrand factor, production of cytokines, the binding of platelets to injured endothelial cells, and the binding of factors IX and X. In addition, endothelial cells promote fibrinolysis through the synthesis of plasminogen activators including tPA and uPA. Endothelial cells also produce inhibitors of plasminogen activators (PAI) that suppress fibrinolysis [24].

2.3 CELL ADHESION

2.3.1 Integrins

The adhesive properties of cells can be largely attributed to the integrin family of cell adhesion receptors. Integrins are heterodimeric matrix receptors consisting of two noncovalently bound glycoprotein units designated as α and β (Figure 2.5). The twelve alpha and nine beta units that have been identified

combine to form at least 21 distinct integrins [25]. Integrins are composed of two domains. A long extracellular domain adheres to the ligands while the cytoplasmic domain links the integrins to the cytoskeleton of the cell. Integrins anchor cells to substrates and transmit signals across plasma membranes. They are capable of binding to numerous ligands including extracellular matrix proteins, circulating proteins, immunoglobulin proteins, viruses, bacterial membrane proteins, snake venom proteins, and even other integrins [25].

Several structurally and functionally distinct integrins are often expressed on the surface of a given cell, although some integrins are cell type specific. Interactions between the cell and basement membrane proteins such as collagen, laminin, and fibronectin are governed by β_1 integrins, whereas adhesion to provisional matrix proteins such as fibrinogen, vitronectin, fibronectin, thrombospondin, and osteopontin during wound repair and tissue reorganization is promoted by α_v integrins [25].

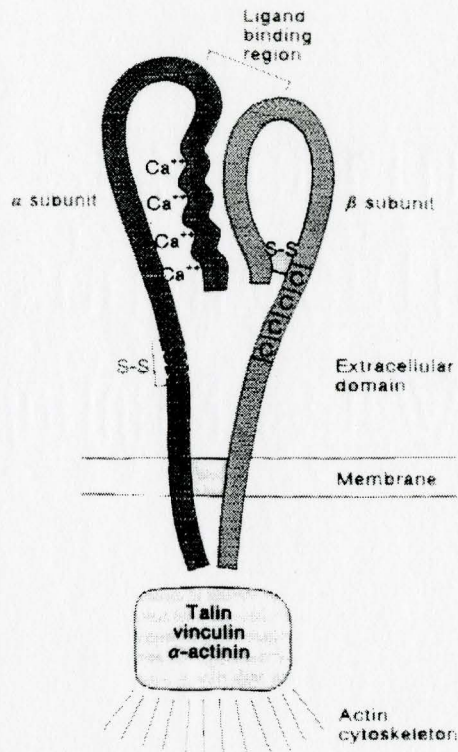


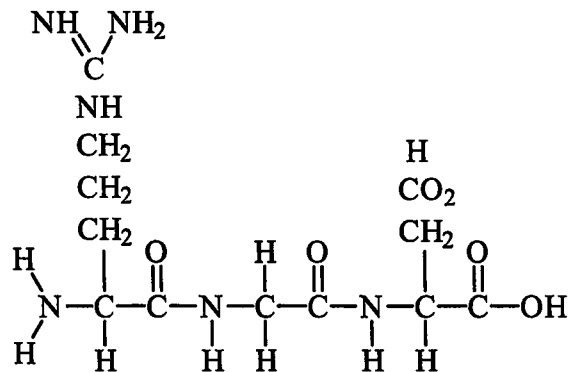
Figure 2.5 Schematic structure of a typical integrin. (Taken from Albelda *et al.*, 1990. [26])

2.3.2 Cell Adhesion Peptides

Peptides are short sequences of amino acids covalently linked together via peptide or amide bonds. In 1984, Pierschbacher and Ruoslahti demonstrated that the amino acid sequence, arginine-glycine-aspartic acid (RGD) is the minimal fragment of fibronectin needed to duplicate fibronectin's cell attachment activity [5]. Variants of this peptide have been found in other adhesive proteins: RGDV (where V is valine) in vitronectin, RGD_X (where X is a variant) in collagen type VI, RGDA (where A is alanine) in thrombospondin, RGDN (where N is asparagine) in laminin, and RGDS in fibrinogen and von Willebrand factor [6].

Surface immobilization of RGD-containing synthetic peptides has been shown to promote cell attachment in a manner similar to that of fibronectin [7], binding to the integrin with nearly the same affinity as the whole protein [6]. Therefore, this technique has been widely used to promote cell adhesion to biomaterial surfaces [4;10;27-30]. The amino acid sequence, arginine-glutamic acid-aspartic acid-valine (REDV), an additional adhesion sequence in fibronectin [31] has been reported to be the minimal active sequence within the CS5 site of the alternatively spliced type III connecting segment (III_{CS}) region of fibronectin [8]. Hubbell *et al.* [32] identified the integrin $\alpha_4\beta_1$ as the endothelial cell receptor for REDV, demonstrating that glass grafted with REDV exhibited a very high degree of selectivity for endothelial cells and that endothelial cells on immobilized REDV exhibited complete spreading. Furthermore, studies by Massia and Hubbell [8] showed that covalent immobilization of REDV-containing peptides resulted in surfaces that selectively supported the attachment and spreading of human vascular endothelial cells (HUVEC) over that of fibroblasts, vascular smooth muscle cells, and platelets.

a) RGD



b) REDV

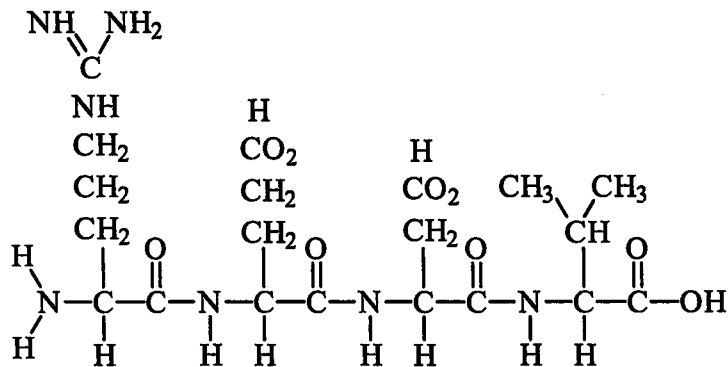


Figure 2.6 Structure of the peptides (a) Arginine-Glycine-Aspartic Acid (RGD), and (b) Arginine-Glutamic Acid-Aspartic Acid-Valine (REDV). The N-terminus refers to the α -amino group and the C-terminus refers to the α -carboxylic acid group.

2.3.3 Vitronectin

Though not commonly associated with the ECM, vitronectin is a multi-functional adhesive glycoprotein that plays key roles in regulating blood coagulation, complement activity and fibrinolytic pathways. More importantly in the current application, vitronectin has been shown in numerous studies with a

variety of different cell types and surfaces to be the primary plasma protein responsible for cell interactions with a biomaterial surface. cDNA sequencing of vitronectin revealed the presence of an RGD sequence. Site-directed mutagenesis studies in vitronectin revealed that the RGD sequence is necessary to promote adhesion and spreading of cells via integrins [33]. The integrins $\alpha_v\beta_3$, $\alpha_v\beta_5$, $\alpha_v\beta_1$ and $\alpha_{IIb}\beta_3$, are established receptors for vitronectin [34] with the classical vitronectin receptor, $\alpha_v\beta_3$, localized to focal adhesion sites, promoting cell spreading and migration on various RGD substrata [34]. Under non-reducing conditions, the molecular mass of vitronectin is 75 kDa by SDS-PAGE, whereas under reducing conditions, vitronectin is in a two-chain (10 kDa and 65 kDa) form [34]. In plasma, vitronectin circulates in both forms. In normal plasma, vitronectin is present at concentrations between 200 and 400 $\mu\text{g/ml}$ [35], accounting for 0.2-0.5% of total plasma proteins. Vitronectin is also found in seminal plasma, urine, amniotic fluid, cerebrospinal fluid, and bronchoalveolar lavage fluid [34]. The liver is the major site for the synthesis of plasma vitronectin. Unlike related proteins fibrinogen and fibronectin, vitronectin concentration in serum is not significantly different from that in plasma due to blood clotting [36]. A second form of vitronectin, accounting for approximately 0.8% of the circulating vitronectin pool [37], is found within platelets in a rapidly releasable form. This vitronectin is thought to be endocytosed from plasma and incorporated into the α -granules of the platelets [38]. Plasma vitronectin is monomeric and in a conformation that does not bind heparin or

glycosaminoglycans, whereas platelet vitronectin is in a multimeric, conformationally altered form that enables it to bind to the anticoagulant heparin [39].

The conformation of vitronectin is an important determinant in specifying biological functions. Treatment of vitronectin with denaturing agents such as urea results in expression of heparin binding activity otherwise present in only 1 to 2 percent of plasma molecules [40]. Altered immunoreactivity and heparin-binding properties were observed by Stockmann *et al.* [41] after vitronectin self-associated into multimers upon treatment with chaotropes, detergents, extreme pH or heat. Modifications of vitronectin conformation may therefore change its function from an anti- to a pro-fibrinolytic co-factor.

Vitronectin plays a role in regulating hemostasis due to its ability to bind heparin, plasminogen, plasminogen activator inhibitors, and thrombin-antithrombin III (TAT) complexes [42]. The initial phase of hemostasis depends on adhesion of cells such as platelets and endothelial cells to the extracellular matrix. Vitronectin has been found to bind to all types of collagen, particularly favouring the helical conformation of collagen [43]. It comprises a high-affinity binding domain for plasminogen activator inhibitor type 1 (PAI-1) which enables the protein to regulate fibrinolysis. Interaction between PAI-1 and vitronectin depends on the conformational state of both proteins. Active PAI-1 binds to urea-purified vitronectin (multimeric) with approximately a 6-fold higher affinity than to native (monomeric) vitronectin [44].

Vitronectin has also been shown to be a plasma protein adsorbed to biomaterials in contact with blood. Initial isolation of the protein resulted from its ability to adsorb to glass bead columns [45]. In cell culture media containing bovine or human serum, cell attachment is mediated by vitronectin and to a lesser extent by fibronectin, and is at least in part due to a 40-fold higher adsorption of vitronectin from plasma or serum to polystyrene copolymer beads compared to fibronectin [46]. Vitronectin has also been found adsorbed to ventriculoperitoneal shunts and temporary ventricular drainage catheters [47]. Collins *et al.* [48] studied the kinetics of platelet deposition onto coated polymeric tubing in canine *ex vivo* shunt model and found differences in response to adsorbed fibronectin and vitronectin. Vitronectin adsorbed more avidly than fibronectin to the various polymers, and vitronectin was most active at shorter blood contact times and promoted more fibrin deposition. The importance of vitronectin for *in vitro* cell adhesion has been well established in many studies with many cell types [49]. For instance, it was found that tissue culture polystyrene (vacuum plasma treated to create a hydrophilic surface with a net negative surface charge) supports good attachment of adherent endothelial cells whereas unmodified polystyrene does not, primarily due to the adsorption of greater amounts of vitronectin from the serum [50]. Though higher levels of fibronectin were also found adsorbed to the tissue culture polystyrene, the levels of fibronectin were not optimal for cell attachment. Likewise, the use of vitronectin-depleted serum with or without fibronectin included resulted in greatly

reduced *in vitro* attachment, spreading, and spatial distribution of bone-derived cells on chemically modified quartz surfaces [51]. Depletion of vitronectin from serum resulted in a nearly 90% reduction in total bone-derived cell area compared to media containing complete fetal bovine serum, while removal of fibronectin had no significant effect on adhesion, spreading, or spatial distribution.

2.4 BLOOD COMPATIBLE MATERIALS

2.4.1 Biomaterials

Biomaterials are natural or synthetic materials used to replace or augment part of a living system and include sutures, artificial heart valves, catheters, dialysers, pacemakers, and bone and joint replacements among others. Various materials, including polymers, metals, ceramics and other composites, may be used. Polymers are ideal candidates for use in many biological applications due to their strength, durability and flexibility. However, the occurrence of undesirable reactions at the interface between many polymeric materials and the biological environment, including coagulation and inflammatory responses, limits their widespread applicability.

2.4.2 Surface Modification for Modulating Protein Surface Interactions

Polymer surface modification to enhance blood compatibility while maintaining other essential properties [2] is commonly used to improve the

biocompatibility. Modification techniques include increasing hydrophobicity, chemical modification, attachment of anti-thrombotic agents, treatment of surfaces with protein, and biomembrane-mimetic surfaces [3].

To reduce protein adsorption and cell adhesion, surface modification with polyethylene oxide (PEO) or polyethylene glycol (PEG) is commonly used. PEG grafted onto a surface can reduce protein adsorption by forming a viscous, neutral, surface-bound layer that modifies the electrical nature of a surface exposed to an aqueous environment [52]. When a protein approaches a PEG-modified surface the conformational degrees of freedom for the polymer are reduced, and this, in turn, causes an entropic repulsion between the surface and the protein [52].

Modulation of the coagulation cascade through the attachment of an anti-coagulant such as heparin has also been used to improve blood compatibility of polymeric materials [53]. Heparin, a naturally occurring thrombin inhibitor, requires the presence of a cofactor (ATIII) limiting its long term usefulness [54]. However, upon overcoming these limitations, a heparin-immobilized surface has the potential to prevent platelet adhesion and complement activation. Sun *et al.* [55] modified gold-coated polyurethane surfaces with thrombin inhibiting peptides to generate thrombin-scavenging surfaces. Compared to the gold and cysteine-modified gold control surfaces, their peptide-modified surfaces adsorbed significantly more thrombin. Alternatively, surfaces have been modified to lyse a clot as it forms through manipulation of the enzymes in the fibrinolytic cascade.

McClung *et al.* [56] used lysine-modified polyurethane surfaces to activate plasminogen and lyse forming clots. The lysine-modified surfaces adsorbed plasminogen specifically in significant amounts (up to 1.2 $\mu\text{g}/\text{cm}^2$) in comparison to controls. Furthermore, the surfaces generated were shown to be able to lyse forming clots in an experimental system, suggesting that the system has significant potential for development.

While modulating protein interactions with the surfaces has significant potential for development of surfaces with good blood compatibility, it has been suggested [57] that conversion of Factor XI to XIa never drops to zero, suggesting that modulation of the proteins in the coagulation cascade may not completely eliminate surface thrombus formation. An alternative method of conferring blood compatibility involves mimicking the native physiology of the body through the generation of a vascular endothelial cell surface.

2.4.3 Endothelialization to Promote Blood Compatibility

One of the more promising approaches to produce blood compatible materials has been to mimic the body's natural physiology by modifying the surface to support the growth of a monolayer of endothelial cells. The end goal of this approach is to reduce blood material contact thereby improving blood compatibility and if possible to mimic the physiology of the *in vivo* layer, including both pro- and anti-coagulant properties. However, the potential for thrombus formation still exists. Some reports have indicated that the production of anti-

thrombogenic molecules such as tissue-type plasminogen activator by endothelial cells seeded onto prostheses is considerable lower than by endothelial cells on native arteries and veins [58], resulting in a decreased ability to dissolve thrombi. There have also been difficulties with cell adherence, cell coverage, and cell retention. Exposure of an endothelialized surface to physiologic shear stresses *in vivo* has been shown to result in cell losses of as much as 40 percent after one hour and more than 80 percent upon implantation *in vivo* for 24 hours [59].

2.4.4 Peptide Modification of Surfaces to Improve Cell Adhesion

To better promote initial cell attachment and to improve the long-term stability of the endothelialized surfaces, surface modification with cell adhesion peptides has been widely used. Massia *et al.* [27] demonstrated that covalently immobilized adhesion peptides (YIGSR and RGD) can promote attachment and spreading of endothelial cells to various materials independently of adsorbed adhesion proteins at very low peptide surface concentrations. Human umbilical vein endothelial cell (HUVEC) attachment to polytetrafluoroethylene was improved by both the coating of the surface with fibronectin and the grafting of RGD in a similar manner. However, proliferation (as measured by DNA activity per cell) was greater on the RGD-modified surface [60]. Peptides (GRGDSY and GRGDVY) grafted onto the backbone of polyurethanes enhanced HUVEC attachment and spreading [61].

Cell adhesion via peptide modification is advantageous over that of adsorption or covalent attachment of cell adhesion proteins for a number of reasons. The smaller peptides show considerably less immunogenicity and more specific surface attachment with one or two possible means for attachment. Furthermore, grafted ligands are more stable [6], and a peptide can be specifically designed for optimum interaction with cells.

Peptide orientation on a substrate may be a crucial determinant in cell binding. While various integrins recognize the RGD sequences in adhesive proteins, the specificity of recognition may be dependent on the conformation of the RGD sequence in the individual proteins [7]. Porte-Durrieu *et al.* [29], suggested that adsorption of attachment proteins may not promote long-term cell attachment *in vivo* due to difficulties in controlling the sequence presentation (C- or N-terminus binding). They believe that the use of small peptides would allow some control over the density and orientation of attached ligands. Duscl *et al.* [62] found a critical peptide concentration on their gold surfaces, where a decreased binding constant was measured at concentrations above this point and implied that above this concentration, peptides were presented in such a way that their antibodies had difficulty in approaching the peptides due to steric hindrance. Xiao and Truskey [63] found that immobilized cyclic RGD exhibited a greater affinity for endothelial cell attachment than did linear RGD. However, the importance of peptide orientation appears to be largely overlooked, and with

covalent attachment, the orientation is arbitrarily selected depending on the chemistry used for attachment.

2.5 GOLD-THIOL CHEMISTRY

2.5.1 Gold-Thiol Chemistry as a Surface Modification Technique

Gold, a relatively inert metal that does not readily oxidize and resists atmospheric contamination, strongly interacts with sulfur enabling the formation of monolayers in the presence of many other functional groups [9]. Moreover, self-assembled monolayers (SAMs) of alkanethiols on gold are stable in a variety of organic and aqueous media. Monolayers of alkanethiols on gold appear to be stable indefinitely in air or in contact with liquid water or ethanol at room temperature [9].

Figure 2.7 illustrates the chemisorption of alkanethiols on gold. The adsorbed thiolates are epitaxially located on the gold surface [64]. Upon contact with the gold, the alkanethiol loses a hydrogen atom to become a thiolate [65]. The sulfur atoms are located in the contiguous three-fold hollow sites on the gold surface. The energy of the bond between the organic thiolate and a gold surface is high (approximately 40-45 kcal/mol) [9] and desorption of organosulfur compounds from the surface is slow. However, the exact nature of the strong chemical bonds at the interface between the alkanethiolate chain and gold is still poorly understood at the molecular level. Bensebaa and colleagues [66], using x-ray photoelectron spectroscopy, detected a significant shift in the sulfur peaks

on thiolated gold colloids confirming a chemical reaction, but did not detect any significant difference between the Au 4f_{7/2} peak of the colloids and that of pure bulk samples of gold. They suggested that the metal atoms did not react, that the XPS features of reacted and unreacted gold were similar or, most likely, that the chemical state of gold atoms reacted with thiol groups similar to the unreacted state and that the Au 4f_{7/2} electron is not affected or is indistinguishably affected by the chemisorption process.

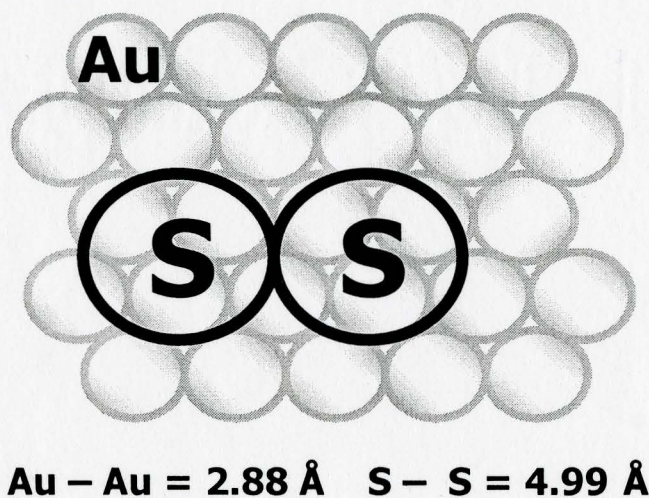


Figure 2.7 Schematic illustration of alkyl thiolate monolayer on Au(111). The sulfur atoms are located in the threefold contiguous hollow sites. The circles surrounding the sulfur atoms suggest the area occupied by the alkyl chain. (Adapted from Whitesides and Laibinis, 1990. [64])

2.5.2 Self-Assembled Monolayers on Gold Substrates

Self-assembled monolayers, (SAMs), are formed by the spontaneous association of molecules under equilibrium conditions into stable, structurally

well-defined aggregates joined by non-covalent bonds [67]. SAMs are the result of bonds weaker and less directional than covalent bonds, such as ionic bonds, hydrogen bonds, and van der Waals forces. Examples of SAMs include carboxylic acids on silver, aluminum or titanium, chloro- and alkoxy-silanes on aluminum, titanium, silicon, gold, silver, or copper, and sulfur-containing compounds on noble metals such as gold, silver, copper or platinum [65].

Dialkyl disulfides, RSSR, have been shown to form oriented monolayers on gold [68] resulting from cleavage of the disulfide bond upon contact with the gold surface [69]. The monolayer formed contains approximately equal proportions of the two different thiolate groups. In addition, it was found that chemisorption of long-chain alkanethiols, RSH, on gold also gives ordered, oriented monolayer films [9;70]. Further studies of SAMs prepared from dialkyl disulfides and alkanethiols chemisorbed onto gold suggests that organosulfur compounds coordinate to the surface as alkyl thiolates [71;72].

2.5.3 Gold-Thiol Surfaces In Biomedical Applications

Prime and Whitesides [73] suggest that a SAM is one of the best-defined model systems available for studying protein surface interactions. Lindblad *et al.* [74] evaluated the biological response induced by true methyl and hydroxyl surfaces by immobilizing alkane thiols onto gold given that surface properties, such as chemical functionality and hydrophobicity, influence specific events in the inflammatory cell response. Their *in vivo* results showed that the methylated

surface had the smallest amount of cells associated with that surface. However, in the fluid space around the implant, a higher number of inflammatory cells were present compared to that of the hydroxylated or gold surfaces. Bovine aortic endothelial cell (BAEC) growth on terminally functionalized, self-assembled monolayers of alkanethiolates on gold was studied by Tidwell *et al.* [75]. Growth varied significantly with surface functionality, increasing in the following order - $\text{CH}_2\text{OH} < -\text{CO}_2\text{CH}_3 < -\text{CH}_3 \ll -\text{CO}_2\text{H}$. However, cell growth was highest on the tissue culture polystyrene, suggesting that although these functional groups affected cell growth, they are not necessarily ideal for optimum cell growth.

While long chain alkanethiols form stable SAMs on gold, smaller molecules containing the thiol moiety, including L-cysteine can also interact with a gold surface to form a monolayer. Figure 2.8 illustrates the chemisorption of L-cysteine to gold. Using x-ray photoelectron spectroscopy, Uvdal *et al.* [76] detected two sulfur peaks, S 2p_{3/2} at 163.8 eV and S 2p_{1/2} at 164.9 eV, on cysteine-modified gold surfaces and suggest an organized double layer of cysteine formed on gold, where the second overlayer partly overlaps the first layer. Based on XPS and photolysis experiments, Kohli and colleagues [77] determined that multilayers are formed through covalent S—S bonds, and that the S—S bonds within the multilayers appear to “protect” the Au-S bond from oxidative attack.

Tengvall *et al.* [78] studied plasma interactions with gold surfaces modified with either L-cysteine or 3-mercaptopropionic acid. Though significant

differences in plasma protein adsorption were observed among the surfaces, no correlation between the patterns could be readily identified. They concluded that the surface biology in complex systems could be conveniently studied through a combination of systematic gold surface modifications, antisera techniques, and ellipsometry. Variations of this technique have since been used in a number of investigations. For instance, Tengvall *et al.* [79] studied complement activation on gold surfaces modified with 3-mercapto-1,2-propanediol. This technique was also used by Lestelius *et al.* [80] to examine plasma protein adsorption and initiation of the coagulation cascade on gold surfaces modified with 3-mercaptopropionic acid, L-cysteine or glutathione. Protein adsorption and platelet activation [81], as well as initial inflammatory cell-surface reactions [82], have been studied using gold surfaces.

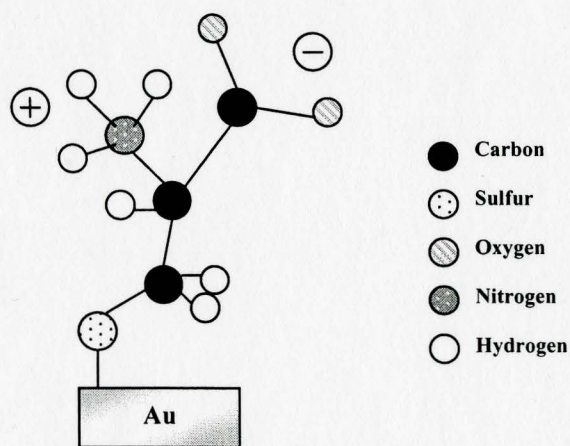


Figure 2.8 Schematic model of L-Cysteine on a gold surface. (Adapted from Tengvall *et al.*, 1992. [78])

Boncheva and Vogel [83] looked at controlling molecular conformation and orientation of polypeptide monolayers on gold surfaces using amphipathic and hydrophobic polypeptide helices. They found that transferring peptides of a stable helical molecular conformation to a surface without altering that conformation was achievable. Parameters that they believe key in controlling molecular conformation as well as orientation include the type of interface, the specific peptide interactions with the support, the amino acid sequence, and the method of layer formation. Moreover, the amino acid sequence of the peptide is particularly important since the orientation of the polypeptide monolayers could simply be controlled via placement of an N- or C-terminal cysteine.

Gold surfaces have also been modified with cell adhesion peptides to improve cell attachment to artificial surfaces. Saneinejad and Shoichet [11] modified gold-patterned glass surfaces with polyethylene glycol (PEG), and then C-cysteine terminated peptides CGYIGSR, CGRGDS, and CSIKVAV, for purposes of attaching hippocampal neurons. The PEG-modified regions of the surfaces promoted neither neuron adherence nor outgrowth. Cell adhesion and neurite outgrowth was greatly enhanced on the peptide-modified gold regions of the surfaces, although the differences among the specific peptides were indistinguishable. Zhang *et al.* [84], using microcontact printing and gold surfaces modified with cysteine-containing peptides, studied cell pattern formation. They designed two peptides having the ligand RADS at the N-terminus with either three or five alanine linkers between the ligand and a C-

terminal cysteine. Several days after seeding the surfaces with various cell types (mouse fibroblast 3T3 cells, human epidermoid carcinoma cells and bovine aortic endothelial cells), recognizable cell patterns were identified. They concluded that this technique is a simple procedure for studying and controlling cell pattern formation. Ferris *et al.* [10] modified gold-coated titanium rods with RGDC and implanted in rat femurs to stimulate increased bone formation *in vivo*. McMillan *et al.* [12] modified gold-coated polyurethanes with the linear peptides, CRGD and CREDV, as well as with the cyclic peptide, CCRRGDWLC, to promote attachment of human vascular endothelial cells and mouse 3T3 fibroblasts. Attachment was appreciably enhanced on the peptide-modified surfaces as compared to the gold and cysteine-modified control surfaces. In particular, endothelial cell attachment was greatest on the surfaces modified with the cyclic peptide, while the 3T3 fibroblasts adhered best to the CREDV-modified surfaces. The preference of the endothelial cells for the RGD-containing cyclic peptide over the linear RGD peptide provides evidence for the importance of peptide orientation in cell-surface interactions.

2.6 CHARACTERIZATION TECHNIQUES

2.6.1 Water Contact Angles

Contact angle measurements provide a convenient probe of the hydrophilicity or hydrophobicity of a surface based on differences in surface energy [64]. The useful characteristics of contact angles include their sensitivity towards polarity of the functional groups on a surface, their ability to detect ionizable functionality, their sensitivity to the local details of the structure at the solid-liquid interface. In addition, the instruments used are straightforward and relatively inexpensive [64].

The most common approach for measuring contact angles is the sessile drop technique. The angle formed between a drop of liquid (often water) and a surface is measured, with this angle providing an indication of the relative hydrophobicity of the surface. Figure 2.9 depicts the setup of the sessile drop technique. Both advancing and receding contact angles can be measured (Figure 2.10). The difference between the measurements is referred to as contact angle hysteresis, and corresponds to the heterogeneity of the surface [19], with a more heterogeneous surface typically yielding greater hysteresis.

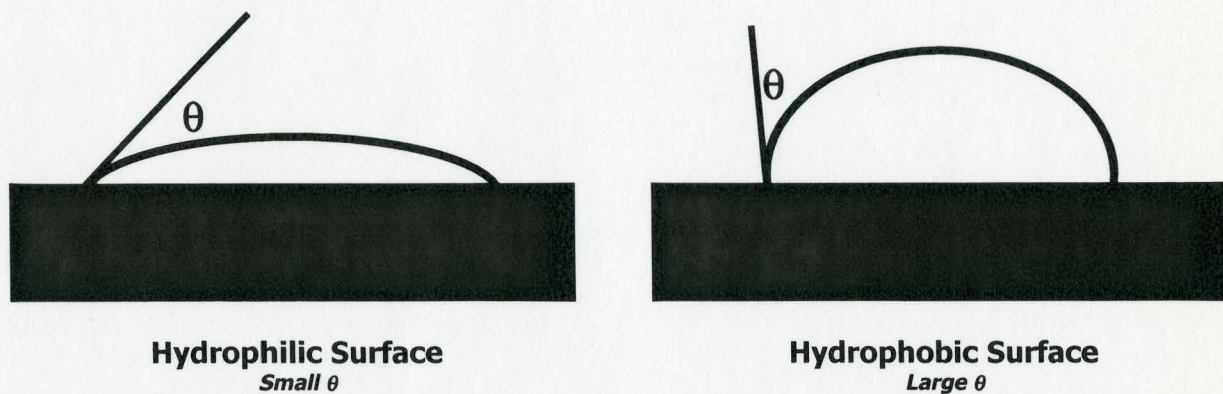


Figure 2.9 Schematic illustration of contact angles on hydrophilic and hydrophobic surfaces. (Adapted from Whitesides and Laibinis, 1990. [64])

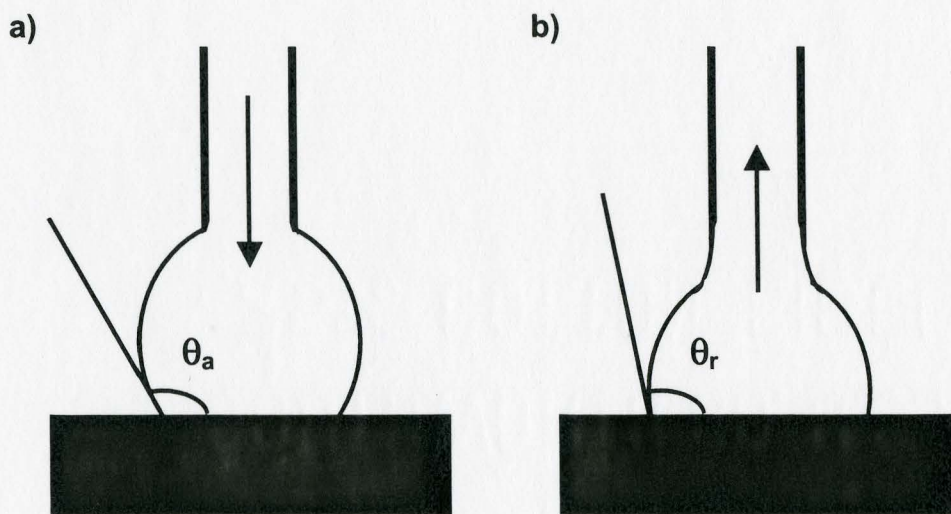


Figure 2.10 Advancing (θ_a) and receding (θ_r) contact angles as measured by the sessile drop method. (Adapted from Lestelius, 1996. [19])

3.2.3 X-Ray Photoelectron Spectroscopy

X-ray photoelectron spectroscopy (XPS) is a surface analysis technique used to determine the elemental composition of the outermost atomic layers of a surface. Both the elemental composition (low resolution) and their bond configurations (high resolution) can be determined. Upon passing x-ray photons through a surface, the electrons become excited. Electrons close to the surface are ejected, and the energy of the emitted photoelectrons is analyzed by an electron spectrophotometer that measures the kinetic energy (E_K) of the electron. From the known photon energy ($h\nu$), the binding energy (E_B) of the electron, which specifically identifies which specifically identifies the electron, and is calculated using the following equation (1) [85]:

$$E_B = h\nu - E_K \quad (1)$$

The surface specificity of this technique comes from the fact that only electrons from a maximum depth of approximately 100Å can escape the material and reach the detector as described by the Beer-Lambert equation (2):

$$I = I_o \exp(-d / \lambda \sin \theta) \quad (2)$$

where I is the intensity of the electrons from depth d , I_o is the intensity from an infinitely thick substrate, θ is the electron take-off angle, and λ is the electron inelastic mean free path [86].

3.2.3 SCANNING ELECTRON MICROSCOPY

Scanning electron microscopy (SEM) is used to probe the topography and composition of a surface. It can also detect potential distributions, subsurface conductivity, surface luminescence, surface composition and crystallography [87]. The scanning electron microscope scans the surface of a specimen with a beam of electrons synchronously with an electron beam in a cathode ray tube [88]. The intensity of the beam in the cathode ray tube is modulated by the signals produced by the probe-specimen interaction. The intensity of the cathode-ray tube is modulated by the signals recorded to form an image. Electron optical systems such as the SEM have much greater resolution and depth of field than light optical systems and can resolve topographical details of less than 50 Å with a depth of focus 500 times that of an optical microscope with equivalent magnifications [87].

3.2.3 SDS-POLYACRYLAMIDE GEL ELECTROPHORESIS

Electrophoresis measures the migration of a charged particle under the influence of an electric field. Gel electrophoresis is a common technique used to separate proteins. In polyacrylamide gel electrophoresis (PAGE), a polyacrylamide gel provides a supporting medium to minimize convection currents and diffusion so that the separated components remain as sharp zones with maximum resolution [89]. The gel consists of polymerized acrylamide monomers cross-linked with a co-monomer, usually N,N'-methylene-bis-

acrylamide (or Bis). The average polymer chain length is determined by the acrylamide concentration, and the extent of cross-linking is determined by the concentration of Bis.

When PAGE is used in conjunction with the detergent sodium dodecylsulphate (SDS), protein separation is based solely on molecular weight and not the charge of the molecule. SDS binds to the proteins in large amounts (up to 1.4g SDS per gram of protein) [90], which masks the intrinsic charges of the protein so that the net charge per unit mass becomes approximately constant. Electrophoresis then becomes proportional only to the molecular weight of the protein. Staining reveals bands corresponding to specific molecular weights. When coupled with an immunological assay (Western blotting), this technique can be used to detect specific proteins and the molecular weight distribution of the proteins.

2.7 PROJECT RATIONALE

Protein adsorption to blood-contacting materials promotes a series of undesirable blood-biomaterial interactions that include platelet adhesion, thrombus formation and inflammation. Since polymers still remain desirable for use in biological applications, various surface modification techniques can improve blood compatibility while maintaining the essential properties of the polymer. Modifying the surface to support the growth of a monolayer of endothelial cells is an attempt to mimic vascular physiology. With this approach,

blood compatibility can be improved both by reducing blood-surface contact and by exploiting the properties of the endothelial cells themselves.

Modifying a surface with cell adhesion peptides can be used to improve the adhesion of cells to the surface. Gold surfaces offer a convenient method for peptide surface modification. It is hypothesized that the orientation of the peptide on a surface, via N- or C-terminal cysteine, will affect both its surface and biological properties, and thus, cell adhesion. Peptides that contain cysteine will readily react with a gold surface via the thiol group. Peptide orientation can simply be controlled by placement of the cysteine in the peptide sequence. Peptide orientation, seemingly chosen arbitrarily or by chemistry in many studies, may prove to be an important factor in determining the effectiveness of endothelialization of an artificial surface, as well as its interactions with the biological milieu.

3. EXPERIMENTAL PROCEDURES

3.1 SURFACE PREPARATION AND MODIFICATION

3.1.1 Polyurethane Synthesis

Polyurethanes were prepared based on the method of Santerre *et al.* [91]. Polytetramethylene oxide (PTMO), with a molecular weight of 650, was degassed under vacuum for at least 4 h prior to polyurethane synthesis. The reactants, PTMO, 4,4'-methylene-di-p-phenyl diisocyanate (MDI), and ethylene diamine (ED), were all dissolved in anhydrous dimethyl sulfoxide (DMSO) in a 5% w/v ratio during the reaction. Though MDI could be distilled prior to use, it was instead aliquotted into smaller quantities, placed in sealed containers, and kept dry and cold to minimize reaction with water. Similarly, although adding some dry sodium hydroxide pellets prior to use will dehydrate ED, it was deemed unnecessary.

The prepolymer was prepared by reacting MDI with PTMO in a 2:1 molar ratio in a dry nitrogen environment. The MDI solution was added to the reaction vessel and heated to 90°C. The PTMO solution was then added to the reaction vessel dropwise over a period of approximately 20 min. The prepolymer reaction then proceeded for an additional 90 min. The temperature was subsequently reduced to 45°C and the prepolymer was reacted with ED in 1:1 stoichiometry to

yield polyurethane. The ED solution was added to the reactor dropwise over a period of 10 min and the chain extension reaction proceeded for 30 min. The polymer was precipitated in water, extensively rinsed and dried under vacuum prior to use. The reaction yield for each of the batches was determined based on the mass of polyurethane produced and the total mass of the reagents used.

3.2.3 Polyurethane Film Casting

Polyurethane films were prepared from a 5% (w/v) solution of the polymer in dimethylformamide (DMF). The solutions were poured into a clean glass dish and placed covered in an air oven at 60°C for five days. The resultant films were approximately 5 mm thick. Prior to subsequent use, the films were dried under vacuum at 60°C and thoroughly rinsed with methanol.

3.2.3 Gold Coating of Polyurethane Films

Gold coating of the polyurethane films were performed by Dr. M. Sayer (Queen's University, Kingston, ON). Gold was coated directly onto both sides of the polyurethane to a thickness of approximately 1000 Å via vacuum (5×10^{-6} Torr) evaporation with an Edward's Auto 306 Coating System.

3.2.3 Peptide Chemisorption

Circular disks (6 or 12 mm diameter) were punched from the gold-coated polyurethane films. The surfaces and all glassware were cleaned in a solution

consisting of 5 parts distilled water, 1 part ammonium hydroxide and 1 part hydrogen peroxide (TL1) for 10 min at 85°C. Following cleaning, all surfaces and glassware were thoroughly rinsed with MilliQ water.

The synthetic cell adhesion peptides chosen for this study, CRGD, RGDC, CREDV, and REDVC, were synthesized by the Peptide Synthesis Laboratory (Queen's University, Kingston, ON). Peptides were purified by high performance liquid chromatography (HPLC) and their purity determined by mass spectroscopy. Chromatograms are included in Appendix B.

The maximum density of gold atoms on a smooth 111 gold surface is 10×10^{18} atoms/m². Therefore, assuming that the gold coating on the polymer surfaces was of a 111 orientation, this corresponds to a maximum of 5.65×10^{12} atoms of gold and 9.4×10^{-12} moles of gold on a two sided 6 mm diameter disk. While surface roughness may increase this number, the orientation of the gold on these surfaces is not of 111 orientation, and it is expected that this provides a reasonable estimate of the maximum possible number of sites for reaction with the peptide. Assuming that the reaction between the gold and the sulfur in the peptides occurs in the contiguous threefold hollows between the gold atoms, 5×10^{-10} moles of peptide is required for each 6mm diameter surface. The amounts of peptide used in these studies (10 mL of 2 mM peptide solution for 12 surfaces) are well above this minimum and it is therefore assumed that the amount of peptide present is not limiting.

For every chemisorption, peptide solutions in water were freshly prepared. The solutions were placed in separate glass beakers. In all studies MilliQ water served as a negative control, while chemisorption from a 2 mM solution of *L*-cysteine served as a positive control. Surfaces were placed in the solutions and were incubated with mild agitation for 24 h at room temperature. After chemisorption, the surfaces were extensively rinsed with MilliQ water. Characterization of the modified surfaces was performed immediately after chemisorption if possible. Otherwise the surfaces were stored in stoppered vials prior to analysis.

3.2 SURFACE CHARACTERIZATION

3.2.3 Water Contact Angles

Both advancing and receding sessile drop contact angles were measured on 12 mm diameter unmodified and peptide modified gold-coated polyurethanes. Following chemisorption, the surfaces were allowed to air dry. Using a goniometer (Model 100-00115, Rame-hart, Inc., Mountain Lakes NJ), a drop of distilled water was placed on the surface. Advancing and receding contact angles were measured taken for each side of the drop and an average angle was determined using multiple measurements ($n > 6$).

3.2.3 X-ray Photoelectron Spectroscopy

XPS was used to determine the elemental composition of both the unmodified and the peptide-modified gold-coated polyurethane surfaces. Take-off angles of 90° and 30° were used to probe the surface depth. Analyses were performed by the ICPET at the National Research Council of Canada. A Kratos AXIS HS X-ray photoelectron spectrophotometer was used for the analysis. The size of the analyzed area was approximately 1 mm². Monochromatized Al K radiation was used for excitation and a 180° hemispherical analyzer with a three-channel detector was employed. The X-ray gun was operated at 15kV and 20mA. The spectrophotometer was operated in Fixed Analyzer Transmission mode (FAT) throughout the study using electrostatic magnification. Survey and high-resolution spectra were collected using 160 and 20 eV pass energy respectively. The pressure in the analyzer chamber was 10⁻⁸ to 10⁻⁹ torr. An electron flood gun was used to neutralize the charge during the experiment. In order to verify that the surfaces were not damaged during angle dependent studies, the surfaces were scanned at the 90° (non-surface specific) take-off angle both before and after the angle dependence measurements. Binding energies were referenced to the hydrocarbon C1s binding energy set to 285 eV. Atomic composition was estimated using standard software provided with the instrument and using the following sensitivity factors: 0.25 for C1s, 0.66 for O1s and 0.42 for N1s relative to F1s at 1.00. Low resolution spectra, as well as high

resolution spectra for gold, carbon, nitrogen and sulfur, were obtained for each of the surfaces.

3.2.3 Scanning Electron Microscopy

SEM was used to determine the surface morphology of both the unmodified and modified surfaces by ICPET at the National Research Council of Canada. Images with magnifications of 2000 and 5000 were obtained.

3.3 PROTEIN ADSORPTION STUDIES

3.3.1 Protein Adsorption from Plasma

Twelve 6 mm diameter gold surfaces were modified via chemisorption with each of the peptides. Following chemisorption, and an extensive water rinse, the surfaces were equilibrated by incubation in 10 mL of phosphate buffered saline (PBS) (pH 7.4) for 1 h with mild agitation at room temperature. Preparation of PBS is shown in Appendix C. The surfaces were then placed in individual wells of a 96-well microtitre plate, and incubated in 300 μ L of pooled normal adult plasma for 2 h at room temperature. Each of the surfaces was subsequently rinsed (3 x 10 min) in 300 μ L PBS. The 12 surfaces for each modification were placed in a single vial and incubated with 300 μ L of 2% sodium dodecyl sulphate (SDS) overnight at room temperature to remove the adsorbed protein. The eluate was removed and stored at -70°C until further use.

3.3.2 Total Protein Assay

Total protein adsorption was determined based on bovine serum albumin standards using Bio-Rad Detergent Compatible total protein microassay for protein concentrations ranging from 5-250 $\mu\text{g}/\text{mL}$ protein using the eluates obtained following protein adsorption from 100% plasma. The assay is a colourmetric assay involving a reaction between an alkaline copper tartrate solution and Folin reagent [92]. The amino acids tyrosine and tryptophan, and to a lesser extent, cystine, cysteine, and histidine, are responsible for colour development [93]. Calibration was based on concentration variation of BSA in 2% SDS. 20 μL of either a standard or a sample was added to a well of a 96-well microtitre plate with all standards and samples run in at least triplicate. Reagent A' was prepared by adding 20 μL of Reagent S (sodium dodecyl sulfate) to each mL of Reagent A (sodium hydroxide) needed. Colour was generated by reacting the protein with 10 μL Reagent A' and 80 μL of Reagent B (Folin reagent) for 15 min as described in the assay. Absorbances were read in a microplate reader at 690 nm. Protein concentration was determined from the calibration.

3.3.3 SDS-Polyacrylamide Gel Electrophoresis

Reduced sodium dodecyl sulfate polyacrylamide gel electrophoresis (SDS-PAGE) was performed on the eluted proteins obtained following protein adsorption from 100% plasma. The detailed SDS-PAGE and Immunoblot procedure is described in Appendix D.

A 12% separating gel solution was prepared and poured into the casting assembly and the gel was allowed to polymerize for 1 h. Subsequently, a 4% stacking gel was prepared and added. An appropriate comb was added and the gel polymerized for another hour. Samples to be loaded onto the gel were then prepared as described in the Appendix. Loadings were such that equal amounts of protein (based on the total protein assay) were loaded onto the gel. Electrophoresis proceeded using a potential difference of 200 V for approximately 1 h. The gels were removed from the electrophoresis assembly and transferred to immobilon (PVDF) membranes using a potential difference of 100V (200 mA) applied for 1 h. The membranes were then stained with colloidal gold or dried and used for immunoblot analysis.

3.3.4 Immunoblotting

Immunoblotting was used to determine specific protein adsorption patterns and the details are described in Appendix D. The sections of the membrane containing the low molecular weight and the prestained molecular weight marker lanes were removed and stained by incubating in Protogold solution (Cedarlane Lab Ltd., Hornby ON) for 1 to 4 h. The remainder of the membrane was cut into 3 mm strips. To block unbound membrane sites and prevent non-specific binding, the strips were incubated for in 5% (w/v) dry skim milk in TBS, pH 7.4 with gentle agitation. The preparation of TBS is shown in Appendix C. Each strip was then incubated in 1% (w/v) dry skim milk and 0.05% (v/v) Tween 20 in

TBS with a 1/1000 dilution of the primary antibody (Table 3.1) to the protein of interest. Strips were then incubated for one h in a 1/1000 dilution of the alkaline phosphatase-linked secondary antibody (Table 3.2). Colour generation, indicative of the presence of the protein of interest was effected by incubation for up to 20 min in the chromogenic substrate solution (see Appendix). The colour reaction ceased upon extensive rinsing with distilled water. The strips were then allowed to air dry.

Table 3.1 Polyclonal antibodies to human proteins in the form of fractionated antisera (IgG fractions) developed in goat, sheep, or rabbit.

PROTEIN	HOST	SUPPLIER
Factor XI	Goat	Cedarlane Lab. Ltd., Hornby, ON
Factor XII	Goat	Cedarlane Lab. Ltd., Hornby, ON
Prekallikrein	Goat	Cedarlane Lab. Ltd., Hornby, ON
HMWK	Goat	Cedarlane Lab. Ltd., Hornby, ON
Fibrinogen	Goat	Cedarlane Lab. Ltd., Hornby, ON
Plasminogen	Goat	Sigma, St. Louis, MO
ATIII	Sheep	Cedarlane Lab. Ltd., Hornby, ON
C3	Goat	Cedarlane Lab. Ltd., Hornby, ON
Transferrin	Goat	Sigma, St. Louis, MO
Alpha-1-antitrypsin	Goat	Enzyme Research Laboratories, Inc., South Bend, IN
Fibronectin	Rabbit	Calbiochem, Bering Diagnostic, La Jolla, CA
Albumin	Goat	Cedarlane Lab. Ltd., Hornby, ON
IgG	Goat	Sigma, St. Louis, MO
Beta-lipoprotein	Goat	Sigma, St. Louis, MO
Alpha-2-macro	Rabbit	Sigma, St. Louis, MO
Vitronectin	Sheep	Cedarlane Lab. Ltd., Hornby, ON
Protein C	Goat	Cedarlane Lab. Ltd., Hornby, ON
Prothrombin	Sheep	Cedarlane Lab. Ltd., Hornby, ON
Haemoglobin	Rabbit	Sigma, St. Louis, MO
Factor B	Goat	Calbiochem, Bering Diagnostic, La Jolla, CA
Factor H	Goat	Calbiochem, Bering Diagnostic, La Jolla, CA
Factor I	Goat	Calbiochem, Bering Diagnostic, La Jolla, CA
Protein S	Sheep	Cedarlane Lab. Ltd., Hornby, ON
Apolipoprotein A1	Goat	Chemicon International Inc., Temecula, CA

Table 3.2 Affinity purified alkaline phosphatase conjugated secondary antibodies.

SECONDARY ANTIBODY	SOURCE
Rabbit Anti Goat IgG Alkaline Phosphatase Conjugate	Sigma Chemical Co., St. Louis, MO
Rabbit Anti Sheep IgG Alkaline Phosphatase Conjugate	Bethyl Laboratories Inc., Montgomery, TX
Goat Anti Rabbit IgG Alkaline Phosphatase Conjugate	Bio-Rad Laboratories, Hercules, CA

3.3.5 Vitronectin Adsorption and Immunoblotting

Human vitronectin, purified from human plasma by immuno-affinity and affinity chromatography (Enzyme Research Laboratories, South Bend IN) (1.0 mg/ml in a buffer consisting of 50 mM Tris-HCl, 0.25 M NaCl, pH 7.3) was used in all studies. Urea was not used in any purification step and thus the vitronectin was primarily monomeric (as determined by SDS-PAGE) and had approximately 10 x the biological activity of urea treated vitronectin.

3.3.5.1 ¹²⁵I Labeled Vitronectin Adsorption to Modified Surfaces

Vitronectin adsorption studies were performed on the gold, cysteine- and synthetic peptide-modified surfaces. Vitronectin was labeled with ¹²⁵I using the iodogen method. 100 μL of vitronectin and 0.5 mCi of ¹²⁵I was added to a glass reaction vial precoated with iodogen iodinating reagent, and the reaction proceeded for 15 min. The labeled vitronectin was then removed from the vial and dialyzed overnight with two changes of PBS buffer and one buffer change to PBS buffer containing a small amount of nonradioactive iodine (PBS-Nal) (Appendix C) to remove unreacted iodine using a Slide-A-Lyzer Dialysis Cassette

(3.0 mL capacity, 10000 MW cutoff) (Pierce Chemical Company, Rockford, IL). The free radioactive iodide concentration was determined by trichloroacetic acid precipitation of the protein (details of this procedure are presented in Appendix E).

3.3.5.2 Vitronectin Adsorption from Plasma

Labeled (30%) vitronectin was added to normal pooled plasma based on an average vitronectin concentration of 300 $\mu\text{L}/\text{mL}$ of plasma. Sheardown *et al.* [94] showed that interaction of the free iodide with the gold surface can lead to significant overestimation of protein adsorption. Du *et al.* [95] found that by adding small amounts of nonradioactive iodide to the protein solution effectively suppresses the binding of $^{125}\text{I}^-$ ion (present in trace amounts relative to nonradioactive iodide) to the gold surface. Thus, in order to reduce the error associated with the interactions of gold and free iodide, the surfaces were pre-incubated with PBS-Nal for 1 h. Furthermore, plasma was diluted with PBS-Nal to yield solutions of 1, 2, 5 and 10% of normal plasma strength. The surfaces were incubated in 300 μL of the plasma solutions for 2 h at room temperature within a 96-well plate, and subsequently rinsed 3 times for 10 min each in 300 μL of PBS-Nal. The surfaces were counted for radiation using a gamma counter and the vitronectin adsorption was assessed by the following equation (3):

$$\text{Adsorbed Vitronectin} = \frac{(CPM_1 \times C_{Vn} \times V)}{(Area \times CPM_2)} \quad (3)$$

where CPM_1 is the radioactivity of the surface in counts per minute [cpm], C_{Vn} is the concentration of vitronectin in plasma [$\mu\text{g/mL}$], V is the volume of the reference vitronectin solution [mL], $Area$ is the total surface area of the gold coated polyurethane disk [mm^2], and CPM_2 is the radioactivity of the reference vitronectin solution [cpm].

3.3.5.3 Vitronectin Immunoblot

SDS-PAGE and immunoblots were performed in order to probe specifically for vitronectin in the eluates obtained following protein adsorption from plasma. The procedure was the same as that described previously (sections 3.3.3 and 3.3.4) except that a 9% separating gel and a 10-well comb were utilized in order to compare different samples on the same immunoblot. Each lane was loaded with approximately 200 μg of protein as determined by a total protein microassay in order to probe for vitronectin specific differences.

3.4 IN VITRO CELL ATTACHMENT STUDIES

3.4.1 Cell Reagents, Maintenance and Subculture

The cell type ECV304, considered until recently to be an immortalized endothelial cell line [96], was used for all of the cell attachment studies. ECV304 cells were grown in Medium 199 supplemented with heat activated 10% fetal

bovine serum and penicillin-streptomycin. All reagents were warmed to 37°C in a water bath prior to use. To maintain the cells, the media was replaced two to three times a week. Upon reaching confluence, the cells were subcultured by trypsinization. Once detachment was visualized microscopically, 5 to 10 mL of fresh media was added to the flask to inhibit trypsinization, the cells were resuspended, divided into 3 equal volumes, and added to new flasks. Media was added to each flask to replenish the volume.

3.4.2 Cell Attachment Assay

Endothelial cell attachment studies were performed on 12 mm diameter modified surfaces sterilized by incubation in 70% ethanol for 30 min, and a subsequent 30 min of UV exposure. The surfaces were placed in a 24-well tissue culture plate and were held in place by sterile stainless steel washers. ECV 304 cells were removed from confluent flasks by trypsinization, and replated into wells containing the surfaces. Studies were carried out in both serum-free and serum-containing (10% FCS) medium to assess the effects of adsorbed proteins. The effect of vitronectin was further examined by using protein-containing media containing either anti-vitronectin or non-immune IgG in molar excess.

Approximately 100000 endothelial cells, as determined by a Coulter Counter® Z1 Series Particle Counter counting particle sizes between 5 and 18.66 μm , were seeded onto each of the surfaces and the surfaces incubated for

4 h at 37°C. Following incubation, loosely adherent cells were removed by dip rinsing in PBS and the surfaces were placed in individual Coulter Counter vials. The attached cells were removed by adding 200 μ L trypsin to each vial. Once the cells were removed, 10 mL IsoFlow™ Sheath Isotonic Fluid was added to each vial. The surfaces were removed from the vials and the number of cells was counted using the Coulter Counter.

The Coulter Counter uses displacement as a measure of volume to measure changes in the electrical resistance produced by nonconductive particles suspended in an electrolyte [97]. In the sensing zone, each particle displaces its own volume of electrolyte and this, in turn, changes the electrical resistance to the current flowing through the orifice [89]. The volume displaced is measured as a voltage pulse, and the height of each pulse is proportional to particle volume.

4. RESULTS

4.1 SURFACE PREPARATION AND MODIFICATION

4.1.1 Polyurethane Synthesis

In this study, a polyurethane urea was used as the substrate for the gold layer. The polyurethanes were prepared in a batch reaction [91] using polytetramethylene oxide (PTMO), methylenedi-p-phenyl diisocyanate (MDI) and ethylene diamine (ED) in a 1:2:1 mole ratio. Numerous batches were prepared to generate adequate polymer for the experiments. Reaction yields ranged between 92 and 98%, with losses likely the result of small amounts of polymer remaining the reaction vessel as well as resulting from the filtration and wash steps.

4.1.2 Gold Evaporation on Polyurethane Films

In order to improve the adhesion of gold to a smooth surface, a thin layer of chromium or titanium often precedes the deposition of a gold layer [98]. However, in the case of a polyurethane surface, the surface is rough enough to allow deposition of gold using evaporative methods without the intermediate layer. A loss of gold from the polyurethane surface was noted in some experiments, mainly as a result of surface manipulation. Improved handling

techniques significantly reduced gold loss. Significant losses were also observed following the 24 hour incubation in either water or cysteine. Incubation with peptides did not usually result in loss of the gold layer, suggesting that the peptide may actually be protecting the underlying gold surface. Similarly, only the unmodified surfaces sustained significant losses of gold following incubation in phosphate buffered saline containing sodium iodide. Though an intermediate layer of titanium or chromium is not needed in order for gold to adhere to the polyurethane, such a layer may improve gold retention during such manipulations. Nevertheless, losses were generally estimated to be less than 5% of the total surface area.

4.1.3 Cleaning Gold Coated Polyurethanes

In order to remove surface contaminants prior to peptide chemisorption, the surfaces were cleaned with a heated ammonium hydroxide hydrogen peroxide solution. No significant loss of gold was observed during the cleaning process. However, following cleaning, cracking on the surfaces could be detected macroscopically, the likely cause of which is the swelling of the base polyurethane during the cleaning process, which swells between 2 to 5% in water at room temperature [99].

4.2 SURFACE CHARACTERIZATION

4.2.1 Water Contact Angles

Figure 4.1 shows sessile drop advancing and receding water contact angle results for unmodified, cysteine-modified, and peptide-modified gold-coated surfaces. On the unmodified gold surface, the average advancing and receding angles were 51.5° and 29.75° respectively. These results compare well to those of Sun *et al.* [98] and McMillan *et al.* [12], but are not likely representative of a pure gold surface due to the contamination that occurs following atmospheric exposure [9].

The cysteine-modified surfaces were slightly more hydrophilic than the gold, with the advancing angle decreasing to 40.5° . Statistically significant increases ($\alpha=0.05$) in the advancing angle to between 56.7 and 59.3° were noted following modification with the peptides, suggesting differences in the surfaces. No substantial differences were noted among the different peptide-modified surfaces, as would be expected because contact angle measurements are not likely sensitive enough to detect differences due to peptide orientation since the overall surface chemistry of the peptide-modified surfaces would be similar. Receding contact angles also showed significant differences between the unmodified and peptide-modified surfaces. The receding angle increased from 29.8° on the unmodified surface and 31.7° on the cysteine-modified surface to an average of 44.5° on the peptide-modified surfaces, again illustrating a change in

surface chemistry. Again, there were no notable differences among the receding contact angles for the peptide-modified surfaces.

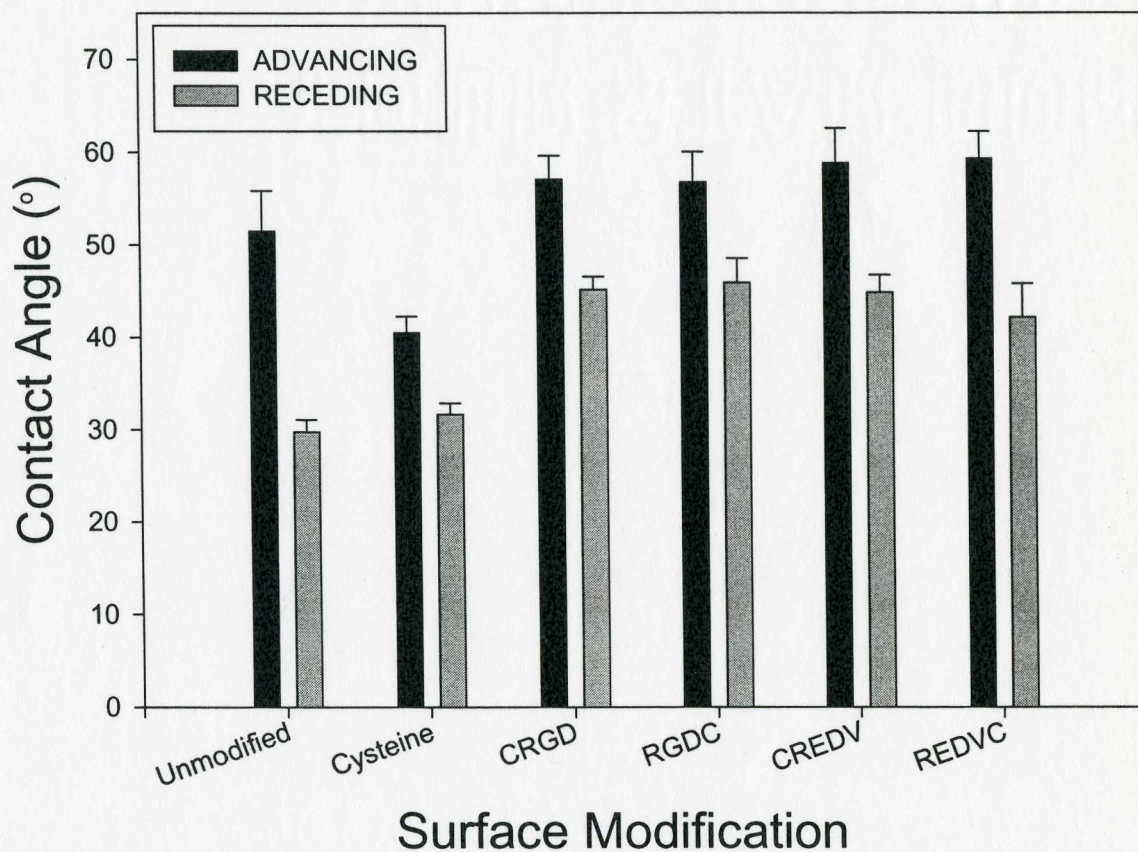


Figure 4.1 Advancing and receding sessile drop water contact angles for the unmodified and peptide-modified surfaces. Error bars represent 1 standard deviation ($n > 6$).

4.2.2 Scanning Electron Microscopy

The SEM images for the unmodified but washed and peptide-modified surfaces are compared in Figures 4.2 and 4.3. A high level of surface cracking is noted on both the unmodified and peptide-modified surfaces. This provides further evidence that the cracking is likely the result of polymer swelling during the wash and chemisorption procedures and it not due to imperfections in the gold layer. Differences between the different modifications were not apparent. Small imperfections, represented by dark areas in the images, can also be seen on the surfaces.

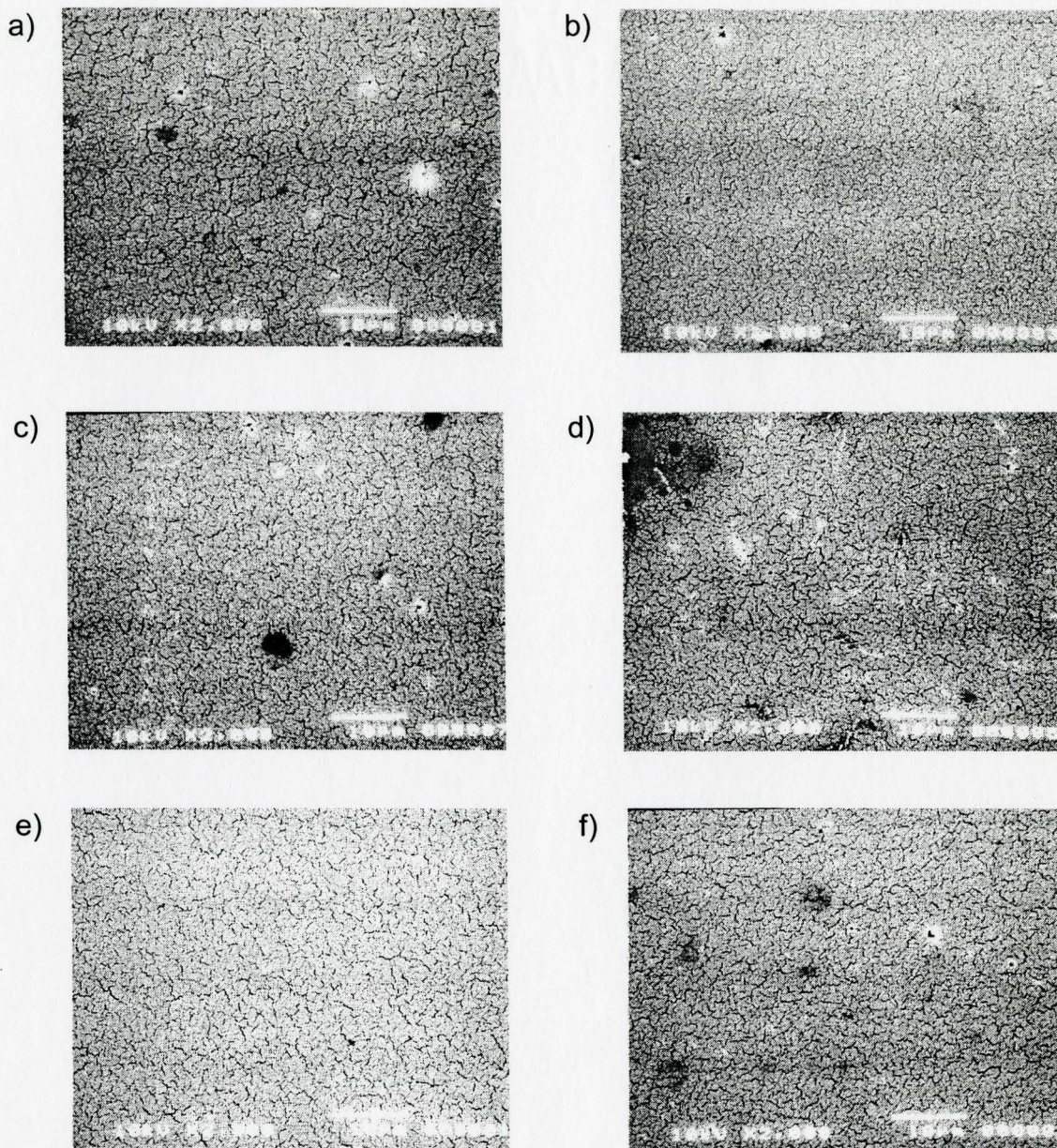


Figure 4.2 Scanning electron microscope images (2000x) of (a) unmodified, and peptide-modified surfaces: b) cysteine; c) CRGD; d) RGDC; e) CREDV; and f) REDVC. The cracking on the surfaces suggests that the cleaning procedure results in the swelling of the polyurethane and hence, the cracking of the overlying gold surface.

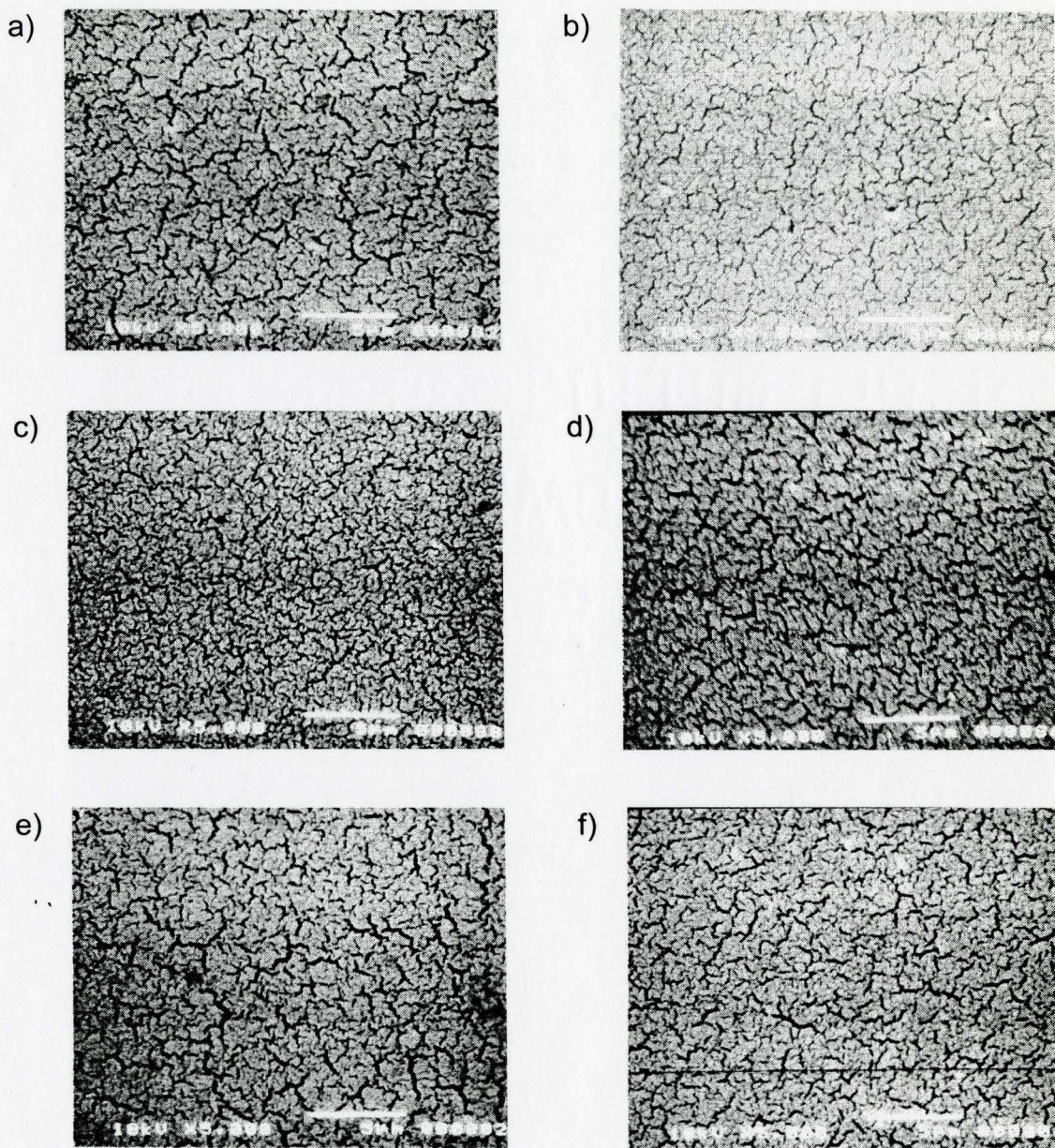


Figure 4.3 Scanning electron microscope images (5000x) of (a) unmodified, and peptide-modified surfaces: b) cysteine; c) CRGD; d) RGDC; e) CREDV; and f) REDVC. The cracking on the surfaces suggests that the cleaning procedure results in the swelling of the polyurethane and hence, the cracking of the overlying gold surface.

4.2.3 X-ray Photoelectron Spectroscopy

Table 4.1 summarizes representative XPS data for the unmodified and peptide modified surfaces, including results for the peptides of different orientation. The washed but unmodified gold control surface showed carbon, oxygen and nitrogen in addition to the gold. Atmospheric contamination, as well as the underlying polyurethane, are likely the sources for the carbon and oxygen signals. Since cracking of the surface exposes the polyurethane substrate, the nitrogen signal is likely resulting from the isocyanate and ethylene diamine in the polyurethane. High-resolution nitrogen envelopes provide additional evidence that this is the case. An amide nitrogen at 399.0 eV and isocyanate nitrogen at 400.5 eV are noted, with the predominance of the isocyanate nitrogen being attributable to the hydrophobic XPS environment. The smaller than expected amount of gold is likely the result of both atmospheric contamination and exposed polyurethane.

On the modified surfaces, signals from both the underlying gold substrate and the peptides are present. While the size of the peptides and packing density are likely not great enough to eliminate a signal from the underlying gold surface, a decrease in the angle of incidence from 90° to a more surface-sensitive 30° resulted in a lower level of gold detected and an increase in both the N1s and S2p signals as expected for peptide chemisorption. Furthermore, the composition of the high-resolution N1s envelope demonstrates that the signal from the polyurethane is eliminated and provides further evidence of peptide

modification. In this case, the nitrogen is either predominantly or entirely in the amide (399.0 eV) rather than the isocyanate (400.5 eV) form as for the unmodified surfaces. In addition, a carboxylic peak (288.5 eV) was noted on each of the modified surfaces, providing further evidence of peptide chemisorption.

Examination of the high-resolution sulfur envelopes in Table 4.1 suggests that the sulfur was directly bonded to gold. A S2p peak at 160.5 eV [66] was observed on all of the modified surfaces. Sulfur peaks at 162.0 eV and 163.5 eV suggest the presence of a second and third layer of cysteine that was not bonded to the gold. Moreover, a peptide orientation effect is apparent. The fraction of bound sulfur was consistently higher on both surfaces modified with C-cysteine terminated peptides, RGDC and REDVC. However, the surfaces modified with the N-cysteine terminated peptides, CRGD and CREDV, show a greater total amount of sulfur due to the presence of unbound peptide. It is interesting to note that the relative atomic amounts of bonded sulfur however are similar on the two surfaces. In subsequent studies, levels of nitrogen were comparable to these values obtained. However, sulfur levels tended to vary by 10-15%.

Table 4.1 Summary of representative XPS results for the unmodified and peptide-modified surfaces.

Surface Modification	Takeoff Angle	C1s				O1s	Au4f	N1s		S2p			
		285.0	286.5	288.5	Total			399.0	400.5	160.5	162.0	163.5	Total
Unmodified	90	40.1	21.5	0	52.5	17.0	19.1	0	2.3	0	0	0	0
Cysteine	90	26.7	8.2	2.5	37.5	39.2	20.1	1.3	0.8	0.70	0.24	0	0.94
CRGD	90	29.7	14.9	0	44.6	17.7	29.2	3.4	0	1.26	2.55	1.31	5.12
CRGD	30	37.7	18.4	5.1	56.1	18.5	12.7	3.7	0	0.82	1.67	1.37	3.86
RGDC	90	33.9	11.4	8.5	53.8	19.0	19.4	6.5	0	0.81	0.54	0	1.35
RGDC	30	49.9	7.2	4.9	62.1	26.7	6.7	4.0	0	0.36	0.22	0	0.58
CREDV	90	36.9	10.9	3.0	50.8	17.1	20.5	3.8	0	1.15	4.46	2.12	7.73
CREDV	30	47.5	12.2	5.0	64.7	18.1	7.0	3.5	0	0.82	3.98	1.90	6.70
REDVC	90	48.1	8.0	5.1	61.2	16.2	18.0	3.4	0	0.83	0.46	0	1.29
REDVC	30	55.7	8.1	5.0	68.9	16.9	8.9	4.2	0	0.71	0.38	0	1.09

4.3 PROTEIN ADSORPTION STUDIES

4.3.1 Total Protein Adsorption

Following exposure to 100% plasma, adsorbed proteins were eluted from the unmodified and the modified surfaces. Figure 4.4 shows the combined results of total protein assays used to quantify the total amount of protein adsorbed to the various surfaces. Measurements show that all surfaces adsorb between 0.3 and 1.0 $\mu\text{g}/\text{cm}^2$ of protein from plasma, with peptide modification increasing protein adsorption. In particular, the surfaces modified with REDV-containing peptides, CREDV and REDVC, adsorb more protein than the other surfaces. Furthermore, the surfaces modified with N-cysteine terminated peptides, CRGD and CREDV, adsorb more protein than their C-cysteine terminated counterparts. These results suggest that the location of the cysteine in the peptides as well as the peptide composition may be significant in determining the biological activity of peptide modified surfaces.

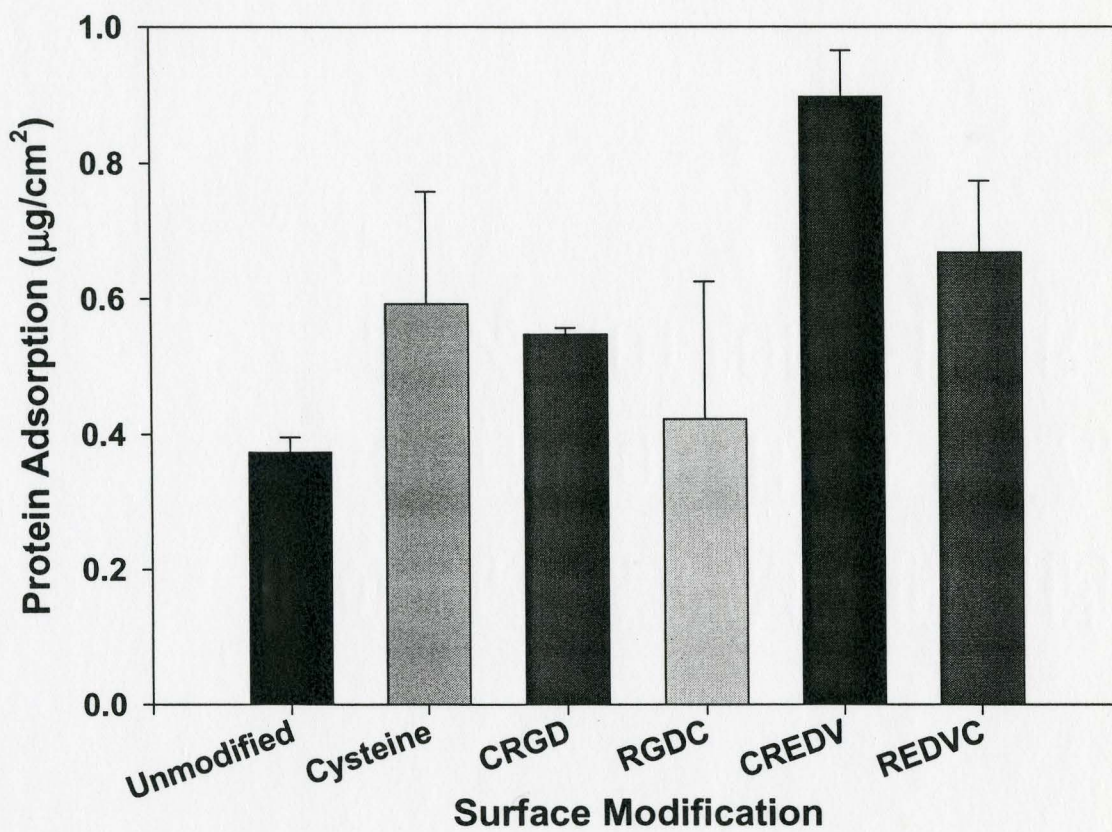


Figure 4.4 Total amount of protein adsorption to the unmodified and peptide-modified surfaces following a two-hour incubation in 100% plasma. Error bars represent 1 standard deviation (n=6).

4.3.2 Total Protein Immunoblot

Immunoblotting for a number of plasma proteins following protein adsorption, including contact activation and complement proteins, suggests protein adsorption differences between the peptides as well as differences dependent on peptide orientation. Western blots (Figures 4.5, 4.6 and 4.7) loaded with equal volumes of eluates show that patterns of protein adsorption vary between surfaces. Blots for the proteins eluted from surfaces are much less complex in comparison to plasma itself [100].

Contrary to results obtained by Sun *et al.* [55], significant amounts of protein were eluted from and detected on the gold surface. Albumin was noted on all of the surfaces including the control. Contact phase coagulation factors, Factor XII, Factor XI, prekallikrein and high molecular weight kininogen (HMWK), were found on the unmodified, CREDV-modified and REDVC-modified surfaces. However, the intensity of the bands was much greater on the surface modified with CREDV. Furthermore, the CREDV-modified surface was the only surface that adsorbed the coagulation factor Protein S. On the cysteine-, CRGD-, and RGDC-modified surfaces, HMWK was the only contact phase coagulation factor found in significant quantities, suggesting that these surfaces are more inert with respect to the intrinsic coagulation pathway.

All of the surfaces exhibited strong bands for essentially all of the complement proteins as well as for IgG. The bands for the complement proteins were more prevalent than the bands for the contact activation factors, in

agreement with results obtained by Lestelius *et al.* [80] and Tengvall *et al.* [78] who demonstrated that cysteine-modified surfaces did not initiate contact activation even though the surfaces adsorbed complement proteins.

The adhesion protein, fibronectin, was found on the unmodified as well as the cysteine- and CREDV-modified surfaces. Vitronectin was found on all of the peptide-modified surfaces. However, the bands were more prevalent on the surfaces modified with CRGD and CREDV.

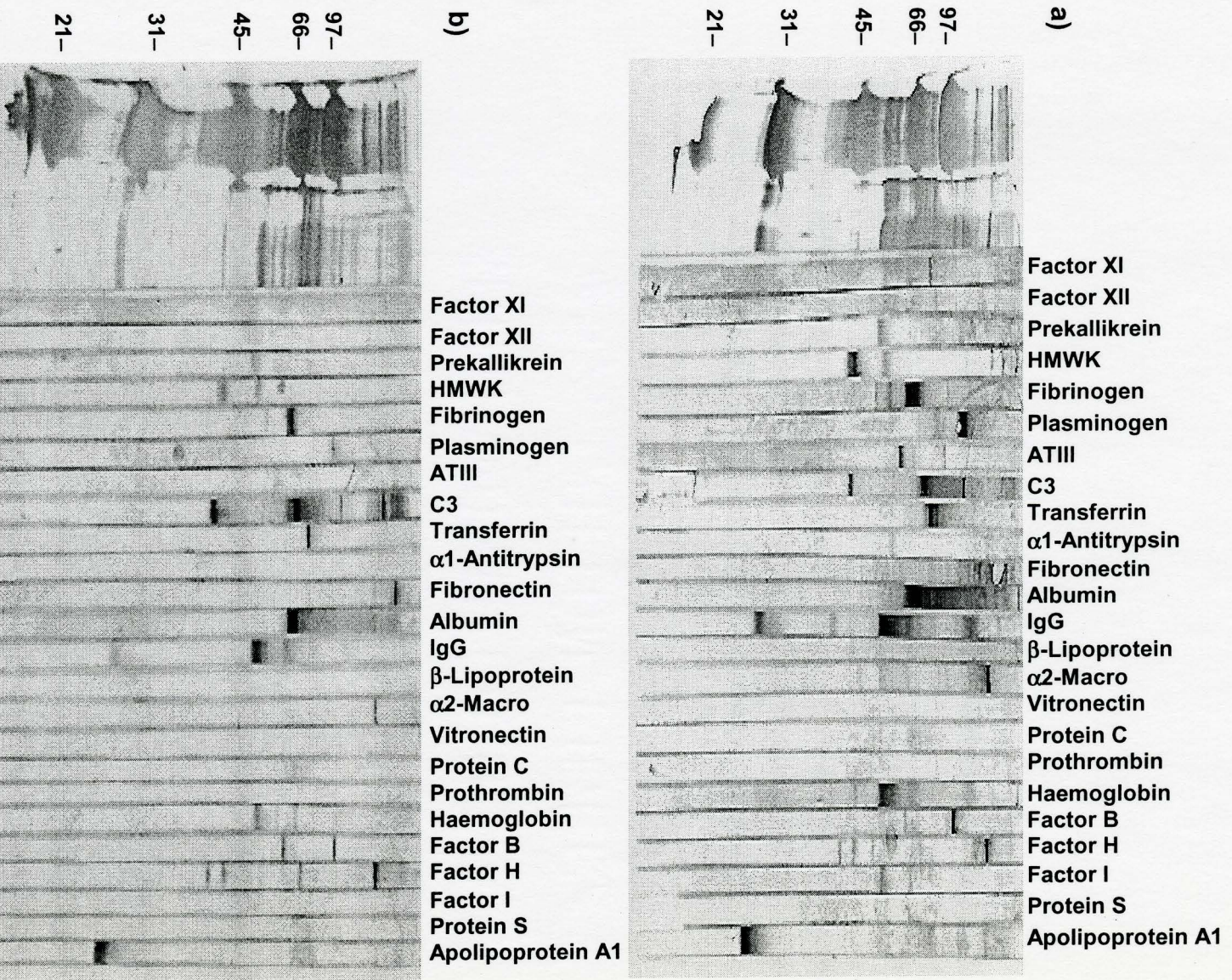


Figure 4.5 Immunoblot from SDS-PAGE 12% reduced gel probing for numerous plasma proteins in the eluate obtained from: a) the unmodified gold surface; and b) the cysteine-modified surface, following a two-hour incubation in plasma.

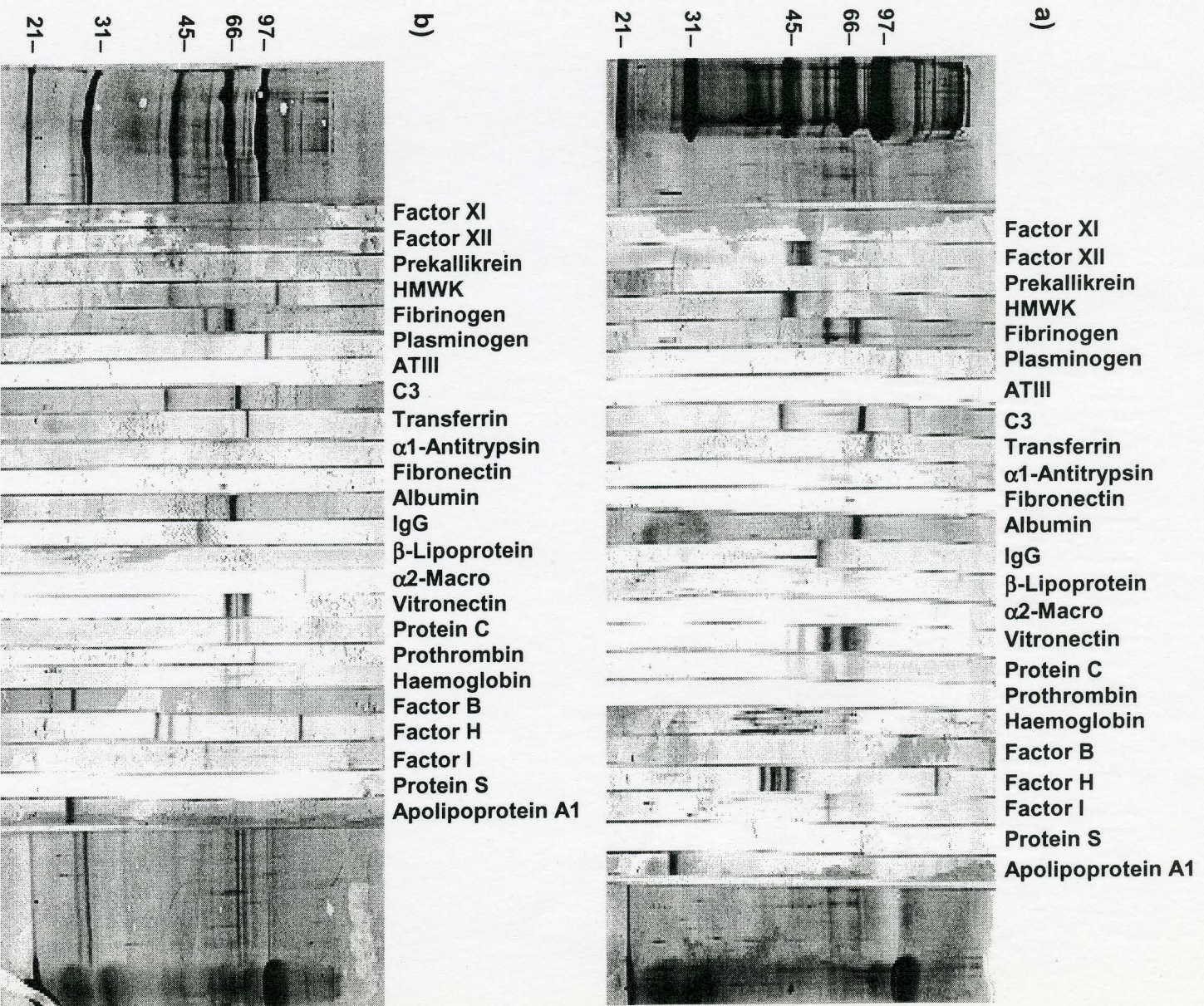


Figure 4.6 Immunoblot from SDS-PAGE 12% reduced gel probing for numerous plasma proteins in the eluate obtained from: a) the CRGD-modified surface; and b) the RGDC-modified surface, following a two-hour incubation in plasma.

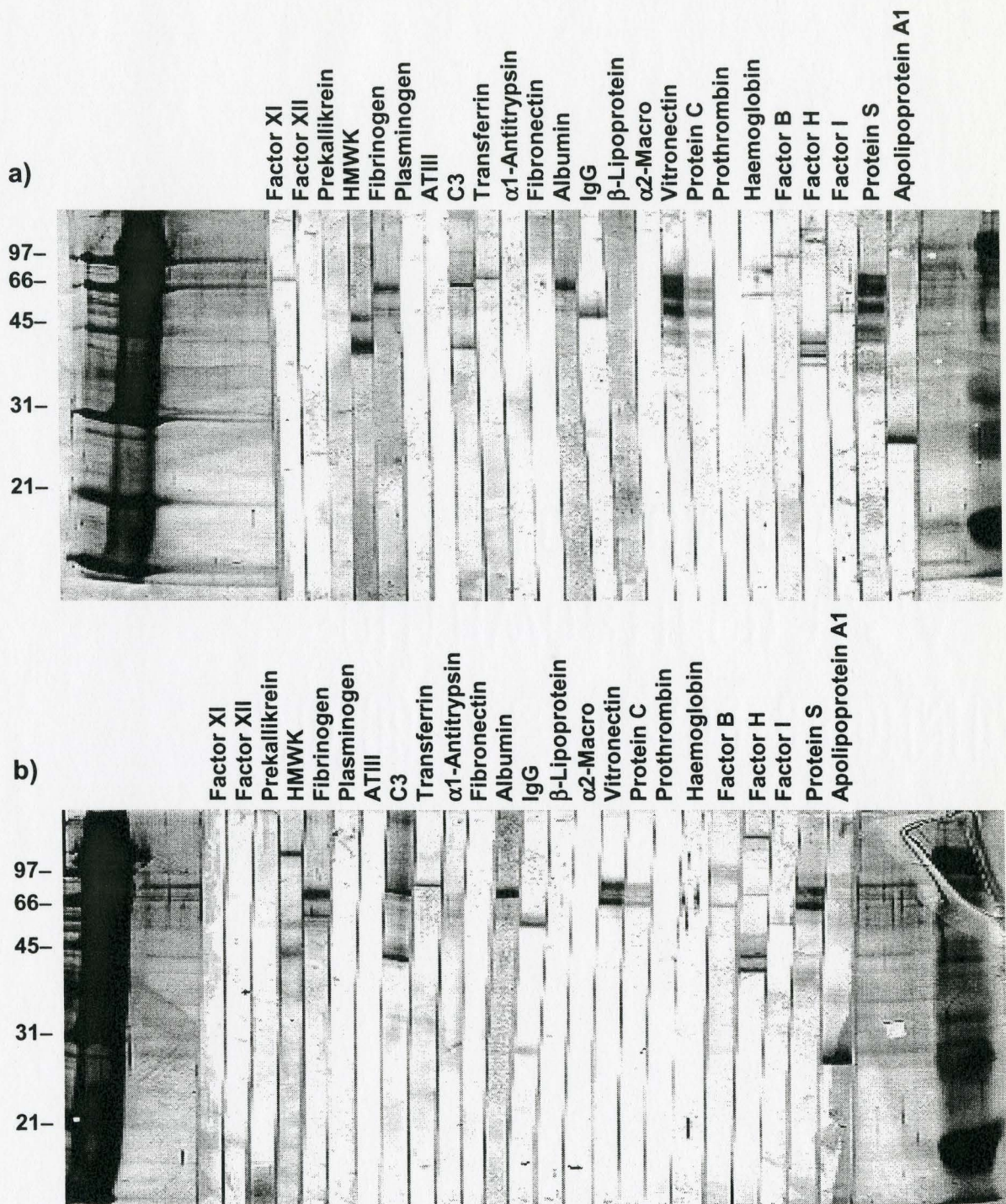


Figure 4.7 Immunoblot from SDS-PAGE 12% reduced gel probing for numerous plasma proteins in the eluate obtained from: a) the CREDV-modified surface; and b) the REDVC-modified surface, following a two-hour incubation in plasma.

4.3.4 Vitronectin Immunoblot

Figure 4.8 shows an immunoblot probing specifically for vitronectin in the eluates obtained following protein adsorption from plasma. Each lane was loaded with approximately 200 μg of protein as determined by a total protein microassay in order to be able to probe for vitronectin specific differences.

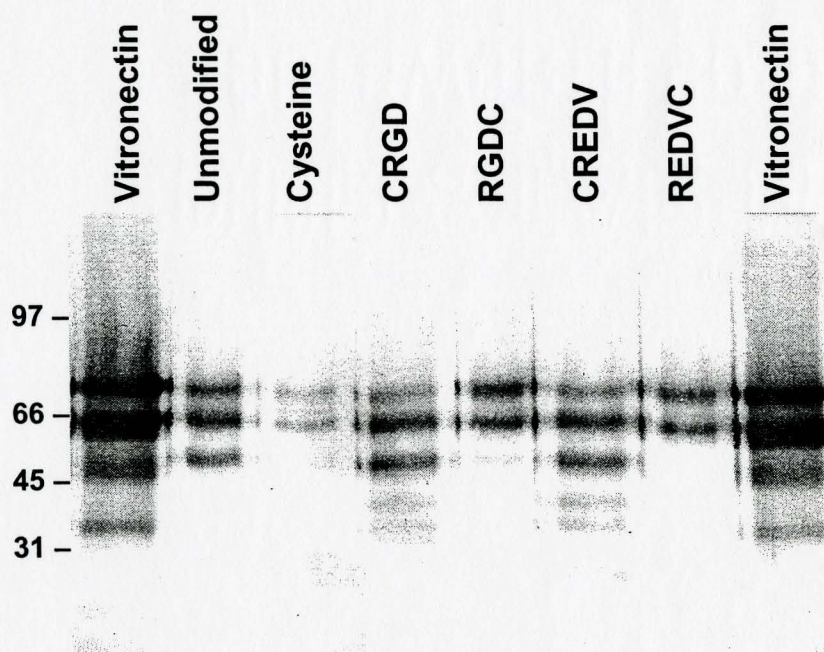


Figure 4.8 Immunoblot from SDS-PAGE 9% gel (reduced) probing for vitronectin in the proteins eluted from the unmodified and modified surfaces following a two-hour incubation in plasma.

A positive response for vitronectin was observed for all of the surfaces. In addition to bands at 75 and 65 kDa, pure vitronectin also showed bands at 54 and 45 kDa [101]. The surfaces modified with N-cysteine terminated peptides, CRGD and CREDV, as well as the unmodified surface, show a pattern of vitronectin fragments similar to that of the pure vitronectin with bands at 75, 65,

54, and 45 kDa. The surfaces modified with CRGD and CREDV also show a band at 37 kDa. However, the cysteine-, RGDC-, and REDVC-modified surfaces show primarily the two traditional fragments of vitronectin at 75 and 65 kDa, with faint bands at 54 kDa were observed on the cysteine- and RGDC-modified surfaces.

4.3.5 Vitronectin Adsorption

The adsorption of radioactive iodine (^{125}I) labeled vitronectin from plasma/buffer solutions to the surfaces was evaluated. The protein was radiolabeled using Iodogen®. Unreacted ^{125}I was removed by dialysis against phosphate buffered saline (PBS) containing trace amounts of nonradioactive iodine in order to suppress the binding of free iodide to gold surfaces [95]. In addition, the surfaces themselves were incubated in PBS-Nal prior to exposure to the protein solution. Incubation of the unmodified surfaces in PBS-Nal resulted in significant loss of gold, and thus, the vitronectin adsorption results for the unmodified surfaces are indicative of both a polyurethane and a gold surface rather than a gold surface alone. No apparent loss of gold was observed on any of the modified surfaces.

The free iodide concentration, determined by trichloroacetic acid (TCA) precipitation of the protein, remained less than 5% (ranging from 3.1% to 4.6%) in all studies. The surfaces were incubated in 1, 2, 5 and 10% plasma solutions in buffer containing approximately 30% radiolabeled vitronectin. A large

percentage of vitronectin was labeled assuming a large amount of vitronectin would be lost during labeling due to its adhesive nature.

The combined results of three experiments for a total of 12 surfaces each, shown in Figure 4.9, demonstrate peptide specific and, in particular, peptide orientation effects. The surfaces modified with N-cysteine terminated peptides, CRGD and CREDV, adsorbed more radiolabeled vitronectin than the other surfaces at all concentrations. Differences between the surfaces modified with N-cysteine terminated peptides and the other surfaces became significant at plasma concentrations of 5 and 10% ($\alpha=0.05$). Contrarily, no significant differences in vitronectin adsorption were observed between the C-cysteine terminated peptide-, cysteine-, and unmodified surfaces, although again in all cases, the peptide modified surfaces adsorbed higher amounts of radiolabeled vitronectin. These results suggest that the vitronectin binding affinity is significantly influenced by peptide orientation on the surface.

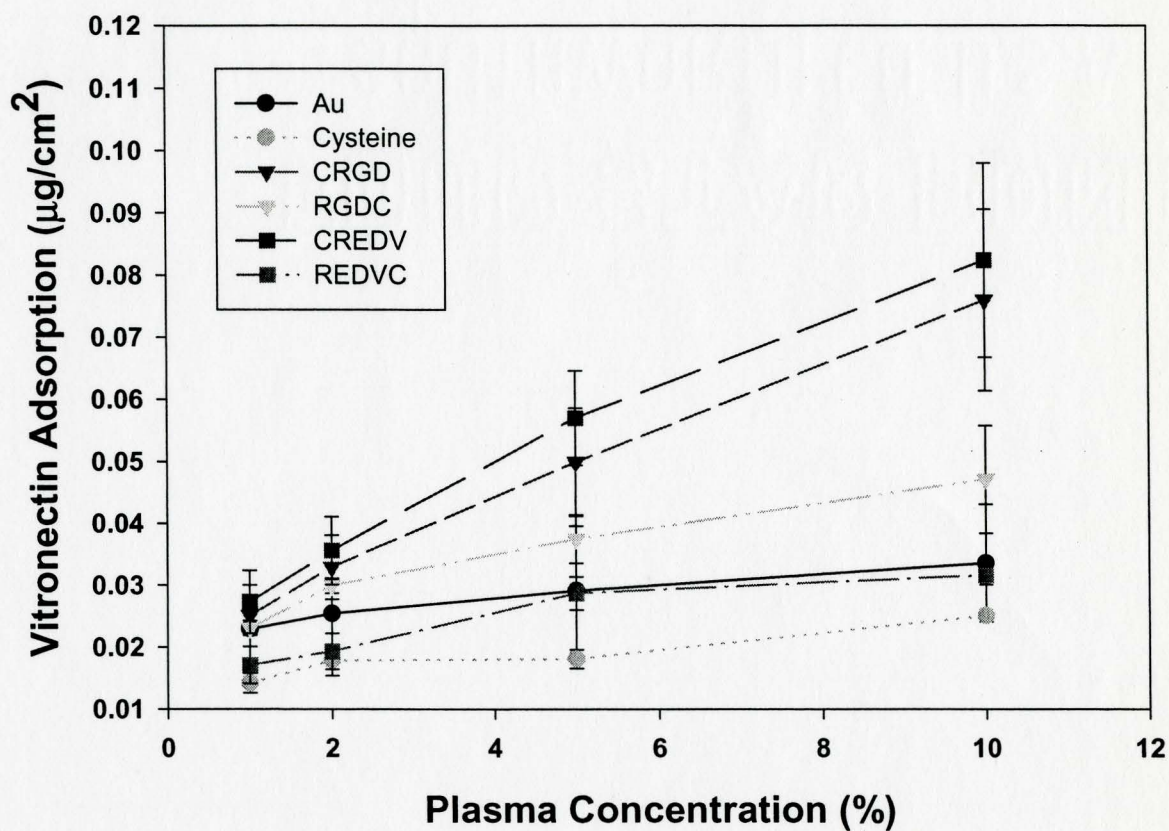


Figure 4.9 The adsorption of ^{125}I labeled vitronectin from plasma solutions to the unmodified and peptide-modified surfaces. The surfaces modified with N-cysteine terminated peptides adsorbed significantly more radiolabeled vitronectin than their C-terminated counterparts. Error bars represent 1 standard deviation ($n=12$).

4.4 IN VITRO CELL ATTACHMENT STUDIES

4.4.1 Peptide and Serum Protein Effects

Incubation of the surfaces with cells in serum-containing media presents a more accurate representation of actual *in vivo* conditions in which exposure of blood to the bare underlying substrate following the inevitable denudation of the cells is likely. However, the presence of serum may potentially confound the effects of the specific peptides. Therefore, studies were performed in both serum-containing and in serum-free media. Figure 4.10 shows the percentage of cells attached to the surfaces in both the presence and absence of 10% fetal calf serum (FCS). In all cases, cell attachment is greater on the peptide-modified surfaces than on the unmodified control surface, indicating that peptide modification enhances cell adhesion, either alone or via an adsorbed protein layer. Furthermore, peptide specific differences were noted, with cell attachment being consistently highest on the surfaces modified with the peptide, CREDV in both serum-free and serum-containing conditions.

In the absence of serum, cell attachment was generally reduced, suggesting that a fraction of the cell attachment is mediated by the adsorption of serum proteins. However, cell attachment on the unmodified surface remained unchanged in both the presence and absence of serum proteins. This may suggest that protein adsorption to the surface not only plays a role in mediating cell attachment, but that the serum proteins may be adsorbing in a specific

manner to the peptide modified surfaces but not to the unmodified surface to improve cell attachment.

In the presence of serum, surfaces modified with N-cysteine terminated peptides, CRGD and CREDV, resulted in greater cell attachment than their C-cysteine terminated counterparts. Additionally, when proteins were absent from the serum, the greatest decrease in cell attachment was detected on the surfaces modified with N-cysteine terminated peptides. Both of these observations are significant ($\alpha=0.05$). Thus, it appears that the surfaces modified with N-cysteine terminated peptides have a greater affinity for the proteins present in the serum-containing media. In the absence of serum, the greatest cell adhesion was noted on the CREDV-modified surface. The level of adhesion was significantly greater than on its C-terminated counterpart. Differences between the RGD based peptides were not significant under serum poor conditions. Small values for adhesion were noted on both the gold and cysteine-modified surfaces.

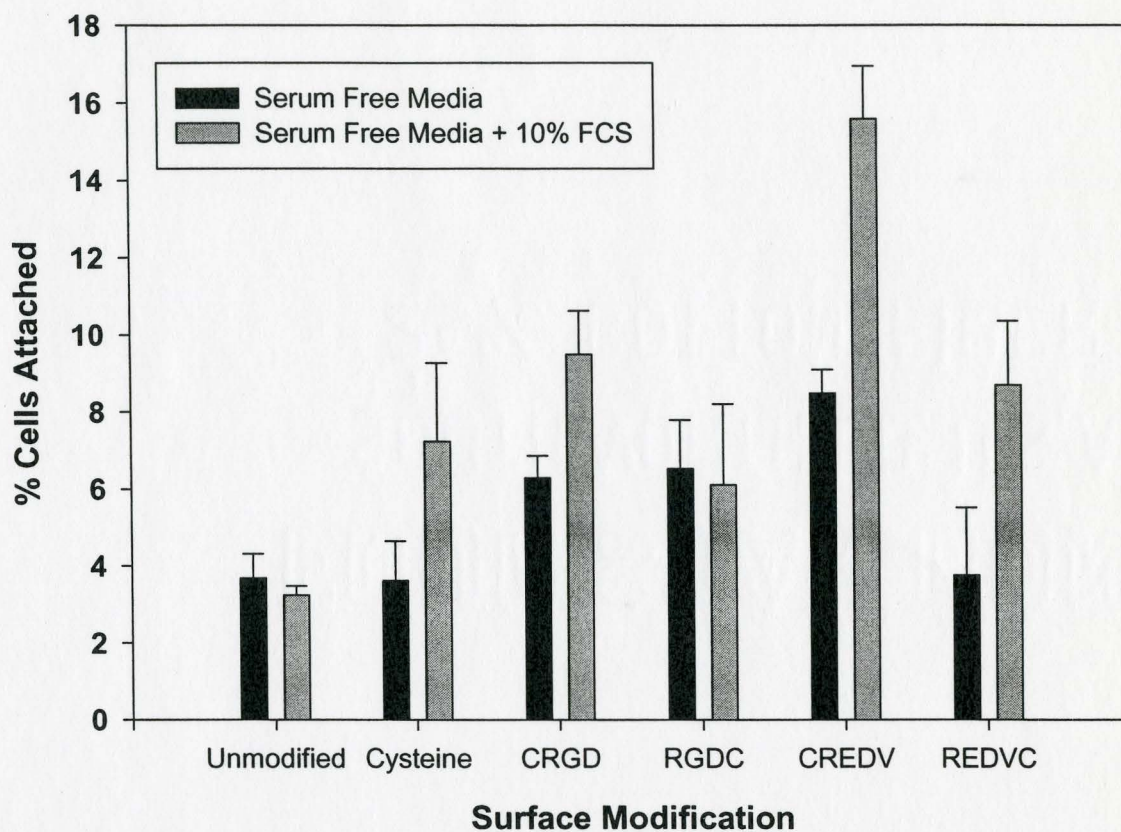


Figure 4.10 Percentage of cells attached on the various surfaces after a four-hour incubation at 37°C. The media was either serum-free or serum-free containing 10% fetal calf serum. Error bars represent 1 standard deviation (n=6).

4.4.2 Peptide and Vitronectin Effects

To further elucidate the role of adsorbed serum proteins on the differences in cell attachment, a vitronectin antibody was added to the media. As a control, media containing non-immune IgG was used. The results of this study on cell attachment are shown in Figure 4.11. Results are normalized to account for differences in the various experiments.

In agreement with the previous results, this study showed that cell adhesion in either the presence of non-immune IgG or anti-vitronectin was greater on the modified surfaces. Furthermore, the trend noted in the presence of non-immune IgG was similar to that noted in previous studies using serum-containing media as would be expected. However, when anti-vitronectin was present in the media, cell adhesion was significantly reduced in most cases, with the most significant reduction being on the surfaces modified with CRGD and CREDV. These observations correlate well to cell adhesion results obtained using serum-free media, suggesting that vitronectin may be primarily responsible for the enhanced cell adhesion observed in the presence of serum proteins, particularly for surfaces modified with N-cysteine terminated peptides.

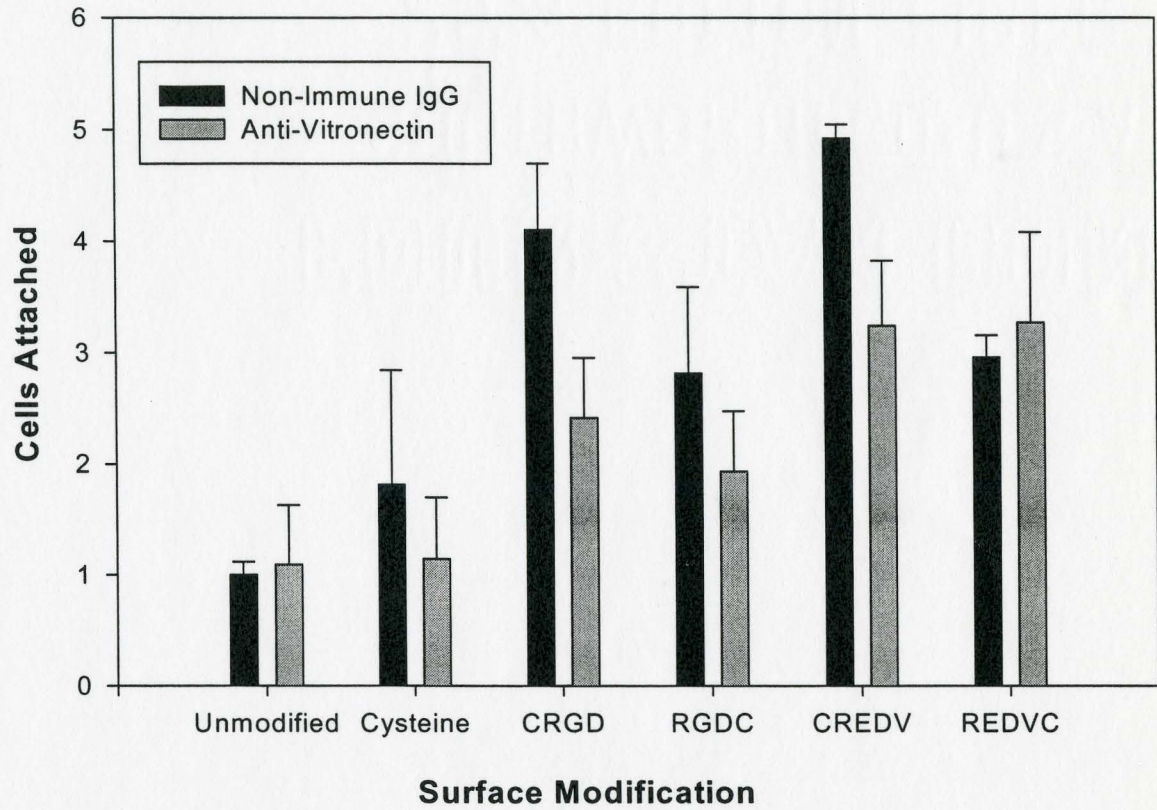


Figure 4.11 Normalized cells attachment on the various surfaces following a four-hour incubation at 37°C. The media was serum-free containing 10% fetal calf serum containing either anti-vitronectin or non-immune IgG. Error bars represent 1 standard deviation (n=5).

5. DISCUSSION

5.1 PEPTIDE MODIFICATION OF GOLD-COATED SURFACES

Surface modification with bioactive peptides is a powerful technique for generating surfaces that interact with a specific biological environment. The chemically well-defined nature of gold-coated surfaces makes them particularly attractive for investigating interfacial phenomena and they have been widely used in biological and biomedical applications [73]. Gold-coated silicon and glass surfaces in particular have been used in previous studies of protein adsorption [78;102], and for studying interactions with various cell types including nerve [11], bone [10], cornea [103], inflammatory cells [104], fibroblast [105], and vascular endothelial cells [12;75]. Specific modifications have been used to generate surfaces useful for modulating the adsorption of plasma proteins [55]. In this work, the reaction between gold and thiol groups was used to study the effect of cell adhesion peptide orientation on surfaces and to further demonstrate the potential of these surfaces for supporting the growth of cells. The substrate in this case, a polyurethane, was selected based on its desirable mechanical properties which it is hoped can eventually be exploited in the development of biomaterials. A thin (100 nm) layer of gold was evaporated onto the polyurethane surface and the gold subsequently modified with cell adhesion

peptides thought to have a degree of specificity for vascular endothelial cells, including the relatively non-specific RGD [5], as well as the more vascular endothelial cell specific REDV [8]. Orientation of the peptide was controlled via the chemisorption reaction of sulfur and gold through the placement of a cysteine in the peptides. SEM results suggest that adhesion between the gold layer and the polymer must be an area of focus in future studies if this surface is to stand up to the rigors of biological implantation. Regardless, a high density of the peptide on the surface should be possible using this technique, making it attractive from a theoretical standpoint. It should be noted however that densities on these surfaces would not be as high as on (111) gold surfaces, although the exact nature of these surfaces is unknown.

5.2 SURFACE CHARACTERIZATION

Surface analysis provides evidence that modification of the surfaces with the peptides has occurred. Small differences in both advancing and receding water contact angles were noted with peptide modification. Specifically, both the advancing and receding angles of the cell adhesion peptide modified surfaces were significantly different from the unmodified gold-coated polyurethane surface and from the cysteine-modified control surface. However, there were no orientation specific differences noted with this analysis technique on these surfaces, as would be expected since the hydrophilicity of the surfaces would be expected to be quite similar.

The unmodified gold coated polyurethane surfaces showed XPS signals from carbon, nitrogen and oxygen in addition to gold, these are likely due to a combination of atmospheric contamination and a signal from the underlying polymer substrate. The level of nitrogen as well as the presence of both an amide and an isocyanate nitrogen in the high resolution nitrogen envelope suggests that the contribution from the polymer may be quite significant. This result is not unexpected given the significant amounts of cracking that were noted on the washed and peptide chemisorbed surfaces by SEM, likely due to swelling of the polymeric substrate under the cleaning and reaction conditions. On the peptide-modified surfaces, the presence of sulfur, an increase in the nitrogen signal, and significant shifts in the N1s high resolution envelopes provide evidence of peptide modification. In particular, the peptide modified surfaces in all cases showed a significant increase in the contribution from the amide nitrogen and a decrease to zero in most cases in the contribution from the isocyanate nitrogen. While there was some variability in the XPS data, in general nitrogen contents were lower and sulfur contents were higher than would be expected for monolayer coverage with the peptide. This may be due to a combination of the formation of a peptide double layer on the gold-coated surface and peptide orientation in the hydrophobic XPS environment. High-resolution sulfur spectra suggest that a significant fraction of the sulfur was bonded rather than physically adsorbed with bonded fractions of greater than 50% in some cases. The presence of a significant amount of unbonded sulfur does however

suggest that at least some of the peptide is physioadsorbed rather than chemisorbed.

XPS analysis suggests that peptide orientation has a significant effect on the composition of the surface. While there were no apparent peptide orientation specific differences noted in the nitrogen signals or in the high resolution carbon envelopes, the amount of sulfur present on the surfaces as well as the ratio of chemisorbed to physioadsorbed sulfur showed definite orientation specific trends. With both of the peptides, the C-terminal peptides had a lower overall surface sulfur content, but a higher level of bound sulfur. Overall, the levels of bonded sulfur on the surfaces were similar. The reaction between gold (111) and thiols has been shown to occur in the threefold hollow sites formed by contiguous gold [64], yielding a maximum thiol coverage of 7.5×10^{-10} mol/cm² if all of the sites were occupied. It is then expected that based on the sulfur levels obtained through XPS, peptide surface coverages ranged from 4.35×10^{-10} to 5.8×10^{-9} mol/cm². Note, however, that the surfaces used in these studies were of unknown gold orientation, and are most likely to show a lower than this maximum amount of peptide. These estimates compare well to the surface concentration of GRGDY grafted onto either a glass or polymer substrates found by Massia *et al.* [27] and to more recent results of surface peptide concentration on gold surfaces found by Sun *et al.* [55]. However, they are higher than the surface concentrations found by Saneinejad and Shoichet [11]. Akiyama *et al.* [106] estimated the number of fibronectin receptors per cell to be 10^5 , averaging 35

receptors per μm^2 in cell surface coverage of receptors. This estimation suggests there are enough adhesion ligands on the substrates to occupy all available receptors on a cell surface, although it is unknown whether this ligand density is optimum for maintaining cell adhesion, spreading and growth.

While significant carbon and oxygen contamination were present and expected on all of the surfaces, differences in the high resolution carbon spectra between the unmodified gold and the peptide modified surfaces provide additional evidence that surface modification with the peptides had occurred. The presence of a carboxyl and amide peak at 288.5 eV is noted on most of the peptide modified surfaces, although the trends appear to be in opposition to the levels of total sulfur. In particular, at higher takeoff angles (less surface specificity), the contribution of the carboxylic peaks is less for the N-terminal cysteine peptides than for the C-terminal cysteine peptides. However, at higher surface specificity, the contribution from the carboxylic group is virtually the same for each of the peptides. Furthermore, there was generally a surface specific increase in this peak on the modified surfaces. While the results suggest that surface modification of the gold-coated polyurethanes with the peptides has occurred, it is difficult with this technique to ascertain the exact surface concentration of peptide. It is not likely that a peptide monolayer is present despite the high levels of sulfur. Optimization of the surface density of the peptides should also be an area of focus for future studies if these surfaces are to be viable in terms of biomaterials applications.

5.3 BIOLOGICAL CHARACTERIZATION

Adhesion of cells from the ECV304 line to the modified surfaces was shown to be affected both by the surface bound peptide, and by its orientation. In medium containing 10% FCS, the greatest adhesion was noted on the CREDV-modified surface. These results are in agreement with those obtained previously by Hubbell *et al.* [32], who suggested that REDV should have a greater affinity for endothelial cells than RGD. Adhesion via the peptide REDV is mediated by the endothelial cell integrin $\alpha_4\beta_1$ [8], whereas RGD is more specific for $\alpha_v\beta_3$, an integrin found on numerous cells [5]. It is interesting to note that previous results by McMillan *et al.* [12], using a different vascular endothelial cell line, suggested that a CRGD-modified gold-coated polyurethane surface has a greater affinity for vascular endothelial cells, while a CREDV-modified gold-coated polyurethane surface showed some degree of specificity for mouse 3T3 fibroblasts. The cells used in the study of Hubbell *et al.* [32] were primary human umbilical vein endothelial cells. The ECV304 cells of the current work, though originally found to retain most of the immunocytochemical, biochemical and morphological characteristics as HUVEC [23], have recently been shown to be identical to bladder epithelial cells [96]. It was noted, however, that because ECV304 displays some endothelial cell characteristics, it is useful for the study of receptor pharmacology. These cells were originally selected based on the assumption that they retain endothelial like characteristics in terms of surface adhesion. While more recent results demonstrated that they are not genetically

identical to human vascular endothelial cells, the adhesion information generated remains useful. Together these results suggest possibly that cell specific effects must be accounted for in addition to other factors, as might be expected from the variable nature of the extracellular matrix *in vivo*.

Adhesion of the cells in the present study to CRGD-modified surfaces was also significant, while adhesion to the comparable C-cysteine terminated peptides was lower in both cases. Interestingly, the adhesion of the cells to the CRGD-modified surface was comparable to that noted on the REDVC-modified surfaces providing further evidence of the specificity of adhesion of the REDV peptide with this cell line. Similar trends were noted in the absence of serum, although adhesion was approximately 40% lower on the peptide-modified surfaces. In particular, the differences between serum-containing media and serum-free media were greatest on the CREVD-modified surfaces, suggesting that on these surfaces adsorption of plasma proteins is such that it is having a significant effect on cell surface interactions. Furthermore, it has been shown that cells bind to peptides with virtually the same affinity as to intact proteins. There should be a higher density of ligand on peptide-modified surfaces compared to surfaces modified with entire proteins, and therefore cell binding should be higher with peptide-modification. The fact that cell adhesion in protein-free media is lower suggests that the immobilization of complementary peptides should enhance binding while eliminating problems associated with protein immobilization.

Vitronectin has been shown in other studies to be the protein primarily responsible for mediating cell adhesion under *in vitro* conditions [46;48-50]. Vitronectin adsorption results suggested both by immunoblotting and adsorption of radioactively labeled proteins suggest the CREDV-modified surface in fact does have some vitronectin specificity. Addition of an anti-vitronectin antibody to the media resulted in a significant reduction in cell adhesion all of the surfaces except the REDVC-modified surface. This observation is in agreement with results obtained by McFarland *et al.* [107] who suggested that vitronectin in serum plays an important role in mediating cell adhesion to synthetic surfaces. Vitronectin has been previously shown to be a plasma protein adsorbed to biomaterials in contact with blood [45] and has been suggested in numerous studies to be the plasma protein responsible for mediating cell adhesion with a variety of cell types [34]. Bale *et al.* [46] suggested that the majority of cell attachment activity in cell culture media containing bovine or human serum is mediated by vitronectin after observing that vitronectin adsorption to tissue culture polystyrene from serum or plasma is approximately 40 times higher than fibronectin. More recent studies have shown that corneal [108] or vascular endothelial cell [109] attachment to tissue culture polystyrene was affected little by fibronectin depletion, but removing vitronectin reduced attachment by about 90%. In correlation with the cell adhesion results, ¹²⁵I-vitronectin adsorption to the N-terminal cysteine peptide modified surfaces was similar, but significantly greater than adsorption to the C-terminal cysteine peptide modified, cysteine-

modified and control surfaces. However, there were notable variations in the trends. According to the radiolabeled vitronectin adsorption assays, the surface modified with CRGD adsorbed more vitronectin than the REDVC-modified surface. Yet in the presence of protein-containing media, cell attachment to the surfaces was similar. Furthermore the most significant reductions in cell adhesion were again noted on the N-terminal cysteine-modified surfaces, suggesting an important role for this cell adhesion protein. It is therefore likely that the orientation of the adsorbed vitronectin on the various surfaces is peptide dependent. Adsorption of vitronectin on the peptide modified and to a lesser extent cysteine-modified surfaces is likely more specific than on the unmodified gold surfaces where the addition of serum to the medium did not significantly alter the adhesion of cells to the surface. This result suggests that the peptides, particularly the CREDV peptide is showing specific interactions with the cell adhesion protein vitronectin present in plasma.

Vitronectin specific immunoblots demonstrate that not only are the levels of vitronectin adsorption greater on the N-terminal cysteine peptide modified surfaces greater, but the interactions of the protein with these are different than those with the C-terminal cysteine-modified surfaces. Though vitronectin generally presents as 75, 65 and 10 kDa fragments, additional fragments at 60, 57, 54, 45, 36 and 6 kDa are possible following proteolytic cleavage or degradation. Proteolytic processing of vitronectin produces two fragments of 54 kDa and 45 kDa [101]. Silnutzer and Barnes [110] incubated vitronectin with

thrombin to produce a thrombin-cleaved vitronectin fragment at 57 kDa. Seiffert [111] found that hydrolysis of vitronectin by calpains resulted in defined vitronectin fragments at 60, 45 and 36 kDa. In another study [112], vitronectin was cleaved into 40, 35 and 6 kDa fragments upon treatment with acid. Therefore it is possible that the differences in the patterns of vitronectin adsorption observed in Figure 4.8 and summarized in Table 5.1 stem from vitronectin cleavage upon contact with and adsorption to the unmodified, CRGD- and CREDV-modified surfaces. It could also be that the surfaces adsorbed proteins such as thrombin that are capable of hydrolyzing vitronectin. However, reduced SDS-PAGE and immunoblotting by Sun *et al.* [55] showed no visible bands for thrombin on unmodified gold surfaces following exposure to plasma. The most plausible explanation, in correlation with the cell adhesion results, is that the N-terminal cysteine peptide modified surfaces are capable of preferentially adsorbing vitronectin fragments previously formed in the plasma in an orientation conducive to supporting cell adhesion to some extent. Specifically, in addition to bands at 75 and 65 kDa, the surfaces modified with N-cysteine terminated peptides also showed significant bands at 54, 45, and 37 kDa, whereas the surfaces modified with C-cysteine terminated peptides showed only a positive response for bands at 75 and 65 kDa. While the amino acid sequences of these fragments are unknown, Suzuki *et al.* [113] found that the 53 and 40 kDa fragments of acid-cleaved vitronectin contained the same N-terminal sequence as intact vitronectin and that the fragments promoted cell attachment

activity. The N-terminal region of vitronectin includes the somatomedin B domain followed by the RGD cell adhesion sequence. Contrarily, Pons *et al.* [101] found that the 45 kDa fragment formed following the proteolytic processing of vitronectin lacked the integrin-binding domain, RGD. Similarly, the 42 and 35 kDa fragments generated from plasminolysis of vitronectin were also not effective in promoting cell adhesion [114]. However, neither the method of fragmentation nor the amino acid sequence of the vitronectin fragments isolated in this immunoblot analysis is known.

Table 5.1 Summary of results for the immunoblot probing for vitronectin in the proteins eluted from the unmodified and modified surfaces.

MW of Vitronectin Fragment (kDa)	Surface Modification					
	Unmodified	Cysteine	CRGD	RGDC	CREDV	REDVC
75	•	•	•	•	•	•
65	•	•	•	•	•	•
54	•	•	•	•	•	•
45	•		•		•	
37			•		•	

Immunoblot results were obtained for approximately 20 plasma proteins in order to assess the potential response of these surfaces to blood exposure. The results demonstrated both surface specific and peptide orientation specific differences. The amounts of adsorbed protein were greater on the N-terminal cysteine peptides. Strong bands for the complement proteins probed for, as well as for IgG, were evident on all of the surfaces. The bands for the complement proteins were more prevalent than the bands for the contact activation factors.

These observations are in agreement with results obtained by Lestelius *et al.* [80] and Tengvall *et al.* [78] who demonstrated that cysteine-modified surfaces did not initiate contact activation despite the adsorption of complement proteins to the surfaces. Nonetheless, due to the significant amount of proteins adsorbed to the surfaces, there remains a potential for thrombus formation if the surfaces were exposed.

Since a small range of plasma concentrations was used in these experiments, the Vroman effect may play an important role in the differences noted. The Vroman effect is based on observations that blood protein adsorption involves a hierarchical series of collision, adsorption, and exchange processes. For instance, the extent of adsorption of fibrinogen and fibronectin depends on the plasma concentration from which they were adsorbed [115]. At low plasma concentrations, the extent of adsorption is maximized. This effect is attributed to the ability of other proteins to displace them from the surface. However, in a study by Bale *et al.* [46], it was found that unlike fibronectin, the amount of vitronectin adsorbed from plasma onto microtitre plates was not dependent on the plasma concentration and therefore the Vroman effect is not likely to be a contributing factor in these results.

The ultimate goal is to place surfaces modified with these peptides into the body, potentially in a blood contacting application. The loss of cells following exposure to the shear stresses of the blood and therefore direct surface contact with plasma proteins is inevitable. Therefore it is important to study the

interactions of plasma proteins with the various surfaces. The presence of contact activating and complement proteins on the surfaces suggests that should the surfaces be exposed to plasma proteins, deleterious effects could result. It is interesting to note that similar to the cell adhesion results, the adsorption of complement and contact activating factors was generally higher on the N-terminal cysteine peptide modified surfaces with the CREDV surface showing the highest levels of adsorption. Therefore, while these surfaces appear to have significant potential in terms of interactions with cells, their inertness with respect to contact activation may need further exploration.

6. CONCLUSIONS

The following conclusions can be drawn from this research:

- Peptide modification of the gold surfaces was confirmed both by sessile drop water contact angles and x-ray photoelectron spectroscopy. Both advancing and receding water contact angles showed significant differences in the hydrophobicity between the unmodified and modified surfaces, reflecting a change in surface chemistry.
- Sulfur detected by XPS analysis revealed the presence of cysteine in the peptide on the surface. Additional evidence of peptide modification included the presence and binding characteristics of nitrogen on the modified surfaces and the appearance of carboxylic groups following peptide chemisorption.
- XPS analysis also showed peptide orientation effects. The fraction of bound sulfur was higher on both surfaces modified with C-cysteine terminated peptides, RGDC and REDVC. However, the surfaces modified with the N-cysteine terminated peptides, CRGD and CREDV, show a greater total amount of sulfur due to the presence of unbound peptide.
- Investigation of the protein interactions with the modified surfaces suggest that both peptide type and orientation may be significant in determining the biological activity of peptide modified surfaces.

- The total protein adsorption assays showed that the modified surfaces adsorbed more protein than the unmodified surface, suggesting that modification with the peptides selected for these studies increases protein adsorption. Furthermore, the surfaces modified with REDV-containing peptides (CREDV and REDVC) adsorbed the most total protein compared with the surfaces modified with CRGD and RGDC. Orientation specific effects were also noted with the N-cysteine terminated peptides, CRGD and CREDV, adsorbing more protein than their C-cysteine terminated counterparts.
- Western blotting showed that patterns of protein adsorption vary between surfaces. The intensity of the bands, which reflect the amounts of adsorbed protein, were greater on the N-terminal cysteine peptides. Strong bands for the complement proteins probed for, as well as for IgG, were evident on all of the surfaces. The bands for the complement proteins were more prevalent than the bands for the contact activation factors.
- Blots probing specifically for vitronectin showed peptide and orientation-dependent results. In addition to bands at 75 and 65 kDa, the N-cysteine terminated peptides (CRGD and CREDV) were positive for bands at 54, 45, and 37 kDa. This suggests that these surfaces are in such a conformation that they are capable of preferentially adsorbing vitronectin fragments most likely previously formed in the plasma. In this conformation, the amino acid arginine (R) is closest to and aspartic acid (D) is farthest from the surface.

- The vitronectin immunoblot results concur with the radioactive iodine labeled vitronectin adsorption to the surfaces, which also showed peptide-specific, as well as, peptide orientation effects. The surfaces modified with N-cysteine terminated peptides, CRGD and CREDV, adsorbed more radiolabeled vitronectin than the other surfaces at all concentrations. When the plasma concentration in buffer was 10%, the CRGD- and CREDV-surfaces adsorbed nearly double the amount of vitronectin than the C-cysteine terminated peptides.
- Cell adhesion assays in both serum-free and serum-containing medium showed that in all cases cell attachment was greater on the peptide-modified surfaces than on the unmodified control surface, indicating that peptide modification enhances cell adhesion.
- There was significant cell attachment in the absence of serum proteins. Cell attachment on the peptide-modified surfaces was augmented by the presence of serum proteins. Cell attachment on the peptide-modified surfaces was increased by an average of 40% in serum-containing media.
- Peptide specific and peptide orientation differences were noted, with cell attachment being consistently highest on the surfaces modified with the peptide, CREDV. In the presence of serum proteins, surfaces modified with N-cysteine terminated peptides, CRGD and CREDV, resulted in 1.5 times greater cell attachment than their C-cysteine terminated counterparts. Additionally, when proteins were absent from the serum, the greatest

decrease in cell attachment (approximately 35%) was detected on the surfaces modified with N-cysteine terminated peptides.

- Furthermore, when anti-vitronectin was present in protein-containing media, cell adhesion on the peptide-modified surfaces was significantly reduced in most cases, with the most significant reduction being on the surfaces modified with CRGD and CREDV (approximately 35%). This reduction in cell adhesion due to the presence of anti-vitronectin concurs with cell attachment in serum-free media suggesting that under these conditions, adhesion may be mediated by the peptides rather than protein adsorbed peptides.
- Peptide orientation affects interactions with vitronectin. The surfaces modified with N-cysteine terminated peptides, CRGD and CREDV, adsorb an increased number of vitronectin fragments, as well as adsorb more radiolabeled vitronectin. Cell attachment on the CRGD- and CREDV-modified surfaces is greatest when vitronectin is present in the media.

7. RECOMMENDATIONS FOR FUTURE STUDIES

- Further evaluation of the effect of peptide type should include the peptides studied in this report as well as other peptides that have been suggested to improve vascular endothelial cell adhesion to biomaterial surfaces. Peptides should be studied both alone and in combination since adhesion proteins often contain more than one cell adhesion sequence in their structure.
- The effect of peptide surface density should be further evaluated through the use of non-cell binding peptides along with radioiodination of the peptides.
- The effects of peptide orientation on cell adhesion and biological function could be evaluated through the use of cyclic peptides that would present the peptide in yet another conformation.
- Direct surface attachment of the peptide should be compared with peptide attachment via a polyethylene oxide spacer molecule.
- Surfaces should be evaluated under conditions of physiologic shear, including a full analysis of endothelial cell adhesion and function.

REFERENCES

1. Brash JL. Role of Plasma Protein Adsorption in the Response of Blood to Foreign Surfaces. In: Sharma CP, Szycher M, eds. *Blood Compatible Materials and Devices*. Lancaster, PA: Technomic, 1991
2. Courtney JM, Yu J, Sundaram S. Immobilization of Macromolecules for Obtaining Biocompatible Surfaces. In: Sletyr UB, Messner P, Purn D, Sara M, eds. *Immobilized Macromolecules: Application Potentials*. London: Springer-Verlag, 1993
3. Courtney JM, Lamba NMK, Sundaram S, Forbes CD. Biomaterials for Blood-Contacting Applications. *Biomaterials* 1994; **15**:737-44.
4. Lin H-B, Garcia-Echeverria C, Asakura S, Sun W, Mosher DF, Cooper SL. Endothelial Cell Adhesion on Polyurethanes Containing Covalently Attached RGD-Peptides. *Biomaterials* 1992; **13**:905-14.
5. Pierschbacher MD, Ruoslahti E. Cell attachment activity of fibronectin can be duplicated by small synthetic fragments of the molecule. *Nature* 1984; **309**:30-3.
6. Hubbell JA, Massia SP, Drumheller PD. Surface-grafted Cell-binding Peptides in Tissue Engineering of the Vascular Graft. *Annals New York Academy of Science* 1992; **665**:253-8.
7. Ruoslahti E, Pierschbacher MD. New Perspectives in Cell Adhesion: RGD and Integrins. *Science* 1987; **238**:491-7.
8. Massia SP, Hubbell JA. Vascular Endothelial Cell Adhesion and Spreading Promoted by the Peptide REDV of the IIIICS Region of Plasma Fibronectin is Mediated by Integrin alpha-4-beta-1. *The Journal of Biological Chemistry* 1992; **267**:14013-26.
9. Bain CD, Troughton EB, Tao Y-T, Evall J, Whitesides GM, Nuzzo RG. Formation of Monolayer Films by the Spontaneous Assembly of Organic Thiols from Solution onto Gold. *Journal of American Chemistry Society* 1989; **111**:321-35.
10. Ferris DM, Moodie GD, Dimond PM, Gioranni CWD, Ehrlich MG, Valentini RF. RGD-Coated Titanium Implants Stimulate Increased Bone Formation *In Vivo*. *Biomaterials* 1999; **20**:2323-31.
11. Saneinejad S, Shoichet MS. Patterned glass surfaces direct cell adhesion and process outgrowth of primary neurons of the central nervous system. *Journal of Biomedical Materials Research* 1998; **42**:13-9.
12. McMillan R, Meeks B, Bensebaa F, Deslandes Y, Sheardown H. Cell Adhesion Peptide Modification of Gold Coated Polyurethanes for Vascular Endothelial Cell Adhesion. *Journal of Biomedical Materials Research* 2000.

13. Keogh JR, Wolf MF, Overend ME, Tang L, Eaton JW. Biocompatibility of Sulphonated Polyurethane Surfaces. *Biomaterials* 1996; **17**:1987-94.
14. *Basic Pathology*, 6 Edn. Philadelphia: W.B. Saunders Company, 1997
15. The Platelet Page. Center of Biomedical Research of the University of Vienna, Austria (<http://www.akh-wien.ac.at/biomed-research>). 1996.
16. Clemetson KJ. Primary Haemostasis: Sticky Fingers Cement the Relationship. *Current Biology* 1999; **9**:110-2.
17. Collen D. The Plasminogen (Fibrinolytic) System. *Thrombosis and Haemostasis* 1999; **82**:259-70.
18. Carmeliet P, Collen D. Molecular Analysis of Blood Vessel Formation and Disease. *American Journal of Physiology* 1997; **273**:H2091-H2104.
19. *Human Anatomy and Physiology*, 4 Edn. California: Benjamin/Cummings Publishing Company, Inc., 1998
20. Horbett TA. The Role of Adsorbed Proteins in Animal Cell Adhesion. *Colloids and Surfaces B: Biointerfaces* 1994; **2**:225-40.
21. *Molecular Biology of the Cell*, 3 Edn. New York: Garland Publishing, Inc., 1994
22. Clowes AW, Kohler T. Graft Endothelialization: The Role of Angiogenic Mechanisms. *Journal of Vascular Surgery* 1991; **13**:734-6.
23. Takahashi K, Sawasaki Y, Hata J, Mukai K, Goto T. Spontaneous Transformation and Immortalization of Human Endothelial Cells. *In Vitro Cell Developmental Biology* 1990; **25**:265-74.
24. Podor TJ, Curriden SA, Loskutoff DJ. The Fibrinolytic System of Endothelial Cells. In: Ryan CJ, Una S, eds. *Endothelial Cells*. CRC Press, Inc., 1988
25. Smith JW, Schwartz MA. Integrins. *Molecular and Biological Responses to the Extracellular Matrix*. San Diego: Academic Press, Inc., 1994
26. Albelda SM, Buck CA. Integrins and Other Cell Adhesion Molecules. *FASEB J.* 1990; **4**:2868-80.
27. Massia SP, Hubbell JA. Human endothelial cell interactions with surface-coupled adhesion peptides on a nonadhesive glass substrate and two polymeric biomaterials. *Journal of Biomedical Materials Research* 1991; **25**:223-42.
28. Drumheller PD, Hubbell JA. Polymer Networks with Grafted Cell Adhesion Peptides for Highly Biospecific Cell Adhesive Substrates. *Analytical Biochemistry* 1994; **222**:380-8.
29. Porte-Durrieu MC, Labrugere C, Villars F *et al.* Development of RGD peptides grafted onto silica surfaces: XPS characterization and human endothelial cell interactions. *Journal of Biomedical Materials Research* 1999; **46**:368-75.

30. Neff JA, Tresco PA, Caldwell KD. Surface Modification for Controlled Studies of Cell-Ligand Interactions. *Biomaterials* 1999; **20**:2377-3293.
31. Humphries MJ, Akiyama SK, Komoriya A, Olden K, Yamada KM. Identification of an Alternatively Spliced Site in Human Plasma Fibronectin that Mediates Cell Type-Specific Adhesion. *Journal of Cell Biology* 1986; **103**:2637-47.
32. Hubbell JA, Massia SP, Desai NP, Drumheller PD. Endothelial Cell-Selective Materials for Tissue Engineering in the Vascular Graft via a New Receptor. *Bio/Technology* 1991; **9**:568-72.
33. Cherny RC, Honan MA, Thiagarajan P. Site-Directed Mutagenesis of the Arginine-Glycine-Aspartic Acid in Vitronectin Abolishes Cell Adhesion. *Journal of Biological Chemistry* 1993; **268**:9725-9.
34. Preissner KT, Seiffert D. Role of Vitronectin and its Receptors in Haemostasis and Vascular Remodeling. *Thrombosis Research* 1998; **89**:1-21.
35. Barnes DW, Silnutzer J. Isolation of Human Serum Spreading Factor. *Journal of Biological Chemistry* 1983; **258**:12548-52.
36. Preissner KT, Jenne D. Structure of Vitronectin and its Biological Role in Haemostasis. *Thrombosis and Haemostasis* 1991; **66**:123-32.
37. Parker CJ, Stone OL, White VF, Bernshaw NJ. Vitronectin (S protein) is Associated with Platelets. *British Journal of Haematology* 1989; **71**:245-52.
38. Hill SA, Shaughnessy SG, Joshua P, Ribau J, Austin RC, Podor TJ. Differential Mechanisms Targeting Type I Plasminogen Activator Inhibitor and Vitronectin Into the Storage Granules of a Human Megakaryocytic Cell Line. *Blood* 1996; **87**:5061-73.
39. Seiffert D, Schleef RR. Two Functionally Distinct Pools of Vitronectin in the Blood Circulation: Identification of a Heparin-Binding Competent Population of Vn Within Platelet alpha-Granules. *Blood* 1996; **88**:552-60.
40. Hayashi M, Akama T, Kono I, Kashiwagi H. Activation of Vitronectin (Serum Spreading Factor) Binding of Heparin by Denaturing Agents. *Journal of Biochemistry (Tokyo)* 1985; **98**:1135-8.
41. Stockmann A, Hess S, Declerck P, Timpl R, Preissner KT. Multimeric Vitronectin. Identification and Characterization of Conformation-Dependent Self-Association of the Adhesive Protein. *Journal of Biological Chemistry* 1993; **268**:22874-82.
42. Felding-Habermann B, Cheresh DA. Vitronectin and Its Receptors. *Current Opinion in Cell Biology* 1993; **5**:864-8.
43. Gebb C, Hayman EG, Engvall E, Ruoslahti E. Interaction of Vitronectin with Collagen. *The Journal of Biological Chemistry* 1986; **261**:16698-703.
44. Lawrence DA, Palaniappan S, Stefansson S *et al.* Characterization of the Binding of Different Conformational Forms of Plasminogen Activator Inhibitor-1 to Vitronectin. *The Journal of Biological Chemistry* 1997; **272**:7676-80.

45. Holmes R. Preparation from Human Serum of an Alpha-1 Protein which Induces the Immediate Growth of Unadapted Cells *In Vitro*. *Journal of Cell Biology* 1967; **32**:297-308.
46. Bale MD, Wohlfahrt LA, Mosher DF, Tomasini BR, Sutton RC. Identification of Vitronectin as a Major Plasma Protein Adsorbed on Polymer Surfaces of Different Copolymer Composition. *Blood* 1989; **74**:2698-706.
47. Lundberg F, Li D-Q, Falkenback D *et al*. Presence of Vitronectin and Activated Complement Factor C9 on Ventriculoperitoneal Shunts and Temporary Ventricular Catheters. *Journal of Neurosurgery* 1999; **90**:101-8.
48. Collins WE, Mosher DF, Tomasini BR, Cooper SL. A Preliminary Comparison of the Thrombogenic Activity of Vitronectin and Other RGD-Containing Proteins When Bound to Surfaces. *Annals New York Academy of Science* 1987; **516(-HD-)**:291-9.
49. Preissner KT, Anders E, Grulich-Henn J, Muller-Berghaus G. Attachment of Cultured Human Endothelial Cells is Promoted by Specific Association with S Protein (Vitronectin) as well as with the Ternary S Protein-Thrombin-Antithrombin III Complex. *Blood* 1988; **71**:1581-9.
50. Steele JG, Dalton BA, Johnson G, Underwood PA. Polystyrene Chemistry Affects Vitronectin Activity: An Explanation for Cell Attachment to Tissue Culture Polystyrene but not to Unmodified Polystyrene. *Journal of Biomedical Materials Research* 1993; **27**:927-40.
51. Thomas CH, McFarland CD, Jenkins ML, Rezania A, Steele JG, Healy KE. The Role of Vitronectin in the Attachment and Spatial Distribution of Bone-Derived Cells on Materials with Patterned Surface Chemistry. *Journal of Biomedical Materials Research* 1997; **37**:81-93.
52. Poly(ethylene glycol) Chemistry and Biological Applications. Washington, DC: American Chemical Society, 1997
53. Larm O, Larsson R, Olsson P. A New Non-Thrombogenic Surface Prepared by Selective Covalent Binding of Heparin via a Modified Reducing Terminal Residue. *Biomaterials, Medical Devices & Artificial Organs* 1983; **11**:161-73.
54. Nojiri C, Kido T, Sugiyama T *et al*. Can Heparin Immobilized Surfaces Maintain Nonthrombogenic Activity During *In Vivo* Long-Term Implantation? *ASAIO Journal* 1996; **42**:M468-M475.
55. Sun X, Sheardown H, Tengvall P, Brash JL. Peptide Modified Gold-Coated Polyurethanes as Thrombin Scavenging Surfaces. *Journal of Biomedical Materials Research* 2000; **49**:66-78.
56. McClung WG, Clapper DL, Hu SP, Brash JL. Adsorption of Plasminogen from Human Plasma to Lysine-Containing Surfaces. *Journal of Biomedical Materials Research* 2000; **49**:409-14.
57. Basmadjian D, Sefton MV, Baldwin SA. Coagulation on Biomaterials in Flowing Blood: Some Theoretical Considerations. *Biomaterials* 1997; **18**:1511-22.

58. Sugawara Y, Sakata Y, Minowada S *et al.* Adenovirus-mediated transfer of tissue-type plasminogen activator gene to human endothelial cells. *Surgery* 1997; **122**:91-100.
59. Rosenman JE, Kempczinski RF, Pearce WH, Silberstein E. Kinetics of endothelial cell seeding. *Journal of Vascular Surgery* 1985; **2**:778-84.
60. Sank A, Rostami K, Weaver F *et al.* New Evidence and New Hope Concerning Endothelial Seeding of Vascular Grafts. *The American Journal of Surgery* 1992; **164**:199-204.
61. Lin H-B, Sun W, Mosher DF *et al.* Synthesis, Surface, and Cell-Adhesion Properties of Polyurethanes Containing Covalently Grafted RGD-Peptides. *Journal of Biomedical Materials Research* 1994; **28**:329-42.
62. Duschl C, Sevin-Landais A-F, Vogel H. Surface Engineering: Optimization of Antigen Presentation in Self-Assembled Monolayers. *Biophysical Journal* 1996; **70**:1985-95.
63. Xiao Y, Truskey GA. Effect of Receptor-Ligand Affinity on the Strength of Endothelial Cell Adhesion. *Biophysical Journal* 1996; **71**:2869-84.
64. Whitesides GM, Laibinis PE. Wet Chemical Approaches to the Characterization of Organic Surfaces: Self-Assembled Monolayers, Wetting, and the Physical-Organic Chemistry of the Solid-Liquid Interface. *Langmuir* 1990; **6**:87-96.
65. Lestelius M. Tailor-Made Monolayer Assemblies for *In Vitro* Studies of Blood Protein-Surface Interactions. Linköping: Linköping University, 1996
66. Bensebaa F, Zhou Y, Deslandes Y, Kruus E, Ellis TH. XPS Study of Metal-Sulfur Bonds in Metal-Alkanethiolate Materials. *Surface Science* 1998; **405**:L472-L476.
67. Whitesides GM, Mathias JP, Seto CT. Molecular Self-Assembly and Nanochemistry: A Chemical Strategy for the Synthesis of Nanostructures. *Science* 1991; **254**:1312-9.
68. Nuzzo RG, Allara DL. Adsorption of Bifunctional Organic Disulfides on Gold Surfaces. *Journal of American Chemistry Society* 1983; **105**:4481-3.
69. Biebuyck HA, Whitesides GM. Interchange Between Monolayers of Gold Formed from Unsymmetrical Disulfides and Solutions of Thiols: Evidence for Sulfur-Sulfur Bond Cleavage by Gold Metal. *Langmuir* 1993; **9**:1766-70.
70. Porter MD, Bright TB, Allara DL, Chidsey CED. Spontaneously Organized Molecular Assemblies. 4. Structural Characterization of n-Alkyl Thiol Monolayers on Gold by Optical Ellipsometry, Infrared Spectroscopy, and Electrochemistry. *Journal of American Chemistry Society* 1987; **109**:3559-68.
71. Nuzzo RG, Fusco FA, Allara DL. Spontaneously Organized Molecular Assemblies. 3. Preparation and Properties of Solution Adsorbed Monolayers of Organic Disulfides on Gold Surfaces. *Journal of American Chemistry Society* 1987; **109**:2358-68.
72. Bain CD, Biebuyck HA, Whitesides GM. Comparison of Self-Assembled Monolayers on Gold: Coadsorption of Thiols and Disulfides. *Langmuir* 1989; **5**:723-7.

73. Prime KL, Whitesides GM. Self-Assembled Organic Monolayers: Model System for Studying Adsorption of Proteins at Surfaces. *Science* 1991; **252**:1164-7.
74. Lindblad M, Lestelius M, Johansson A, Tengvall P, Thomsen P. Cell and Soft Tissue Interactions with Methyl- and Hydroxyl-Terminated Alkane Thiols on Gold Surfaces. *Biomaterials* 1997; **18**:1059-68.
75. Tidwell CD, Ertel SI, Ratner BD, Tarasevich BJ, Atre S, Allara DL. Endothelial Cell Growth and Protein Adsorption on Terminally Functionalized, Self-Assembled Monolayers of Alkanethiolates on Gold. *Langmuir* 1997; **13**:3403-13.
76. Uvdal K, Bodo P, Liedberg B. L-Cysteine Adsorbed on Gold and Copper: An X-Ray Photoelectron Spectroscopy Study. *Journal of Colloid and Interface Science* 1992; **149**:162-73.
77. Kohli P, Taylor KK, Harris JJ, Blanchard GJ. Assembly of Covalently-Coupled Disulfide Multilayers on Gold. *Journal of American Chemistry Society* 1998; **120**:11962-8.
78. Tengvall P, Lestelius M, Liedberg B, Lundstrom I. Plasma Protein and Antisera Interactions with L-Cysteine and 3-Mercaptopropionic Acid Monolayers on Gold Surfaces. *Langmuir* 1992; **8**:1236-8.
79. Tengvall P, Askendal A, Lundstrom I. Complement Activation by 3-Mercapto-1,2-propanediol Immobilized on Gold Surfaces. *Biomaterials* 1996; **17**:1001-7.
80. Lestelius M, Liedberg B, Lundstrom I, Tengvall P. *In Vitro* Plasma Protein Adsorption and Kallikrein Formation on 3-Mercaptopropionic Acid, L-Cysteine and Glutathione Immobilized onto Gold. *Journal of Biomedical Materials Research* 1994; **28**:871-80.
81. Kanagaraja S, Lundstrom I, Nygren H, Tengvall P. Platelet Binding and Protein Adsorption to Titanium and Gold After Short Time Exposure to Heparinized Plasma and Whole Blood. *Biomaterials* 1996; **17**:2225-32.
82. Kanagaraja S, Alaeddine S, Eriksson C *et al.* Surface Characterization, Protein Adsorption, and Initial Cell-Surface Reactions on Glutathione and 3-Mercapto-1,2-propanediol Immobilized to Gold. *Journal of Biomedical Materials Research* 1999; **46**:582-91.
83. Boncheva M, Vogel H. Formation of Stable Polypeptide Monolayers at Interfaces: Controlling Molecular Conformation and Orientation. *Biophysical Journal* 1997; **73**:1056-72.
84. Zhang S, Yan L, Altman M *et al.* Biological Surface Engineering: A Simple System for Cell Pattern Formation. *Biomaterials* 1999; **20**:1213-20.
85. Santerre JP, ten Hove P, VanderKamp NH, Brash JL. Effect of Sulfonation of Segmented Polyurethanes on the Transient Adsorption of Fibrinogen from Plasma: Possible Correlation with Anticoagulant Behaviour. *Journal of Biomedical Materials Research* 1992; **26**:39-57.
86. Watts JF. *An Introduction to Surface Analysis by Electron Spectroscopy*. New York: Oxford University Press, 1990

87. Principles and Techniques of Scanning Electron Microscopy. Toronto: Litton Educational Publishing, Inc., 1974
88. Reimer L. Scanning Electron Microscopy. Physics of Image Formation and Microanalysis, 2 Edn. New York: Springer, 1998
89. Freshney RI. Culture of Animal Cells. A Manual of Basic Technique., 3 Edn. New York, NY: Wiley-Liss, Inc., 1994
90. Andrews. AT. Electrophoresis. Theory, Techniques, and Biochemical and Clinical Applications, 2 Edn. New York: Oxford University Press, 1986
91. Santerre JP, ten Hove P, Brash JL. Polyurethanes Bearing Pendant Amino Acids: Fibrinogen Adsorption and Coagulant Properties. Journal of Biomedical Materials Research 1992; 26:1003-18.
92. DC Protein Assay Instruction Manual. 2000. Bio-Rad Laboratories.
93. Peterson GL. Review of the Folin Phenol Protein Quantitation Method of Lowry, Rosebrough, Farr, and Randall. Analytical Biochemistry 1979; 100:201-20.
94. Sheardown H, Cornelius RM, Brash JL. Measurement of Protein Adsorption to Metals using Radioiodination Methods: A Caveat. Colloids and Surfaces B: Biointerfaces 1997; 10:29-33.
95. Du YJ, Cornelius RM, Brash JL. Measurement of Protein Adsorption to Gold Surface by Radioiodination Methods: Suppression of Free Iodide Sorption. Colloids and Surfaces B: Biointerfaces 2000; 17:59-67.
96. Brown J, Reading SJ, Jones S *et al.* Critical Evaluation of ECV304 as a Human Endothelial Cell Model Defined by Genetic Analysis and Functional Responses: A Comparison with the Human Bladder Cancer Derived Epithelial Cell Line T24/83. Laboratory Investigation 2000; 80:37-45.
97. The Coulter Principle. Beckman Coulter. (<http://www.beckmancoulter.com/>). 2000.
98. Sun, X. Peptide Modified Gold Coated Polyurethane Surfaces as Thrombin Scavengers. 1998. M.Eng. Thesis, McMaster University.
99. Meeks, B. Degradation of Polyurethane Ureas. 1998. B.A.Sc. Thesis, University of Ottawa.
100. Cornelius RM, Brash JL. Identification of Proteins Adsorbed to Hemodialyser Membranes from Heparinized Plasma. Journal of Biomaterials Science Polymer Edition 1993; 4:291-304.
101. Pons S, Mart'i E. Sonic Hedgehog Synergizes with the Extracellular Matrix Protein Vitronectin to Induce Spinal Motor Neuron Differentiation. Development 2000; 127:333-42.

102. Tengvall P, Lundstrom I, Liedberg B. Protein Adsorption Studies on Model Organic Surfaces: An Ellipsometric and Infrared Spectroscopic Approach. *Biomaterials* 1998; **19**:407-22.
103. Franco M, Nealey PF, Campbell S, Teixeira AI, Murphy CJ. Adhesion and Proliferation of Corneal Epithelial Cells on Self-Assembled Monolayers. *Journal of Biomedical Materials Research* 2000; **52**:261-9.
104. Kalltorp M, Askendal A, Thomsen P, Tengvall P. Inflammatory Cell Recruitment, Distribution, and Chemiluminescence Response at IgG Precoated- and Thiol Functionalized Gold Surfaces. *Journal of Biomedical Materials Research* 1999; **47**:251-9.
105. McClary KB, Ugarova T, Grainger DW. Modulating Fibroblast Adhesion, Spreading, and Proliferation using Self-Assembled Monolayer Films of Alkylthiolates on Gold. *Journal of Biomedical Materials Research* 2000; **50**:428-39.
106. Akiyama SK, Hasegawa E, Hasegawa T, Yamada KM. The Interaction of Fibronectin Fragments with Fibroblastic Cells. *Journal of Biological Chemistry* 1985; **260**:13256-60.
107. McFarland CD, Thomas CH, DeFilippis C, Steele JG, Healy KE. Protein Adsorption and Cell Attachment to Patterned Surfaces. *Journal of Biomedical Materials Research* 2000; **49**:200-10.
108. Underwood PA, Bennett FA. A Comparison of the Biological Activities of the Cell-Adhesive Proteins Vitronectin and Fibronectin. *Journal of Cell Science* 1989; **93**:641-9.
109. Steele JG, Johnson G, Norris WD, Underwood PA. Adhesion and Growth of Cultured Human Endothelial Cells on Perfluorosulphonate: Role of Vitronectin and Fibronectin in Cell Attachment. *Biomaterials* 1991; **12**:531-9.
110. Silnutzer J, Barnes DW. A Biologically Active Thrombin Cleavage Product of Human Serum Spreading Factor. *Biochemical and Biophysical Research Communications* 1984; **118**:339-43.
111. Seiffert D. Hydrolysis of Platelet Vitronectin by Calpain. *The Journal of Biological Chemistry* 1996; **271**:11170-6.
112. Seiffert D, Loskutoff DJ. Evidence that Type 1 Plasminogen Activator Inhibitor Binds to the Somatomedin B Domain of Vitronectin. *Journal of Biological Chemistry* 1991; **266**:2824-30.
113. Suzuki S, Pierschbacher MD, Hayman EG, Nguyen K, Ohgren Y, Ruoslahti E. Domain Structure of Vitronectin. *Journal of Biological Chemistry* 1984; **259**:15307-14.
114. Kost C, Benner K, Stockmann A, Linder D, Preissner KT. Limited Plasmin Proteolysis of Vitronectin. Characterization of the Adhesion Protein as Morpho-regulatory and Angiostatin-binding Factor. *European Journal of Biochemistry* 1996; **236**:682-8.
115. Brash JL. The Fate of Fibrinogen Following Adsorption at the Blood-Biomaterial Interface. *Annals New York Academy of Science* 1987; **516**:206-22.

APPENDIX A

REAGENTS, SOLVENTS, AND MATERIALS

Reagents and Materials	Acronym	Supplier
0.5% (w/v) Bromophenol blue	-	Bio-Rad Laboratories Inc., Hercules CA
2-Mercaptoethanol	-	EM Science, Gibbstown NJ
4,4'-methylene-di-p-phenyl diisocyanate	MDI	Aldrich Chemical Company, Milwaukee WI
5-bromo-4-chloro-3-indolyl phosphate	BCIP	Bio-Rad Laboratories Inc., Hercules CA
Acrylamide	Acryl	BioShop Canada Inc., Burlington ON
Ammonium Hydroxide	-	BDH Incorporated, Toronto ON
Ammonium Persulfate	-	BRL Life Technologies, Gaithersburg MD
Anhydrous Dimethyl Sulfoxide	DMSO	Aldrich Chemical Company, Milwaukee WI
Arg-Glu-Asp-Val-Cys	REDVC	Queen's University, Kingston ON
Arg-Gly-Asp-Cys	RGDC	Queen's University, Kingston ON
Bovine Serum Albumin	BSA	Sigma Chemical Co., St. Louis MO
Cys-Arg-Glu-Asp-Val	CREDV	Queen's University, Kingston ON
Cys-Arg-Gly-Asp	CRGD	Queen's University, Kingston ON
Dimethylformamide	DMF	Caledon Laboratories Ltd., Georgetown, ON
Endothelial Cell Line ECV304	ECV304	Henderson
Ethanol	(CH ₃) ₂ OH	BDH Incorporated, Toronto ON
Ethylene Diamine	ED	Fisher Scientific, Nepean ON
Glycerol	-	BDH Incorporated, Toronto ON
Glycine	-	BioShop Canada Inc., Burlington ON
Hydrogen Peroxide	H ₂ O ₂	BDH Incorporated, Toronto ON
Immobilon (PVDF) membranes	-	Millipore, Mississauga ON
IsoFlow™ Sheath Isotonic Fluid	-	Beckman Coulter
L-cysteine	Cys	Sigma Chemical Co., St. Louis MO
Magnesium Chloride	MgCl ₂ ·6H ₂ O	BDH Incorporated, Toronto ON
Medium 199	-	Gibco BRL, Grand Island NY
Methanol	CH ₃ OH	Caledon Laboratories Ltd., Georgetown, ON
N,N'-Methylenebisacrylamide	Bis	BioShop Canada Inc., Burlington ON
Nitroblue tetrazolium chloride	NBT	Bio-Rad Laboratories Inc., Hercules CA

Penicillin-Streptomycin	Pen-Strep	Gibco BRL, Grand Island NY
Polytetramethylene Oxide	PTMO	QO Chemicals, West Lafayette IN
Prestained SDS-PAGE Standards, Low Range	-	Bio-Rad Laboratories Inc., Hercules CA
Protogold solution	-	Cedarlane Lab Ltd., Hornby ON
Purified Human Vitronectin	Vn	Enzyme Research Laboratories, South Bend IN
Pyronin Y Dye	-	Bio-Rad Laboratories Inc., Hercules CA
Radioactive Iodide	¹²⁵ I	ICN Pharmaceuticals, Inc., Montreal PQ
Reagent A	-	Bio-Rad Laboratories Inc., Hercules CA
Reagent B	-	Bio-Rad Laboratories Inc., Hercules CA
Reagent S	-	Bio-Rad Laboratories Inc., Hercules CA
SDS-PAGE MW Standards, Low Range	-	Bio-Rad Laboratories Inc., Hercules CA
Sodium Chloride	NaCl	BDH Incorporated, Toronto ON
Sodium Dodecyl Sulphate	SDS	BioShop Canada Inc., Burlington ON
Sodium Hydrogen Carbonate	NaHCO ₃	BDH Incorporated, Toronto ON
Sodium Iodide	Nal	BDH Incorporated, Toronto ON
TEMED	TEMED	Gibco BRL, Grand Island NY
Trichoroacetic Acid	TCA	Sigma Chemical Co., St. Louis MO
Tris	-	BioShop Canada Inc., Burlington ON
Tris Base	-	Boehringer Mannheim Corp., Indianapolis IN
Trypsin-EDTA	-	Gibco BRL, Grand Island NY
Tween 20	-	Bio-Rad Laboratories Inc., Hercules CA

APPENDIX B

PEPTIDE CHROMATOGRAMS

Peptide Sequence CRGD
Formula Weight 449.49

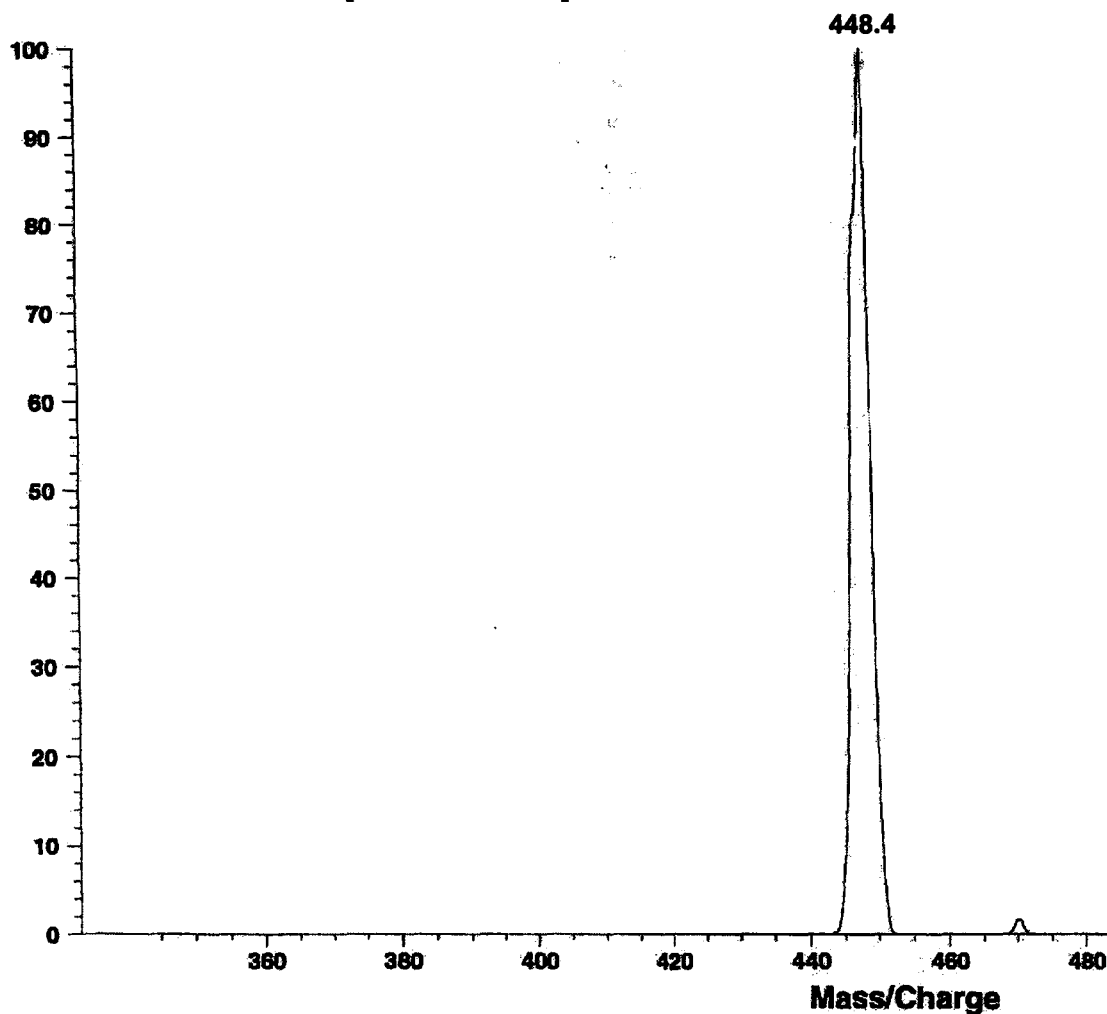
Queen's Univ. SS-12-22-99

Meeks#2ssc(ACHA)

Data:<none>.4 3 Jan 100 16:22 Cal: Insulin 26 Oct 99 18:42

Kratos Kompact MALDI 3 V4.0.0: + Linear High Power: 96

%Int. 100% = 10 mV [sum= 1032 mV] Shots 1-100 Smooth AV26

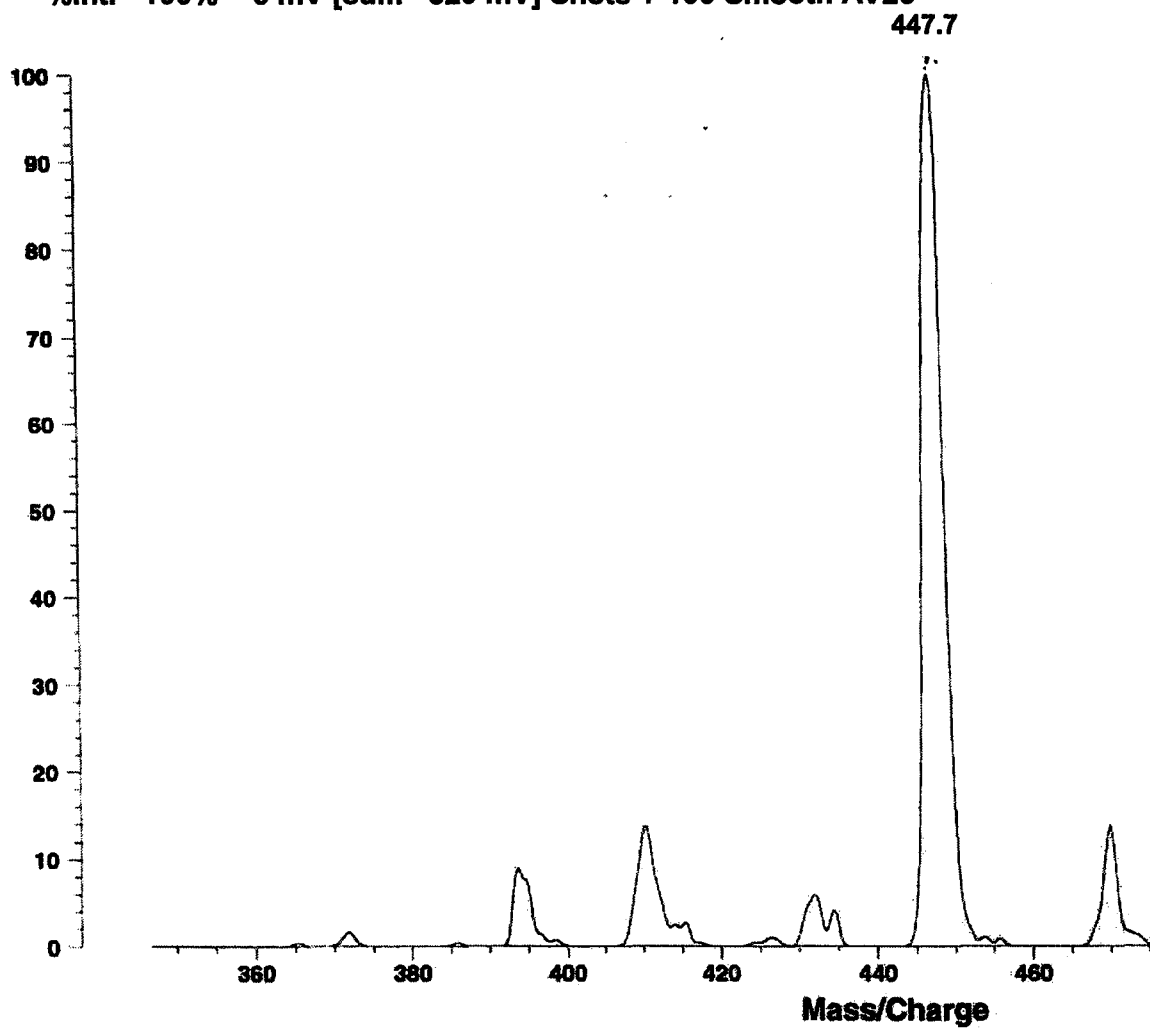


Peptide Sequence RGDC
Formula Weight 449.49

Queen's Univ. SS-3-1-2000
Meeks#3LSC

Data:<none>.6 5 Jan 100 16:21 Cal: Insulin 26 Oct 99 18:42
Kratos Kompact MALDI 3 V4.0.0: + Linear High Power: 104

%Int. 100% = 5 mV [sum= 520 mV] Shots 1-100 Smooth AV26

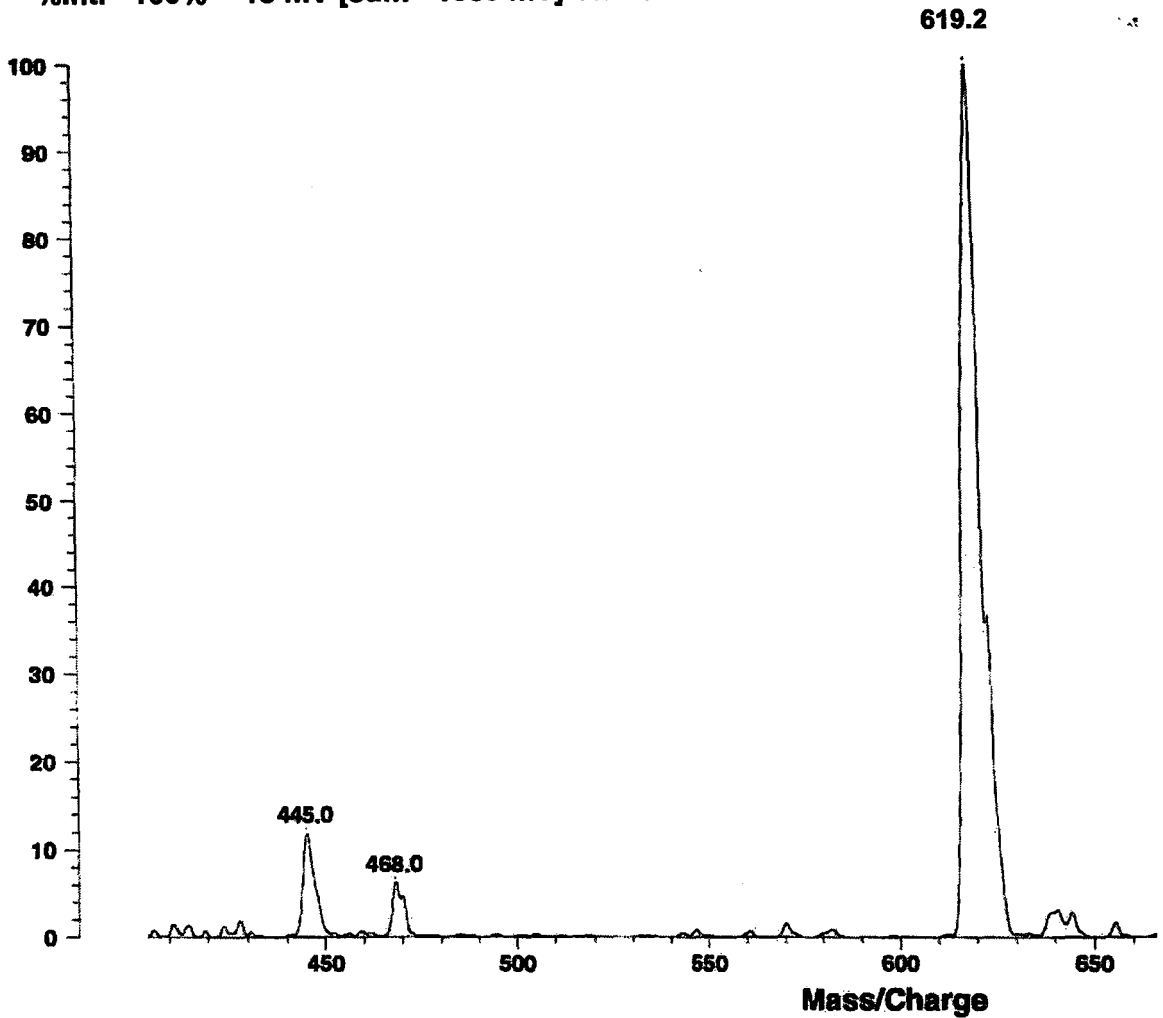


Peptide Sequence CREDV
Formula Weight 620.68

Queen's Univ. SS-3-1-2000
Meeks#4(SA)

Data:<none>.17 11 Jan 100 21:03 Cal: Insulin 26 Oct 99 18:42
Kratos Kompact MALDI 3 V4.0.0: + Linear High Power: 96

%Int. 100% = 18 mV [sum= 1853 mV] Shots 1-100 Smooth AV26

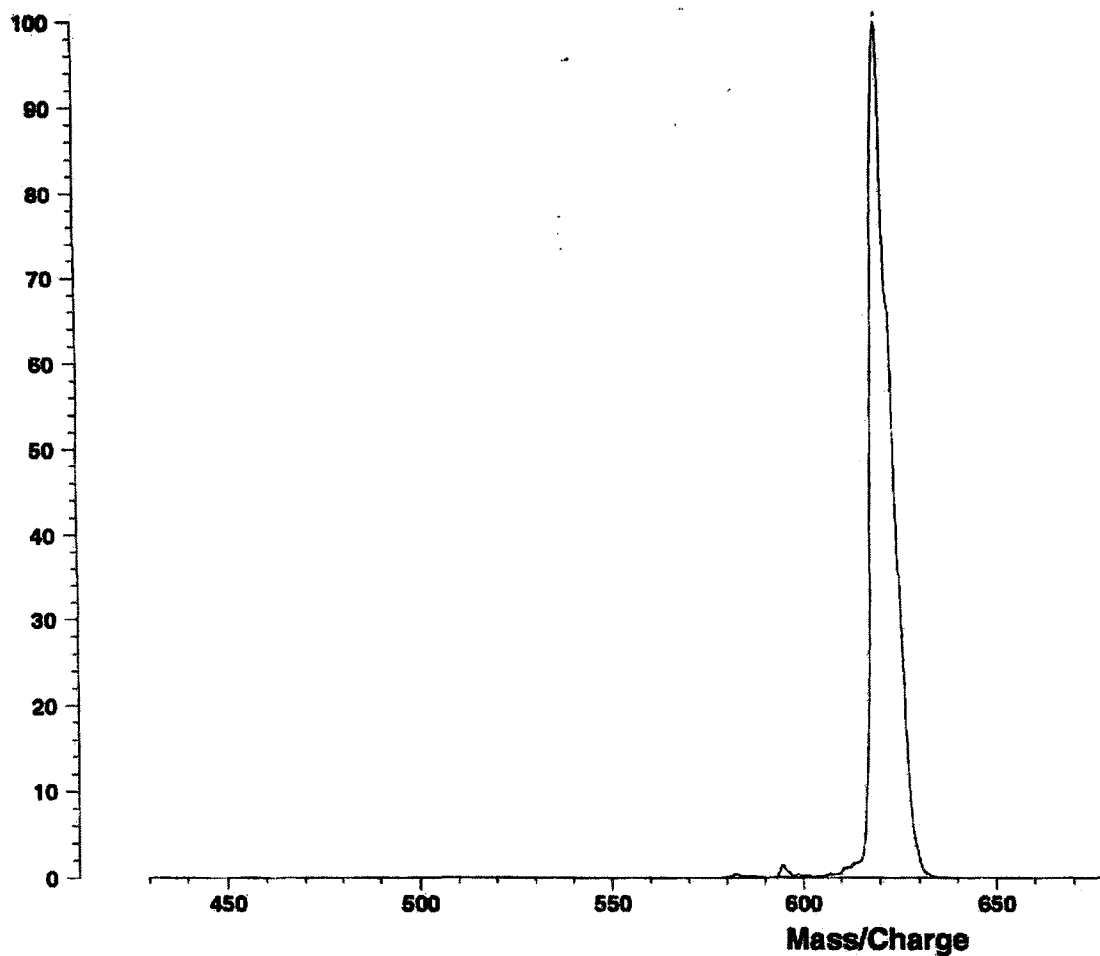


Peptide Sequence REDVC
Formula Weight 620.68

Queen's Univ. SS-12-22-99
Meeks#5

Data:<none>.19 12 Jan 100 16:49 Cal: Insulin 26 Oct 99 18:42
Kratos Kompact MALDI 3 V4.0.0: + Linear High Power: 129

%Int. 100% = 36 mV [sum= 3644 mV] Shots 1-100 Smooth AV26
620.8



APPENDIX C

PREPARATION OF BUFFERS

Phosphate Buffered Saline (PBS)

1.32 g Disodium hydrogen phosphate
0.345 g Sodium dihydrogen phosphate
8.5 g Sodium chloride
Fill to 1 L with distilled water.
Adjust pH to 7.38.

Phosphate Buffered Saline with Sodium Iodide (PBS-Nal)

1.32 g Disodium hydrogen phosphate
0.345 g Sodium dihydrogen phosphate
8.08 g Sodium chloride
1.09 g Sodium iodide
Fill to 1 L with distilled water.
Adjust pH to 7.4.

Tris Buffered Saline (TBS)

6.05 g Tris
8.76 g NaCl
Fill to 1 L with distilled water.
Adjust pH to 7.4.

APPENDIX D

DETERMINATION OF FREE IODIDE CONCENTRATION BY TRICHLOROACETIC ACID (TCA) PRECIPITATION OF THE PROTEIN

- Into two groups of 3 vials (Group A and B), 0.9 mL of a 1% (w/v in MilliQ water) bovine serum albumin (BSA) and 0.1 mL of the iodinated protein solution were added.
- To 3 of the vials (Group B), 0.5 mL of TCA was added. These vials were mixed with a vortex and left to stand for 10 minutes. After the ten minutes, the three vials were spun in a microcentrifuge for 1 minute.
- To a third set of 3 vials (Group C), 0.5 mL of buffer (PBS-NaI) was added to each.
- 0.5 mL of the supernatant from the precipitated Group B vials was added to the Group C vials.
- The vials from both Group A and Group C were counted in the gamma counter for 1 minute. The free iodide content was calculated as follows (equation 4):

$$\%FreeIodide = \left(\frac{3 \times GroupC_{AVERAGE}}{GroupA_{AVERAGE}} \right) \times 100 \quad (4)$$

APPENDIX E

SDS-PAGE AND IMMUNOBLOTS PROCEDURES

Polyacrylamide Gel Preparation (9% or 12% separating gel, 4% stacking gel)

The acrylamide/bis solution is prepared by dissolving the following reagents in distilled water, diluting to 100 mL and filtering the final solution:

Acrylamide	29.2 g
N,N'-Methylenebisacrylamide	0.8 g

The reagents for the 9% and 12% separating gel were mixed and degassed for 15 min at room temperature:

<i>Separating Gel</i>	9%	12%
Distilled water	4.4 mL	3.35 mL
1.5 M Tris, pH 8.8	2.5 mL	2.5 mL
10% (w/v) SDS	0.1 mL	0.1 mL
30% (w/v) Acrylamide/Bis	3.0 mL	4.0 mL

Immediately prior to casting the gel, the following reagents are added to initiate polymerization in the above mixture:

10% (w/v) ammonium persulfate (fresh)	50 μ L
TEMED	5 μ L

The casting plates were cleaned with distilled water and 95% ethanol. Once dry, the plates were inserted into the casting assembly. The assembly was then secured to the casting stand. Using a syringe, the gel plates were filled with polymerising 9% or 12% acrylamide solution, leaving enough space to pour the stacking gel. After 2 min, a small quantity of water was layered over the gel. The gel was allowed to polymerize for 1 h.

The reagents for the 4% stacking gel were mixed and degassed for 15 min at room temperature:

Distilled water	3.0 mL
0.5 M Tris, pH 6.8	1.2 mL
10% (w/v) SDS	0.1 mL
30% (w/v) Acrylamide/Bis	0.65 mL

Immediately prior to casting the gel, the following reagents are added to initiate polymerization in the above mixture:

10% (w/v) ammonium persulfate (fresh)	25 μL
TEMED	5 μL

Using a syringe, the remainder of the gel plates was filled with polymerizing 4% acrylamide solution. An appropriate comb was added and the gel allowed to polymerize for 1 h.

Sample Preparation

The sample buffer used in sample preparation consists of the following reagents, mixed and stored at 4°C in 225 μL aliquots:

Distilled water	4.0 mL
0.5 M Tris, pH 6.8	1.0 mL
10% (w/v) SDS	1.6 mL
Glycerol	0.8 mL

Immediately prior to use, the following reagents are added to an aliquot, yielding tracking dye (TD):

2-Mercaptoethanol	30 μL
0.5% (w/v) Bromophenol blue	30 μL

Samples and standards used for SDS-PAGE only are prepared as follows:

- 1 μL SDS-PAGE MW Standards, Low Range, 10 μL TD
- 10 μL Protein sample, 10 μL TD
- 7.5 μL Prestained SDS-PAGE Standards, Low Range

Samples and standards used for western blotting are prepared as follows:

- 1 μL SDS-PAGE MW Standards, Low Range, 10 μL TD
- 150 μL Protein sample, 100 μL TD
- 7.5 μL Prestained SDS-PAGE Standards, Low Range

Once mixed, the samples are placed in a 95°C water bath for 10 min.

Electrophoresis

Once the gel polymerization was complete, the combs were gently removed and the wells rinsed with distilled water. The gels were removed from the casting stand and placed into the clamp assembly. The assembly was then placed into the buffer chamber. A 5X stock solution of electrophoresis buffer was prepared by mixing the following reagents in distilled water and diluting to 1 L (Note: the pH of this solution should be 8.3 ± 0.3):

Tris Base	15 g
Glycine	72 g
SDS	5 g

Just prior to use, the 5X stock solution was diluted to 1X with distilled water. The upper buffer chamber was filled to a level 3 mm below the edge of the outer (long) glass plate with electrophoresis buffer. The lower buffer chamber was filled to a level that covered the bottom 1 cm of the gel. The comb was subsequently removed and the well flushed with transfer buffer. The sample was then loaded into the wells and a potential difference of 200 V applied across the gel for approximately 1 h. When performing an immunoblot, a small quantity of pyronin Y dye (dissolved in sample buffer) was layered into the wells just before the tracking dye had reached the bottom of the separating gel. Electrophoresis was stopped once the pyronin Y dye had reached the top of the separating gel.

Gel Equilibration

Transfer buffer was prepared by mixing the following reagents in distilled water and diluting to 1 L (Note: the pH of this solution should be 8.3 ± 0.3):

Tris Base	3.03 g
Glycine	14.4 g
Methanol (HPLC grade)	200 mL

The gels were removed from the electrophoresis assembly and equilibrated in fresh cold (4°C) transfer buffer for 30 min.

Electrophoretic Transfer

Immobilon (PVDF) membranes were cut to gel-size, prewetted in methanol (1-3 seconds), incubated in water (1-2 min) and soaked in transfer buffer (15 min). The gels and membranes were loaded in the transfer cassettes according to specifications and placed in the transfer chamber. The chamber was then filled with transfer buffer so that the entire gel surface was covered. A potential

difference of 100V (200 mA) was applied for 1 h. The membranes can then immediately be stained with colloidal gold or dried and used for immunoblot analysis.

Gold Staining

The PVDF membranes were washed two times in phosphate buffered saline (PBS), pH 7.4. PBS was prepared by mixing the following reagents in distilled water, adjusting the pH to 7.4 and diluting to 1 L:

Na ₂ HPO ₄	1.32 g
NaH ₂ PO ₄ ·H ₂ O	0.345 g
NaCl	8.5 g

The membranes were then incubated in 0.3% (v/v) Tween 20 solution in PBS for 1 h at 20°C to block unbound membrane sites. This was followed by three further washings of 5 min with this blocking solution. The membranes were then rinsed in water three times for 1 min.

The membranes were then placed in Protogold solution and stained for 1 to 4 h. Following the staining, the membranes were rinsed extensively with distilled water and air dried.

Immunoblotting

The sections of the membrane containing MW markers lanes and a small section of the sample lane were removed to be stained with the gold staining procedure described above.

Tris-buffered saline (TBS) was prepared as follows:

50 mM Tris
150 mM NaCl
Adjust pH to 7.4

The remainder of the membrane was sliced into 3 mm strips. The strips were prewet in methanol, rinsed in distilled water and placed into plastic wells. In order to block unbound membrane sites and prevent non-specific binding, the strips were incubated for 1 h in 5% (w/v) dry skim milk in TBS, pH 7.4 with gentle agitation. This treatment was followed by three 5 min rinses in 0.1% (w/v) dry skim milk in TBS.

Each strip was then incubated for 1 h in 1 mL 1% (w/v) dry skim milk and 0.05% (v/v) Tween 20 in TBS with a 1/1000 dilution of the primary antibody to the protein of interest. This treatment was followed by three 5 min rinses in 0.1% (w/v) dry skim milk in TBS. Each strip was then incubated for 1 h in 1 mL 1% (w/v) dry skim milk and 0.05% (v/v) Tween 20 in TBS with a 1/1000 dilution of the alkaline phosphatase-linked secondary antibody. Again followed three 5 min rinses in 0.1% (w/v) dry skim milk in TBS. Finally, the strips were incubated for up to 4 h with a solution to develop the colour reaction and detect the bands. The buffer for this solution is prepared by dissolving the following reagents in distilled water, adjusting the pH to 9.8 and diluting to 100 mL:

NaHCO ₃	840 mg
MgCl ₂ ·6H ₂ O	20 mg

The final solution is prepared by mixing 1 mL NBT stock (30 mg NBT in 1 mL 70% DMF in distilled water) and 1 mL BCIP stock (15 mg BCIP in 1 mL DMF) in 100 mL buffer: This reaction was terminated by rinsing the strips in distilled water twice for 5 min.